Biotechnology Advances xxx (xxxx) xxx–xxx

Contents lists available at ScienceDirect

Biotechnology Advances

journal homepage: www.elsevier.com/locate/biotechadv

Research review paper

Essential steps in bioprinting: From pre- to post-bioprinting

Pallab Datta[a], Ananya Barui[a], Yang Wu[b,c], Veli Ozbolat[b,c,d], Kazim K. Moncal[b,c], Ibrahim T. Ozbolat[b,c,e,f,*]

[a] Centre for Healthcare Science and Technology, Indian Institute of Engineering Science and Technology Shibpur, Howrah 711103, West Bengal, India
[b] Engineering Science and Mechanics Department, Penn State University, University Park, PA 16802, USA
[c] The Huck Institutes of the Life Sciences, Penn State University, University Park, PA 16802, USA
[d] Ceyhan Engineering Faculty, Cukurova University, Adana 01950, Turkey
[e] Biomedical Engineering Department, Penn State University, University Park, PA 16802, USA
[f] Materials Research Institute, Penn State University, University Park, PA 16802, USA

ARTICLE INFO

Keywords:
Bioprinting
Biofabrication
Bioink
Bioprinter
Extrusion-based bioprinting
Droplet-based bioprinting
Laser-based bioprinting

ABSTRACT

An increasing demand for directed assembly of biomaterials has inspired the development of bioprinting, which facilitates the assembling of both cellular and acellular inks into well-arranged three-dimensional (3D) structures for tissue fabrication. Although great advances have been achieved in the recent decade, there still exist issues to be addressed. Herein, a review has been systematically performed to discuss the considerations in the entire procedure of bioprinting. Though bioprinting is advancing at a rapid pace, it is seen that the whole process of obtaining tissue constructs from this technique involves multiple-stages, cutting across various technology domains. These stages can be divided into three broad categories: pre-bioprinting, bioprinting and post-bioprinting. Each stage can influence others and has a bearing on the performance of fabricated constructs. For example, in pre-bioprinting, tissue biopsy and cell expansion techniques are essential to ensure a large number of cells are available for mass organ production. Similarly, medical imaging is needed to provide high resolution designs, which can be faithfully bioprinted. In the bioprinting stage, compatibility of biomaterials is needed to be matched with solidification kinetics to ensure constructs with high cell viability and fidelity are obtained. On the other hand, there is a need to develop bioprinters, which have high degrees of freedom of movement, perform without failure concerns for several hours and are compact, and affordable. Finally, maturation of bioprinted cells are governed by conditions provided during the post-bioprinting process. This review, for the first time, puts all the bioprinting stages in perspective of the whole process of bioprinting, and analyzes their current state-of-the art. It is concluded that bioprinting community will recognize the relative importance and optimize the parameter of each stage to obtain the desired outcomes.

1. Introduction

In the last few years, the applications of tissue engineered constructs have expanded from clinical tissue regeneration to fabrication of tissue models for drug discovery (Knowlton et al., 2016; Peng et al., 2016), pathological understanding (Elson and Genin, 2016; Gomes et al., 2017) and controlled drug delivery systems (Do et al., 2017). The key enablers for these applications are advanced fabrication techniques that allow generation of tissue constructs mimicking the complex native extracellular matrix (ECM) organization (Guo et al., 2016). One of the most emerging techniques is bioprinting, which allows for precise deposition of cells and biomaterial components in pre-defined computer generated designs (Cornelissen et al., 2017). Indeed, experimental evidences on bioprinting have accrued at very rapid pace with increasing number of publications and involved research groups worldwide in recent times (Rodríguez-Salvador et al., 2017). These concoctions of cells and biomaterials (in some cases only cell aggregates) are often referred to as bioinks (Hölzl et al., 2016). The success of bioprinted tissue constructs is invariably determined by the properties of bioink. Usually, the process of generating bioprinted tissue constructs involves several steps. The first step is the creation of a computer-aided design model, suitable for bioprinting, whose resolution is determined by the applied image acquisition techniques, such as three-dimensional (3D) laser scanning, micro-computed tomography (μ-CT) and magnetic resonance imaging (MRI). In the design stage, it is also important to note if the methods used for generating a 3D model could be easily deployed in a surgical setting (e.g. short computational interval, and good compatibility between software and hardware).

* Corresponding author at: Engineering Science and Mechanics Department, Penn State University, University Park, PA 16802, USA.
E-mail address: ito1@psu.edu (I.T. Ozbolat).

https://doi.org/10.1016/j.biotechadv.2018.06.003
Received 7 January 2018; Received in revised form 15 May 2018; Accepted 10 June 2018

After the design is finalized, the fabrication process commences along with obtaining cells with sufficient quantity and robustness. Bioink can be characterized by different parameters prior to bioprinting. In addition, clinical application becomes more feasible if the cellular and biomaterial components are obtained by minimally-invasive surgical procedures and if the protocols followed for expansion of cells are cost effective and achievable under general good laboratory practice (GLP) conditions. Thereafter, at the bioprinting stage, multiple factors influence the properties of engineered constructs. Cell densities that can be printed along with appropriate physicochemical properties become important determinants of dispensation through printheads. Such physicochemical properties include rheology, surface properties and most importantly, the gelation kinetics of the bioink. One of the most important challenges is to figure out a balance between printability and immediate solidification after bioprinting, so that the desired structure is retained. Alternatively, bioprinting can be performed in a microgel (e.g. carbopol) support bath or using nanoclays (e.g. laponite) to directly print structures in air without the need for instantaneous gelation (Bhattacharjee et al., 2015; Hinton et al., 2015, 2016; Jin et al., 2016, 2017). Bioink formula must also be affordable and biocompatible. In particular, for fabrication of hollow organ structures, it is required to use sacrificial inks and hence, the difference in properties of two types of bioink becomes important. In turn, the use of sacrificial inks is determined by the physical properties of the functional inks and aspect ratio of the vascular network to be fabricated. Subsequently, the applied bioprinting technique makes an important contribution to the mechanical and structural properties of constructs.

Current bioprinting technologies are based on one amongst extrusion-based bioprinting (EBB), droplet-based bioprinting (DBB) or laser-based bioprinting (LBB), as depicted in Fig. 1. EBB exploits automated three-axis robotic system for continuous extrusion of bioinks in filament forms. Herein, pneumatic or mechanical driven dispensing systems are mostly employed. In EBB, high extrusion pressure and resulting shear stress are the cause of concern for cell survival, but the modality usually produces most mechanically-robust constructs amongst all bioprinting techniques. In DBB, the bioink made up of living cells and other biological materials (e.g. hydrogels) in culture media is deposited in droplets form with precise noncontact positioning. The droplets are generated by one of thermal-, piezoelectric- or electrostatic- drop-on-demand technologies. DBB generally provides appreciable cell viability, though electrohydrodynamic jetting or micro-valve bioprinting can facilitate 80-90% viability (Gudapati et al., 2016; Ng et al., 2017a). DBB is a relatively rapid technique with a low cost and high resolution, but it can result in non-homogenous droplet size and cause nozzle-clogging while printing high density bioinks (Gudapati et al., 2016). LBB operates on the principle of a laser energy beam utilized for precise patterning of cells. Laser energy can be used in two different modalities, one of which involves photopolymerization (e.g., stereolithography or two-photon polymerization), and the other modality is based on cell transfer (e.g. laser guided direct writing and laser induced forward transfer). LBB is advantageous over the other modalities as it causes minimal clogging and damage to cell survival. Several advances in digital projection stereolithography techniques have been applied for bioprinting applications (Gauvin et al., 2012; Gou et al., 2014). Though LBB also provides high resolution, it is an expensive and time consuming modality (Datta et al., 2017a; Peng et al., 2017). Each bioprinting technique has advantages and disadvantages with respect to cell survival against the process. Apart from the basic processes associated with each bioprinting modality, several innovations like aerosol assisted crosslinking, use of electric fields to reduce shear stresses, hybrid electrospinning-bioprinting and core/shell bioprinting has been developed (Lee et al., 2017a, 2017b). In all cases, it is important that cellular biomaterials are printed in a manner that allows intricate cell-material interactions, which are crucial for the tissue development. During this phase, it is essential that cells are printed with sufficient resolution to facilitate proper cell-cell interactions. Finally, bioprinted tissue constructs are required to become mature in suitable bioreactors before they can be implanted. Degradation of the biomaterial support, if present, also demonstrates significance during the post-bioprinting stage.

In this review, we critically present the current literature on abovementioned aspects of bioprinting technology from the design phase to post-bioprinting steps. The complete bioprinting process, including pre-bioprinting, bioprinting and post-bioprinting along with their components, is schematically illustrated in Fig. 2. As shown in the Fig. 2, bioprinting is multi-disciplinary area, and the successful fabrication of tissue constructs requires understanding the dynamic interaction between different disciplines. However, most reviews available till date only concentrate on single domain specific analysis of current literatures, and a comprehensive presentation on all aspects has not been demonstrated yet. Therefore, we provide all the stages involved in this process for the first time in literature and thoroughly discuss these stages including pre-bioprinting, bioprinting and post-bioprinting with their essential components.

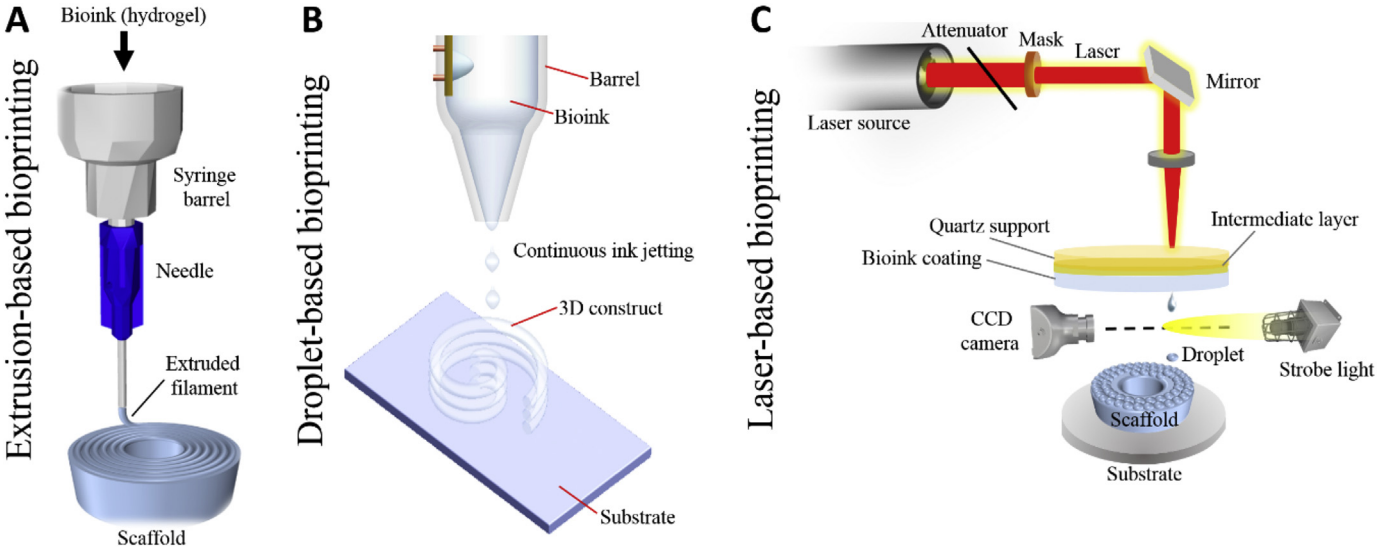

Fig. 1. Mechanisms of bioprinting techniques: A) extrusion-based bioprinting, B) droplet-based bioprinting, C) laser-based bioprinting.

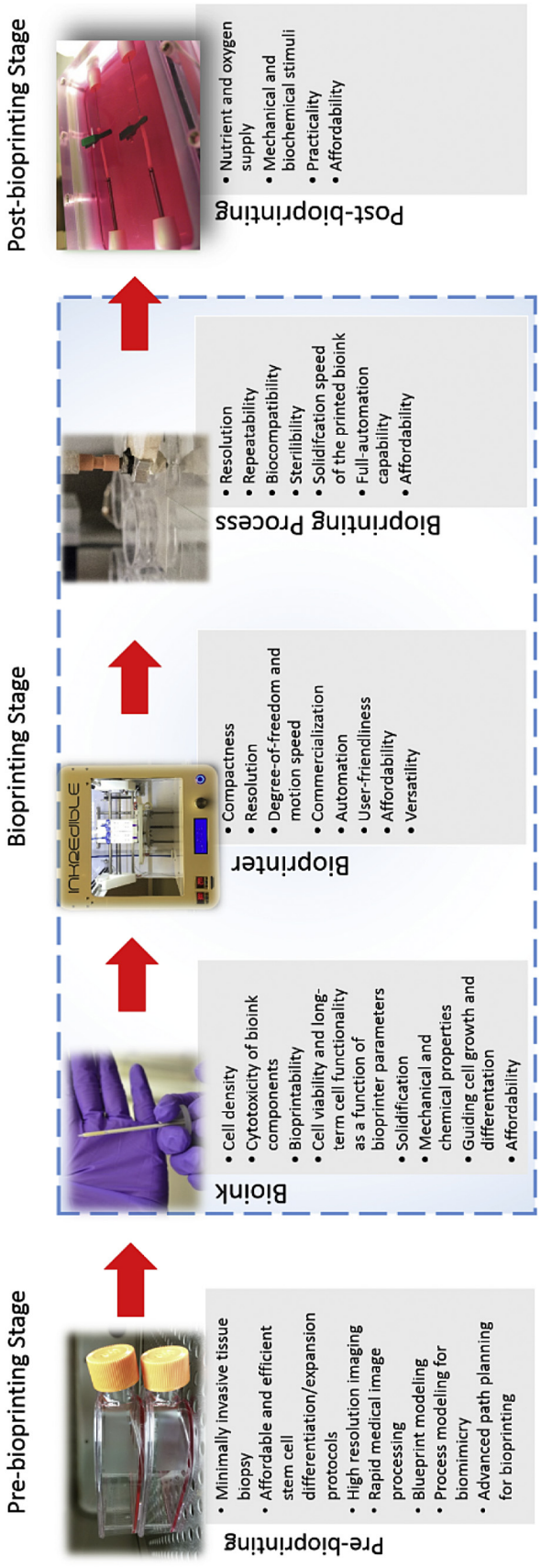

Fig. 2. Stages in the entire 3D bioprinting process, including pre-bioprinting, bioprinting and post-bioprinting, and their major components (bioreactor image taken with permission from (Norotte et al., 2009).

2. Pre-bioprinting Stage

The pre-bioprinting stage plays an extremely crucial role in determining the properties of bioprinted constructs. To ensure that the adequate quality of cells is obtained along with anatomically-correct tissue models and appropriate process planning for bioprinting, it becomes extremely important in pre-bioprinting stage that the correct procedures are adopted. Fig. 3 demonstrates the essential components of pre-bioprinting stages including minimally invasive tissue biopsy, affordable and efficient stem cell differentiation/expansion protocols, high resolution imaging, rapid medical image processing, blueprint modeling, process modeling for biomimicry, and advanced path planning for bioprinting, which are thoroughly discussed in the following subsections.

2.1. Minimally invasive tissue biopsy

In order to minimize the chance of immune-rejection of bioprinted tissues, patient's own cells are preferred as the cell source. Cell acquisition methods are important since most laboratories working on bioprinting primarily focus on material, process and structure development, in which model/standard cell lines are employed. However, for bioprinting to overcome the barrier of clinical translation, primary cells obtained from the patients are essential should be provided equal importance. A patient-lab-patient strategy is essential for the success of the process. Cells with different phenotypes and genotypes are bound to show different survival, proliferation and maturation kinetics under the bioprinting conditions and hence topical overview is provided as the roadmap that should be followed to obtain functional constructs by bioprinting. Similarly, in situ tissue engineering using recruitment of host cells is a useful strategy but limited to younger patients or patients with good nutritional status. Additionally in vitro tissue engineering is advantageous for generating vascularized constructs. Therefore, the acquisition of cells is an important aspect for bioprinting. For collecting cells, minimally invasive biopsy is gaining importance for successful 3D bioprinting and other regenerative approaches. In medical diagnosis, biopsy has been the gold standard and sometimes the only choice of harvesting tissue for disease prognosis (Obeng-Gyasi et al., 2018; Pohlig et al., 2012); however, the need of routine screening has increased dramatically with increase in healthcare awareness. To meet up the requirement, surgical oncology has been evolving towards minimally invasive biopsy methods. For example, through special vacuum assisted needle biopsy system (Park and Kim, 2011), a tiny amount of skin sample can be collected which was not earlier possible with conventional systems. Another advantage of such system is to introduce a very little deformation or secondary wound at the biopsy site, which recovers within minimal time without any scar formation. Upon early diagnosis, the treatment of primary tumor site without surgical intervention can be performed through different emerging minimally invasive procedures such as focused ultrasound, MRI or X-ray, CT-guided biopsy. Another approach called percutaneous stereotactic method has been recently applied for biopsy collection (Fine et al., 2003). Amongst several minimally invasive approaches, the most extensive work has been done on radiofrequency ablation (Vlastos and Verkooijen, 2007). In this method, under imaging guidance, a radio frequency probe is inserted at the tumor site, and high frequency alternating current is applied through the probe that causes an irreversible destruction of tumor cells (Hamazoe et al., 1991). Another approach for such treatment is focused ultrasound ablation, in which ultrasound is focused on the target tumor and temperature increase rapidly through converting the acoustic energy to heat (Chen et al., 1999). For this method, high resolution imaging guide (e.g., MRI) is required for diagnostic accuracy (Cline et al., 1995; McDannold et al., 1998).

In bioprinting, apart from harvesting of cells as source for in vitro tissue engineering, harvesting of a volumetric tissue sample (i.e., adipose) is gaining importance for preparation of decellularized ECM-

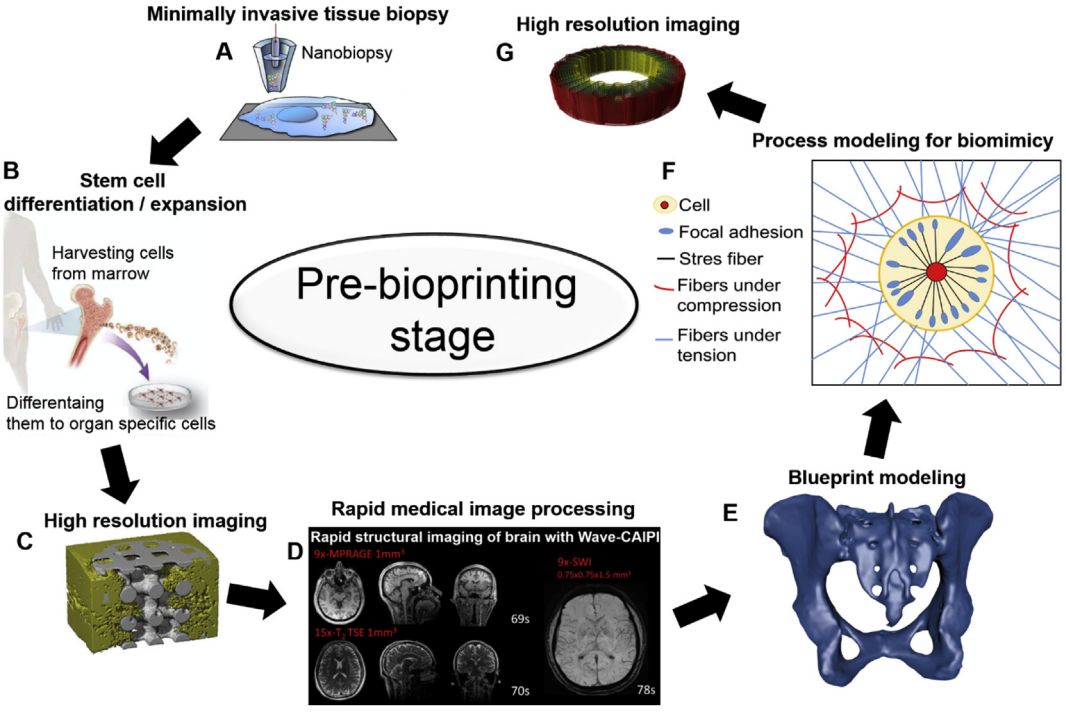

Fig. 3. The major components of the pre-bioprinting stage: A) A schematic of nanobiopsy (modified with permission from (Actis et al., 2014)); B) A schematic of stem cell isolation (modified with permission from (Lanza et al., 2007)); C) 3D Reconstruction of scaffold (white) and bone ingrowth (yellow); only part of the cylindrical scaffold is displayed, as to be able to look inside the scaffold (modified with permission from (Van Lenthe et al., 2007)); D) A high resolution whole brain imaging of MPRAGE, T2-TSE and SWI (modified with permission from (Poser and Setsompop, 2017)); E) A STL file of a pelvis (National Institutes of Health 3D Print Exchange (https://3dprint.nih.gov/)); F) A schematic of a cell adhered to fibrous ECM; G) Advanced path planning for multi-layered structure printing (modified with permission from (Ozbolat and Khoda, 2014)).

based bioink (Pati and Cho, 2017). In this regard, minimally invasive biopsy is becoming popular for obtaining live tissues. Although there are several ways for harvesting tissues (Levin et al., 1989), they require incisional process to collect the tissue and multi-layered suturing to close the incision site, which sometime give rise to different clinical complications such as stitch abscesses and formation of hematoma or seroma. Due to fast development of tissue engineering technology, minimally invasive technique will play the critical role in making the autologous tissue engineering a clinical reality (Megerian et al., 2000).

Researchers have explored the possibility of microbiopsy or needle biopsy, in which a small amount of tissue of approximately 15 to 20 mg is collected through an automatic 14 gauge microbiopsy needle. In this method, a small skin puncture is sufficient for successful collection of a biopsy sample (Ceusters et al., 2017). Though it is at present a challenge if adequate cell numbers can be generated from single cell biopsy and may require conjunction with cloning techniques in the future, some authors have started exploring their potential in tissue engineering (Tait et al., 2017). Recently, a research team has reported robotic 'nanobiopsy' method for collection of extremely tiny amount of samples (even isolation of single cell) is possible (Actis et al., 2014). A nanopipette (50 nm) is inserted through cell membrane by minimally invasive method without damaging the target cell (see Fig. 3A).

2.2. Affordable and efficient stem cell differentiation/expansion protocols

In the field of regenerative medicine, there is a growing interest to apply bioprinting methods (Collins, 2014); however, there remain a plethora of biological challenges. One of the important hurdles is the viability of stem cells and their long-term functionality during sequential differentiation. Researchers are continuously trying to identify optimum source of stem cells and develop appropriate and efficient protocols for isolation and explosion of stem cells through affordable and rapid methods (see Fig. 3B). Several stem cell sources including embryonic stem cells (ESCs) and human mesenchymal stem cells (hMSC) isolated from bone marrow and adipose tissue have already been explored for bioprinting (Gruene et al., 2011a; Gruene et al., 2011b; Xu et al., 2011). ESCs are the ideal source of stem cells since they are able to differentiate into any cell type. Prior to differentiation into target lineage, ESCs aggregate into embryoid bodies (EBs) demonstrating early stage of embryogenesis (Itskovitz-Eldor et al., 2000). Overall, the EBs establish the microenvironment for lineage-specific differentiation of stem cells (Kurosawa, 2007; Tasoglu and Demirci, 2013). However, the application of ESCs is limited in many countries due to ethical restriction. Other than ethical constrains, another disadvantage of ESCs is that the cellular differentiation process is not always readily controlled, and cells may exhibit immunogenicity. To overcome such limitations, induced pluripotent stem cells (iPSCs) offer an alternative approach that is subject to neither ethical nor immunogenic concerns (Youssef et al., 2016). The differentiation state of stem cells depicts its immunogenic potential. It has been observed that undifferentiated stem cells are more immune-tolerated in comparison to the differentiated stem cells. Such immune-modulatory behavior of undifferentiated stem cells allows successful implantation and reduces host rejection of grafts (Gao et al., 2016a, 2016b; Irvine and Venkatraman, 2016; Madrigal et al., 2014). Despite the continuous effort for the development of robust and rapid protocols for differentiation of stem cells into target cell lineages, most of the available methods are time consuming and lack reproducibility (Cohen and Melton, 2011). A recent approach reported by some research groups (Huang et al., 2014; Ieda et al., 2010) reveals that the forced expression of lineage specific master regulators induces direct reprogramming of somatic cells, and it has potential to be an alternative to direct rapid cellular differentiation. In this process, the differentiation of human pluripotent stem cells (hPSCs) is modulated by forward programming that enables scalable and faster production of lineage-specific cell types (Zhang et al., 2017). The forward programming method presently used

in regenerative biology is based on lentiviral transduction of hPSCs (Darabi et al., 2012); however, transgenes are inserted randomly into the genome in lentiviral method, probably resulting in unwanted interference with cellular endogenous transcription program. To overcome this limitation, researchers have been trying to develop an alternative forward programming system by identifying more specific dual genomic safe harbor targeting strategies, which are required to induce expressions of transcription factors (Pawlowski et al., 2017; Sadelain et al., 2011). For neurogenic differentiation of ESCs or iPSCs, the available protocols require the animal factors for EBs formation, which reduces yield and efficiency of differentiation process. A recent study by Lukovic *et al.* has demonstrated a method for neural conversion of ESCs/iPSCs without employing any animal factors (Lukovic et al., 2017). They have fortified the culture media with insulin to promote direct differentiation of stem cells into functional neural cell lineage.

Monocytic cells are important cells for promoting immune response under pathological condition. These cells are generally differentiated from ESCs or iPSCs through embryonic body or feed co-culture method. However, all these methods employ xenogeneic material, which subsequently compromises the reproducibility of the differentiation process. Recent studies have reported a highly efficient alternative for differentiation of monocytic cells without using serum and feeder layer (Yanagimachi et al., 2013). Since the isolation of embryonic stem cells from mouse embryo by Martin (1981), considerable progress has been made in stem cell research. However, till date several challenges still exist, such as definition of the culture conditions that are adequately compatible with the clinical applications. Although most of adult stem cells derived from tissues are able to maintain considerable self-renewal capacity and lineage specificity, challenges remain in expanding the lineage-specificity of the stem cells for generating more patient-specific cell types. The cellular reprogramming is one approach for fulfilling this need, although it is often proved that large scale production is inefficient, and the number of fully-reprogrammed cells are very limited (< 0.01%) (Hasegawa et al., 2010; Takahashi and Yamanaka, 2006). Application of small molecules (e.g. epigenetic-related compounds valproic acid (VPA), BIX-01294, parnate, pluripotin) may provide an alternative approach to overcome this situation (Zhou et al., 2010). Effect of small molecules on biological systems is rapid, reversible and dose dependent. By modulating the synthesis process, shape and size of these molecules can be tailored, and functional optimization is also possible. Although handling of such molecules is relatively easier than genetic intervention, some researchers reported the disadvantages of these molecules in terms of their target specificity and toxic effects observed *in vivo*. Chen *et al.* proved that small molecule such as pluripotin (also known as SC1) was able to maintain the long term self-renewal of mouse embryonic stem cells (mESC), even in absence of any feeder layer or animal serum in culture media (Chen et al., 2006). Identification of this small molecule revealed the possible strategy of maintaining self-renewal capacity of stem cells by effectively balancing the endogenous differentiation pathway of stem cells. In 2008, Buehr *et al.*, applied combination of two inhibitors, PD0325901 and CHIR99021, for maintaining the self-renewal of mESCs without any feeder layer or exogenous cytokines (Buehr et al., 2008). In addition to maintaining the self-renewal capacity, these small molecules have also played role in dictating lineage specificity of their differentiation (Buehr et al., 2008; Li et al., 2008). One such compound, StemRegenin1 (SR1) in combination of growth cytokines was reported to promote the *ex vivo* expansion of hematopoietic stem cells (HSCs) and their differentiation towards the lineage of blood cells (Boitano et al., 2010; Zhang et al., 2013).

2.3. High resolution imaging

Designing of tissue constructs before bioprinting assumes great significance in the process workflow. Bioprinted constructs must not only conform to injury-specific geometrical dimensions, but also match the tissue-specific ECM attributes. Thus, the importance of medical imaging, especially 3D imaging in tissue engineering exhibits increased significance (see Fig. 3C) (Appel et al., 2013; Nam et al., 2014; Teodori et al., 2017). In addition, as cell viability inside a construct is a critical bottleneck for their clinical application, medical imaging techniques must also provide accurate information on geometry of vessel networks to ensure adequate nutrient transport. For optimal patient compliance, medical imaging techniques should be non-invasive and ensure minimum radiation exposure. Presently, X-ray, MRI and CT are the most popular imaging technique to design, preferably 3D, implants with anatomical geometries (e.g. cardiovascular, orthopedic, and nervous tissues), from amongst several other modalities including modality angiography, fluoroscopy, 3D photogrammetry, optical coherence tomography (OCT) or ultrasound (Ballyns and Bonassar, 2009; Reiffel et al., 2013). MRI is the mostly recommended imaging method for soft tissue visualization, which produces contrast in images based on state of water molecules in the tissue. An underlying pathology alters the proton density and/or how water molecules of tissue are bound with tissue, thus altering the intensity of absorption of magnetic energy or relaxation time of constituent protons upon excitation in an external magnetic field changes, which can be detected by magnetic resonance coils. Since its discovery, the resolution of MRI imaging has been constantly improving. The most common method of achieving a higher resolution is to increase the strength of external magnetic field. Presently, MRI machines with range of field strengths from 1.5 to 11.7 T are often employed. Typically, they can attain resolution up to $0.22 \times 0.22 \times 0.41\ mm^3$ in certain brain cancer tissues, though resolution of 250 μm and above are more common with 3T MRI scans, and spatial resolutions of ~100 μm can be achieved in 7–9 T machines. The use of contrast agents (e.g. super paramagnetic iron oxide nanoparticles) further enhances the resolutions achievable with MRI (Iyer et al., 2016). It must be noted that high resolution scanning increases scan time and distorts signals due to patient movements. On the other hand, though MRI does not use ionizing radiation and is considered safe to some extent, patients might feel discomforts due to high magnetic field exposures. MRI has been used in observation of tissue engineered constructs. For example, the technique can efficiently record cell distribution in polymeric scaffolds, vascularization in hydroxyapatite hydrogels or glycosaminoglycan secretion and production in tissue engineered scaffolds *in vivo* (Appel et al., 2013). Generally, imaging techniques have been applied to investigate the scaffold behavior and visualization after implantation (Nam et al., 2014). Recently, their utility for prosthetics or as templates for scaffold design is being realized. Khoda have designed scaffolds with interconnected pores with different spatial distributions by suitable processing of geometric and topology of target tissue, tessellating the 3D contours of tissue volume with triangles using a mesh or stereolithography (STL) model (Ahsan et al., 2017; Khoda, 2014). Researchers also have described scaffold fabrication from MRI images (Fu et al., 2017; Park et al., 2017).

Typically, CT imaging renders higher resolution compared to MRI with less scan time, but requires contrast agents to image tissues, which results in significant radiation exposure. CT images are more convenient to be processed into 3D anatomical geometry. Micro-computed tomography (μ-CT) provides very high resolutions (1–200 μm), but cannot be used to image higher volumes (Nam et al., 2014). On the contrary, ultrasound techniques do not cause exposure to ionizing radiation with a short scan time, and at the same time they can image a wide scope; however, the resolution of ultrasound is limited to $1 \times 1.5 \times 0.2\ mm^3$. 3D Photogrammetry can provide images with resolution up to 150 μm with an extremely short scan time (< 1 min), but it is only applicable for external tissues.

The selection of the most appropriate imaging method depends on the target tissue. For example, the approach to obtain medical imaging data from a patient to generate a femoral head articular surface and bony structure without contrast agents is very different from imaging

the meniscus or heart leaflet valve. In the case of the femoral head, although CT would provide the highest resolution for the bony structure, cartilage or soft tissues could not be imaged readily. Also, the size of femoral head is highly large to fit into current CT devices. In the case of meniscus, the most medically effective choice is MRI. High-resolution images of the meniscus can be obtained via MRI by increasing the scan time. The alternative would be to extract the tissue from the joint, and soak it in a contrast agent to allow for CT scanning. It is important to note that MRI can acquire geometries under loaded condition, whereas CT may have altered geometry due to being soaked in a contrast agent. In the case of the heart valve, MRI and CT both require contrast agents to visualize the inner workings of the heart and have similar image resolutions. Due to the high radiation exposure needed to perform a CT scan of the heart and the high expense associated with MRI usage, echocardiography (cardiac ultrasound) is becoming a more widely used non-invasive method to obtain 3D geometric models of mitral valves (Ballyns and Bonassar, 2009). However, to maximize resolution, the valve can still be extracted, soaked in a contrast agent and scanned via CT.

Recently, Park *et al.* have shown fabrication of 3D scaffold using MRI imaging for bile duct regeneration (Park et al., 2017), and other study on brain tissue engineering from MRI image processing have been also reported. Duan *et al.* have used the CT image to demonstrate the design of bioprinted heart valves (Duan et al., 2013). Apart from the tomographic imaging, developments in molecular imaging also enable high resolution images with functional information about the target tissues. In the future, molecular imaging could be combined with tomographic imaging for target tissue design for bioprinting (Mycek, 2015).

2.4. Rapid medical image processing

3D printing is rapidly expanding in the field of healthcare and medical applications including fabrication of customized prosthetics, implants or tissue and organ fabrications. The exact anatomical model of target organ can be acquired through various medical imaging modalities as discussed in the previous sub-section. To generate the design of tissue constructs, it is necessary to perform suitable processing steps such as image segmentation and pattern recognition (McCormick et al., 2014; Sun et al., 2004). Presently, most image acquisition is performed in common digital formats such as Analyze, Nifti, Minc, VPX, Interfile, though sometimes specific formats like Digital Imaging and Communications in Medicine (DICOM) are necessary (Larobina and Murino, 2014). Image processing steps include image pre-processing, image segmentation, feature extraction, and data mining. In image pre-processing, image scaling is performed, followed by image enhancement through noise removal and brightness, illumination or contrast correction. After the image registration is conducted, image segmentation is a crucial step to seek to identify the region of interest, which is performed by thresholding, edge, region or cluster-based methods. Image segmentation can be further performed by supervised or unsupervised methods, and conform to deformable, parametric or geometric models. Segmentation software is vital for convenient extraction of surface structures of interest from 3D images (see Fig. 3D). After image segmentation, extraction of morphological and textural features or identification of specific spatial patterns is performed. It must be noted that in many cases, image processing is necessary, not only to depict the architecture of construct to be bioprinted, but also to obtain optimal stress distribution and oxygen perfusion for incorporated cells through the optimization of the internal architecture (Shen et al., 2011; Xu et al., 2013a, 2013b). Furthermore, design software is required for 3D modelling, such as MIMICS, TSIM, Solidworks, 3D slicer, MATLAB, and OsiriX. For example, the use of finite element analysis (FEA) for creating tissue engineering constructs by stereolithography has been reported (Lin et al., 2007). In another work, Mahmoud *et al.* have shown the use of an automated scaffold design technique by use of k-means clustering algorithm and isosurface rendering technique for reconstruction and visualization of 3D volume of bone defects (Mahmoud et al., 2015). Moreover, a computer-aided system for tissue scaffolds (CASTS) has been reported, which could automatically design 3D porous constructs in accordance with a defined external geometry (Sudarmadji et al., 2012). Such methods are required for rapid scaffold design in bioprinting for clinics. CAD models are also useful to design scaffolds with gradient porosity for bioprinting (Khoda et al., 2013). Recently, Bücking *et al.* have described an optimized workflow, in which CT images were taken as input, followed by segmentation by means of thresholding, connected-component-filter or fill-holes-filter (Bücking et al., 2017). Subsequently, mesh refinement was performed and CAD models were further converted to slices, which was fed into numerical control (NC) coding for bioprinting (Arai et al., 2011; Lee and Yeong, 2016).

2.5. Blueprint modeling

For most bioprinters, it is essential that the CAD model of defect site is converted to a STL format (see Fig. 3E), or a 3D graphics or virtual reality modeling language (VRML) (Coakley et al., 2014; Ozbolat and Gudapati, 2016). After the conversion, they can be further analyzed with FEA software to rapidly evaluate properties of bioprinted constructs *in silico* before performing the physical bioprinting. To generate models for bioprinting, different CAD systems have been developed, including constructive solid geometry (CSG), spatial occupancy enumeration and boundary-representation methods (B-rep) (Requicha, 1980). Amongst these methods, CSG and SOE utilize the joining of primitives and cubic unit cells to build a large model, which is computationally expensive. Sun *et al.* has reported an example of combining unit primitives to build spine models using Boolean operations (Sun et al., 2004). On the other hand, B-rep uses the boundary elements (e.g. edges and vertices) to define closed objects. Alternately, models can be built by algorithm which can identify negative geometry in CT-scanned models by image segmentation, and subsequently subtract the negative geometry to create the porous internal architectures. Moreover, an extension of B-rep methods using iso-geometric analysis (IGA) with volumetric representation (V-rep) involving trimmed B-spline trivariates are also developed, which may have applications in more precise defining of interior architecture of heterogenous scaffolds (Massarwi and Elber, 2016). However, the efficiency of CAD-based systems is inadequate for rapid model generation.

In a different approach, 3D images extracted from CT scan can be used to directly define the external contours of tissue constructs, which can be filled by unit cells to generate the bioprinting file rapidly. Moreover, the limitation of CSG, which is that the porosity of the generated construct is identical, can be overcome by using a freeform systems approach, in which the whole structure can be partitioned into different sub-regions and each one is further assigned different porosity and material properties. An example of using this method has been already reported for a wound device design. In this method, a 3D image was extrapolated from a 2D scan and processed in ImageJ software (Ozbolat and Koc, 2012). Further, the image was rationally partitioned into non-uniform B-spline surfaces, which were then filled with different material properties. Printing of bioink with different sodium alginate concentrations was then performed for each surface. 3D models of different organs have been shown using this method. Another major limitation of most CAD based designs is the inability to model irregular and complex geometrical patterns. This can be addressed by the use of implicit functions with periodic minimal surfaces, which can divide the geometrical space into periodic interconnected domains. Using minimal surfaces, design of scaffolds with gyroid and diamond structures as well as structures with heterogeneous porosity have been illustrated (Afshar et al., 2016; Elomaa et al., 2011; Melchels et al., 2009). Another important limitation of the traditional CAD design is their incompatibility with most common extrusion-based bioprinters. It can be stated that

most of the abovementioned approaches are more suitable for LBB or DBB. The extrusion-based bioprinters rely on deposition in a 0/90° raster pattern. To address this challenge, toolpaths using space filling curves can be employed, which with lay-down angles of 0/45/90/135° have been reported (Ozbolat and Gudapati, 2016). In this respect, Hilbert curves, a continuous fractal plane-filling function that allows for precise mapping from 1D to 2D space to fill a square, are also very useful (Ćwikła et al., 2017; Li et al., 2010). One important requirement for development of bioprinting is to make open source software available, which allows end users to generate their own toolpath using G-codes (Hinton and Feinberg, 2016; Lee et al., 2017a, 2017b).

2.6. Process modeling for biomimicry

In the realm of bioprinting for tissue engineering, biomimicry can be one of the most effective tools to optimize process parameters for enhanced cell growth and differentiation. In natural tissues, cells with the ECM are in dynamic interaction with each other, which impacts cell fate at various levels (Daley and Yamada, 2013; Goody and Henry, 2010). In certain tissues, one primary cell type interacts with another cell type, which influences the overall tissue functionality (Nagahara and Matsuda, 1996; Pirraco et al., 2010). The ECM forms the essential cell microenvironment and hence, it is necessary that all design should consider adequately the incorporation of proper ECM into the scaffolds (see Fig. 3F) (Cheng et al., 2006). For example, many tissues require a porosity gradient or a spatiotemporal gradient of certain matrix proteins, which exerts important influence on cell behavior (Smadbeck and Stumpf, 2016). Apart from the chemical and architectural factors, biophysical attributes of microenvironment (e.g. matrix stiffness) also impact on cell behavior (Cavo et al., 2016).

In the literature, several studies have attempted to perform processing modeling for biomimicry. Fuzzy modeling approach is described as one of the powerful mathematical tools for biomimicry (Margaliot, 2008). In general, modeling tissue growth can be performed by adopting a continuum viscoelastic tissue approach or discrete cell-based approach. Although the former considers tissue as a deformable substance conforming to principles of continuum mechanics, which is capable of generating small system using coupled partial differential equations with a few non-linear parameters, it is insensitive to identify the morphology and properties at the cellular level. On the other hand, discrete cell-based models allow for analysis of cellular-level features but contain more free parameters (Kim and Sun, 2009; Lyu et al., 2016; Murray et al., 2011). In a comparative study, Gardiner *et al.* modeled cell behavior by considering various cell components including membrane, nucleus, cytoskeleton and ECM as groups of particles. Thereafter, particle-particle interaction laws were employed to understand phenomena such as cadherin mediated cell-cell adhesion and integrin-mediated cell-substrate adhesion. The advantage of discrete modeling was clearly evidenced by the results of simulation study (Gardiner et al., 2015). Further, it is important that tissue growth models are adequately testified by experimental data. The experimental results of developmental biology and tissue self-assembly are often important data source for such modeling. Discrete cell-based modeling has demonstrated the effect of cell seeding on cell growth and dynamics for tissue engineering, which can become an important source for bioprinting modeling (Cheng et al., 2009). Recently, Cao *et al.* have developed a multi-scale model showing the relationship between matrix stiffness and cell adhesion, which can be further extended for design of bioprinting tissue constructs (Cao et al., 2017). In addition, the agent-based models involved biomaterial degradation kinetics and vascularization, and could substantially aid in the process modeling (Mehdizadeh et al., 2015).

2.7. Advanced path planning for bioprinting

Path planning for bioprinting is sufficient for converting a digital CAD model into a physical tissue construct with desired accuracy. For bioprinting, there are two methods for generating path plan, namely Cartesian and parametric forms. In Cartesian form, path planning has been implemented for almost all types of bioprinting modalities. For example, studies on EBB have shown that 0/90° lay-down pattern generated constructs with high mechanical integrity compared to 0/45° and 0/135° patterns (Jin et al., 2015). However, the distortion of structure is mostly observed at the turning points, where the bioprinting speed decelerates or accelerates. This limitation might be addressed by a tangential continuity of the substrate. At the turning points, it also becomes difficult to incorporate functional gradients as bioink deposition does not follow the designed amount due to the speed variation of the substrate deposition. These limitations can be overcome to a certain extent by providing smaller raster sizes as input. Moreover, Cartesian path plan is also not suitable for hollow construct bioprinting. In the parametric form, path planning is performed using parametric coordinates for complex heterogeneous geometries. A method has been demonstrated by Ozbolat and co-worker in which CAD file was sliced into different layers, and each layer was assigned a spline curve (Ozbolat and Khoda, 2014). The path plan was generated for two consecutive layers, wherein the first layer was printed based on the parametric line, whereas the spiral toolpath was fed for the next layer (see Fig. 3G). This toolpath algorithm allowed tangential continuity, and enabled better printing for heterogeneous bioink compositions. Wang *et al.* has also shown a parametric path planning algorithm including mesh parameterization, distance transform, contouring and smooth interpolation steps (Wang et al., 2015b). In the future, it is expected that path planning algorithms could be tailored according to the material properties of different bioink solutions (Wojcik et al., 2015). One of the interesting works has demonstrated the use of predictive algorithms to generate the path plan that compensates for shape distortions due to differences in buoyancy of bioinks (Christensen et al., 2017). Such predictive compensatory algorithms are required not only for 2-dimensional (2D) but also for 3D during bioprinting.

3. Bioprinting Stage

The physical bioprinting stage is predominantly composed of three phases including bioink, bioprinter and bioprinting process. Several parameters require strict optimization to obtain successful fabrication of tissue constructs, which may include physicochemical properties (rheological properties, gelation kinetics, etc.), biological properties (cell density, viability, and biocompatibility) and process parameters (bioprinting time, presence of radiation, etc.). The different quantitative aspects of the bioinks under the three different major bioprinting modalities are summarized in Table 1 and discussed below.

3.1. Bioink phase

Bioink is the bioprintable material consisting of various biologics including cells, media, serum, genes, proteins, etc. (see Fig. 4A). Bioinks can be composed of cells with biomaterials like hydrogel or only cell aggregates and spheroids (in scaffold-free bioprinting) (Akkouch et al., 2015). The ideal bioink formulation is an optimization of material properties (printability and degradation) and biocompatibility. Printability is influenced by rheological properties of bioinks including the viscosity, gelation kinetics, shear thinning properties, yield stress and shear recovery (see Fig. 4B). Such properties are directly associated with print fidelity and mechanical strength. However, improvement in one such property often comes at the cost of other, thus making bioink formulation design and selection an extremely vital process in bioprinting workflow as detailed in the following subsections. Embedding cells in a bioink poses several challenges. To start with, in order to obtain effective bioprintability with hydrogel-based bioinks, concentrations of each ingredient must be precisely optimized (Jia et al., 2014). An ideal bioink should not require any pre- or post-printing

Table 1
Quantitative comparison of bioink properties under different bioprinting modalities.

Parameters	Extrusion-based bioprinting (EBB)	Laser-based bioprinting (LBB)	Droplet-based bioprinting (DBB)	Reference
Rheological properties viscosity	$3–6 \times 10^7$ mPa·s	1 to 300 mPa·s	< 10 mPa·s	Peltola et al., 2008; Guillemot et al., 2010; Guillotin et al., 2010; Kim et al., 2010; Xu et al., 2005)
Cell density	Very high cell density such as cell aggregates	Medium cell density ($\sim 10^8$ cells/ml)	Lower cellular density (< 16×10^6 cells/ml)	Peltola et al., 2008; Guillemot et al., 2010; Guillotin et al., 2010; Axpe and Oyen, 2016
Gelation speed	Fast gelation (i.e., ionic cross-linker)	Slow gelation	Medium gelation speed	Axpe and Oyen, 2016
Definition of Bioprintability	Extrudability or the formation of continuous filaments	Formation of jets on the substrate	Formation of well-defined dotted patterns	
Surface tension	+	+ +	+ + +	
Factors affecting cell viability	Dispensing pressure, nozzle size, bioink viscosity, cell density	Laser radiation, bioink viscosity	Dispensing pressure, droplet generation mechanism, bioink viscosity, cell density	Nair et al., 2009; Blaeser et al., 2016; Ouyang et al., 2016
Cell viability	+	+ + +	+ +	
Mechanical strength	+ + +	+	+ +	Murphy et al., 2012; Seidlits et al., 2010
Resolution	+	+ +	+ + +	Suntornnond et al., 2016); Murphy and Atala, 2014; Bakhshinejad and D'souza, 2015; Jose et al., 2016
Application	Tissue engineering and regenerative medicine, disease modeling and research	Tissue models for toxicity testing, tissue engineering	Stem cell research, high-throughput screening, drug testing, tissue engineering	

processes such as chemical-, physical-, or photo-crosslinking to make bioinks cell-friendly, homogenously mixed within other components and reduce cell encapsulation time (Nicodemus and Bryant, 2008). One of the major limitations in cell-laden bioink is that cells are required to be suspended in an aqueous precursor solution, along with other water-only soluble constituents (Nicodemus and Bryant, 2008). Further, volume of suspension can affect stability and strength of the hydrogel-based bioink by changing the final concentrations of cells and hydrogels in bioink (Ji and Guvendiren, 2017). In addition, it can delay crosslinking time for the bioink and affect other major properties such as swelling, mechanical and gelation time (Derakhshanfar et al., 2018).

In addition, cells can be bioprinted without encapsulating in any other support hydrogel or media requirement on substrate surfaces. This technique is known as scaffold-free cell bioprinting such as bioprinting spheroids or tissue strands as demonstrated by Yu et al (Yu et al., 2016). In such cases, if adequate liquid precursor is not available, cells delivered with scaffold-free bioprinting technique or within the bioink solution will not have enough oxygen and nutrients to sustain viability during the bioprinting process and undergo necrosis due to hypoxia and starvation. In order to avoid starvation, researchers have prepared bioink solutions using ingredients within the culture media. Another approach was to combine bioink with microspheres filled with oxygen to allow oxygen to permeate through the pores into microenvironment avoiding hypoxia and thus maintaining high cell viability during the bioprinting process (Lee et al., 2015).

Mixing cells uniformly within bioink solutions is another common issue especially when hydrogels are also a constituent, and affects the subsequent bioink extrusion in a homogenous manner. If the bioink solution has substantial chain entanglements, it is difficult to break down the structure and suspend cells homogenously within the bioink. In many cases, even after breaking down the entanglements, cells do not attach on the surface of crosslinked network and are likely to accumulate in certain regions due to phase compartmentalization of polymers. Thus, mechanical mixing systems have been used to homogenously suspend cells in fibrous hydrogels such as collagen, methylcellulose, and fibrin (Möller et al., 2017; Seidel et al., 2017). Encapsulating cells uniformly in hydrogels should be carefully carried out in order to minimize any possible bubble formation within the solution, which otherwise may influence the bioprintability. Depending on ingredients of the bioink, cells can be suspended either initially or after the addition of all other ingredients of the bioink to avoid non-homogenous suspension. However, cell encapsulation within hydrogels is not always desirable depending on the stability of the bioprinted constructs as well as pH, toxicity of the bioink reagents (Rutz et al., 2017). Depending on ingredients of the bioink, cells can be suspended either initially or after addition of all other ingredients of the bioink to avoid non-homogenous suspension. However, cell encapsulation within hydrogel-based bioink is not always desirable always depending on the stability of the bioprinted constructs as well as pH, toxicity of the bioink reagents (Nicodemus and Bryant, 2008), biocompatibility of hydrogels and/or their degradation products. For example, Pluronic F127 is a thermo-reversible material, which behaves like a gel at 37 °C (Newby et al., 2009) but dissolves rapidly in aqueous media affecting the stability of bioprinted constructs (Matthew et al., 2002). At the same time, high concentration of Pluronic could be detrimental for cells (Khattak et al., 2005). Thus in such cases, seeding cell on bioprinted constructs is much more desirable instead of encapsulating cells within bioink.

3.1.1. Cell density

In a bioprinting process, the bioink principally comprises of target/progenitor cells of target tissue and/or hydrogel biomaterial. Unlike traditional scaffold fabrication techniques, bioprinting skips the cell-seeding process, as the cells are dispersed into desired locations inside constructs during the fabrication process itself. In order to construct the desired tissue, it is essential to understand the relation among various parameters including bioink types, the required cell density, and the

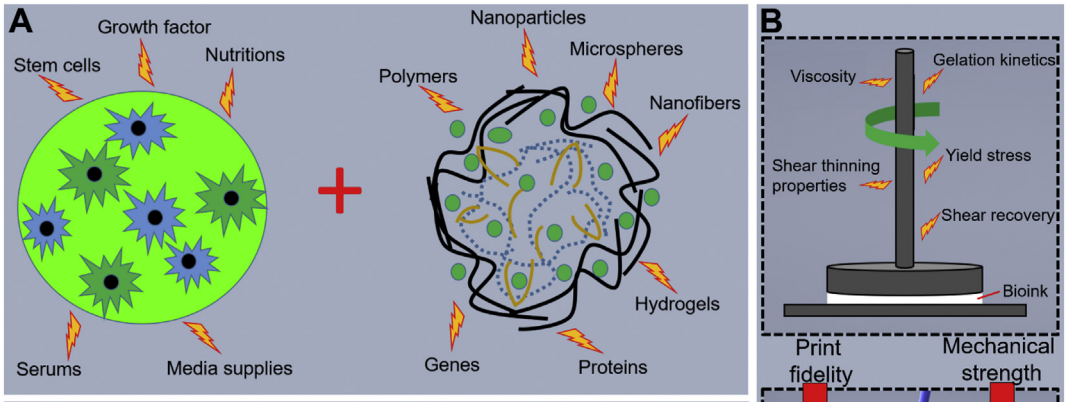

C

	EBB	DBB	LBB
Resolution	Medium-low	Medium	High
Accuracy	Medium-low	Medium	High
Mechanical/structural integrity	High	Low	Low
Cell viability	Medium-high	High	Medium
Hydrogel viscosity	High	Low	Medium
Gelation speed	Medium	High	High

Fig. 4. A) Essential components of bioink; B) Rheological properties affecting print fidelity and mechanical strength; C) Comparison of bioink-induced properties among different bioprinting techniques (further details are presented in Table 1).

crosslinking mechanism (Hölzl et al., 2016). Bioprinting can also be performed using scaffold-free bioinks, wherein cells at much higher densities can be bioprinted without the use of exogenous biomaterials. Scaffold-free bioprinting additionally avoids the biocompatibility-related limitations of common scaffold biomaterials. Though tissue development can be faster compared to scaffold-based approaches, mechanical strengths of the constructs may be compromised in the scaffold-free approach (Leberfinger et al., 2017). Initially, it was expected that high cell density may lead to faster tissue formation. Several reports are available regarding the selection of optimum cell density for 3D printing process. The selection of cell density will also depend upon target tissue to be bioprinted e.g. values of about in articular cartilage 10 cells per unit area (0-22 mm^2), in costal cartilage and 7 cells per unit area and trabecular osteons at 2×10^6 per m^2 in healthy human adults are found (Clarke, 2008; Stockwell, 1967). Details about the total number of cells in different tissues can be found in (Bianconi et al., 2013).

Shear stress during bioprinting has a negative influence on cellular viability and damage to cell membrane (Hölzl et al., 2016) (Ouyang et al., 2016), and hence it is desirable to select low viscous (< 10 mPa·s) bioink with low initial cell density (< 10^6 cells/ml) (Kim et al., 2010; Xu et al., 2005). In LBB (i.e. laser induced forward transfer (LIFT)), the viscosity range of a bioink should be selected between 1 to 300 mPa·s, and medium cell density (~10^8 cells/ml) is suitable for the process (Guillemot et al., 2010; Guillotin et al., 2010). EBB is extensively used for construction of cell-laden tissue constructs (Chung et al., 2013). Such system is able to print viscous bioinks (3–6 × 10^7 mPa·s) with a very high cell density without affecting cellular viability (Peltola et al., 2008). In contrast, inkjet bioprinting employs less viscous bioinks (< 10 mPa·s) with lower cellular density (< 16 × 10^6 cells/ml) (Axpe and Oyen, 2016). The MEMS-based printer head of inkjet bioprinter cannot squeeze viscous bioinks, as relatively small deformation take place by the thermal/piezoelectric actuation at the nozzle opening. Generally, higher cell densities increase the average viscosity of the bioink resulting in clogging of the printer head (Gillette et al., 2010; Mandrycky et al., 2016; Pepper et al., 2012). Billiet *et al.* have compared the printability of methacrylamide-modified gelatin (Gel-MOD) both in the presence and absence of hepatocytes (Billiet et al., 2014). Results demonstrated that above gelation temperature, the viscosity of bioink was reduced to half for cell density up to 1.5 × 10^6 cells/ml. With the increased cell density (2.5 × 10^6 cells/ml), further reduction was obtained. Skardal *et al.* reported that density of human intestinal epithelial cells above certain threshold (> 25 × 10^6 cells/ml) interfere with the hyaluronan-based hydrogel formation (Skardal et al., 2010b). Fig. 4C presents the comparison of bioink-induced properties, including cell density, among different bioprinting techniques.

The relationship between cell density and mechanical properties of the hydrogels was also studied by Mauck et al. (2003), in which chondrocytes were cultured on agarose hydrogels over a period of two months in free-swelling and dynamic loading conditions. Initially, constructs containing low cell concentration (10 × 10^6 cells/ml) were stiffer in comparison to that with high cell concentration (60 × 10^6 cells/ml). As the culture time increased, the constructs with higher cell density exhibited similar Young's modulus to constructs prepared with lower cell density. For example, the initial cell density of 20 × 10^6 cells/ml is preferable for cartilage tissue engineering, and cell density below this concentration may reduce cartilage formation (Möller et al., 2017). Chang and coworkers have demonstrated the effect of different cell densities on remodeling of hydrogels depending on external loading conditions (Chang et al., 2001). Based on such studies, numerous models have been developed to understand the effect of cell density on the properties of bioprinted constructs (Eshraghi and Das, 2012).

3.1.2. Cytotoxicity of bioink components

While an ideal bioink must meet the requirement of printing process, its cytocompatibility is another crucial criteria for successful bioprinting (Levato et al., 2014; Skardal et al., 2015). As a bioink, hydrogels are preferred due to their higher water content and low cytotoxicity (Van Hoorick et al., 2015; Van Vlierberghe et al., 2008). An overview on cytocompatibility of various hydrogels fabricated through different techniques is available (Malda et al., 2013). A study showed that 3D printing with methacrylamide-modified gelatin hydrogels

resulted in > 97% cellular survival. Hsieh *et al.* reported excellent compatibility and proliferation of neural stem cells embedded on 20–30% polyurethane hydrogels (Hsieh et al., 2015). A composite bioink of nano-fibrillated cellulose and alginate was tested by Markstedt *et al.*, and constructs exhibited 86% viability of chondrocytes several days after printing (Markstedt et al., 2015). Construct bioprinted using silk fibroin-gelatin bioink showed multilineage differentiation of encapsulated stem cells for targeted tissue formation (Das et al., 2015). To enhance the cytocompatibility, researchers have also tried to prepare a bioink from biological samples. For example, decellularized liver matrix (dLM)-based bioink was prepared (containing the intrinsic proteins of dLM), which improved the compatibility of encapsulated cells (Khati, 2016). Similarly, to improve cell-adhesiveness of alginate bioinks, enzymatic crosslinking schemes exploiting phenolic hydroxyl moieties and horseradish peroxidase have been attempted (Arai et al., 2016).

Amongst various bioprinting techniques, printing of live cells with DBB is relatively challenging as the increased viscosity of bioink and higher cell density requires excessive forces to eject the droplets, which can cause damage to cells (Kim et al., 2010). Another limitation is the aggregation of cell suspension within the reservoir that causes clogging within narrow tubing of droplet-based bioprinters, which also increases the mechanical stress, and hence affects the cellular viability. Non-uniform droplet formation may also take place. Bioink additives may overcome this problem; however, surfactant materials affect the cellular membrane integrity (Ahmed et al., 2008; Xu et al., 2013a, 2013b). The cytotoxic effect of various nanocellulose bioink was studied against different cell lines (Alexandrescu et al., 2013; Vartiainen et al., 2011). Due to the absence of toxic effect, nanocellulose bioink is considered as suitable wound dressing material. Although the compatibility of natural materials (i.e., alginate, silk, fibrin and collagen) are preferable, due to their weak structure and fast degradability in physiological condition, crosslinking is necessary to improve the mechanical strength. However, crosslinking agents may decrease the material homogeneity, cellular compatibility and enhance the complexity of bioprinting (Rodriguez et al., 2017).

3.1.3. Bioprintability

The printability of a bioink depends on certain factors. First, the bioink should be in liquid form without clogging the printer nozzle before/after printing. Secondly, the applicability of the bioink is determined by the 'biofabrication window' (He et al., 2016). The term has been recently proposed to define the compromises necessary to obtain bioinks with adequate print fidelity and cell viability (Chimene et al., 2016). Though depending upon the bioprinting modality, printability have different definitions. For example, printability of EBB refers to the extrudability or the formation of continuous filaments followed by formation of the integrated 3D structure. In DBB and LBB, printability is used to characterize formation of well-defined dotted patterns and jets on the substrate, respectively. This property of the bioink determines its printability, cell viability, structural resolution, etc. For printability, several parameters such as rheological properties, gelation kinetics, and surface tension of the bioink are necessary to be characterized. Moreover, the viscosity of bioink should be tunable with temperature for certain biomaterials while shear thinning is necessary for EBB. Colosi *et al.* printed low viscous bioink of alginate and gelatin methacroyl (GelMA) blend through a coaxial nozzle (Colosi et al., 2016). Initial concentration of GelMA was kept low, which up-regulated cellular viability; however, it was not printable. Blending with alginate produced mechanically-stable crosslinked fibers (Zhang et al., 2015). The coaxial system is able to tune the gelation kinetics of bioink by modulating the ink composition. Two-step polymerization system was used by Skardal *et al.* for printing of bioink comprising methacrylated ethanolamide derivative of gelatin and methacrylated hyaluronic acid with high viscosity (Skardal et al., 2010a). The construct was completely photopolymerized to obtain the final constructs. In addition, there is a relation between the concentration of cells and the printability of bioink. Higher cellular load increases the viscosity of bioink which may affect its printability. Hence, selection of optimum cell concentration is also important for successful bioprinting (Hölzl et al., 2016).

Other process parameters have also great influence on the fate of bioprinting, such as the fusion of hydrogels, deformation due to gravity, non-uniform droplet size and non-uniform extrusion due to alteration in printing speed. The density of the crosslinker also influences the printing fidelity. In general, high crosslinker concentration limits the cellular migration but possess better printability, whereas low crosslinker concentration reduces the bioprintability (He et al., 2016). For most optimization studies, a "biofabrication window" thus becomes a useful tool to quantify the suitability for fabrication.

Apart from viscosity, other relevant rheological parameters are the shear thinning properties, gelation kinetics and yield stress of the bioink. Shear thinning defines the shear-rate dependent viscosity of bioink, which essentially behaves as a non-Newtonian fluid. Shear induces a reorganization of macromolecules to a less entangled configuration decreasing the viscosity. The viscosity of the most commonly used bioink, sodium alginate is several times lesser at shear rates of 100–500 s^{-1} (most commonly encountered for bioprinting), compared to plateau region at lower values of shear suggesting strong shear thinning behavior, which are more prominent at higher concentrations. Shear thinning is desirable for bioprinting as it enables smooth flow avoiding clogging during extrusion but regaining of the viscosity after bioprinting contributing to improved bioprinting fidelities (Malda et al., 2013; Rezende et al., 2009). Thus along with shear-thinning, shear-recovery is also an essential rheological property in order to attain a better construct resolution (Kesti et al., 2016). During bioprinting, another rheological property of importance is the yield stress, which is the initial minimum stress that is required to be supplied to initiate flow. Yield stress can potentially improve the bioprinting fidelity and reduce cell sedimentation. An example of yield stress effect on bioprinting is demonstrated by addition of the gellan gum to gelMA hydrogels (Malda et al., 2013). Likewise, shear elastic modulus determines deformations and ease of printing hydrogel due to shear forces exerted during extrusion. The evolution of gel parameters is also important as the gelation kinetics will determine the crosslinking time. The major mechanisms of hydrogel gelation are physical (i.e. ionic), chemical or covalent and enzymatic crosslinking. Physical gelation is achieved at bioprinting duration and provides ignorable viscosity fluctuations during bioprinting but result in formation of relatively weaker constructs and crosslinking can be reversible. Chemical crosslinking requires appreciable gelation times, which are impediment to fabrication of multilayered constructs. Also, the toxic crosslinkers must be removed completely before implantation (Chimene et al., 2016; Guvendiren et al., 2016; Hospodiuk et al., 2017; Kirchmajer et al., 2015). Crosslinking under light irradiation is another option for instantaneous crosslinking, but the effect of light wavelengths and duration of exposure on cells must be considered (Wang et al., 2016). On the other hand, enzymatic crosslinking offers a more biologically acceptable process, but it increases the cost and decreases practicality of the process. Ionic crosslinking is also achieved at rapid rates and can be carried out at physiologically-amenable conditions. For example, alginate forms an ionotropic bond with calcium ions, while chitosan with phosphate ions. However, ionic crosslinking is prone to undergo rapid dissociation in physiological fluids. Ideally, solidification should occur at fast enough rate so that bottom layers acquire sufficient mechanical characteristics to withstand loads of subsequent layer. In addition, faster solidification prevents flowability of bioink after bioprinting and improves the structure fidelity.

Another parameter of importance, especially for DBB is the surface tension of bioink to determine high fidelity bioprinting. Surface tension is determined by the net balance of cohesive forces amongst all components of the bioink and influence if either a jet or droplet would be

formed after ejection. Since cells tend to adsorb at the air-water interface, surface tension of a bioink is reduced as cell density increases. Surface tension influences printing resolution, quality, fidelity and dimensions of printed lines and proper matching of the surface tension can be engineered by contact angle measurements. In fact, it has been proposed that hydrogels could be printed with smaller dimensions such that the desired dimensions are achieved after swelling post-bioprinting (Kyle et al., 2017). The physicochemical properties of a bioink including rheological behaviour, surface tension, gelation kinetics, and swelling property are not only important for its printability but also for maintenance of its post-printing integrity (Hölzl et al., 2016). Tuning of these parameters is important for the reproducibility and fidelity of bioprinted constructs. Incorporation of physical/chemical cues can improve the printability of polymers. In EBB, it has been observed that incorporation of cues (e.g. metal ions and gluteraldehyde) can improve bioprintability (Ozbolat and Hospodiuk, 2016). For example, Na^+ was incorporated in gelatin by replacing Ca^{2+} and Fe^{2+} present in gelatin. This significantly altered the molecular interactions and improved the crosslinking density and mechanical strength of gelatin gels (Xing et al., 2014).

3.1.4. Cell viability and long-term cell functionality as a function of bioprinting parameters

Bioprinting enables spatial manipulation of cells, where the viability of cells during pre- and post-bioprinting is crucial. Researchers have been exploring different combinations of biomaterials and cell types in order to understand cell-biomaterial interactions. However, of the optimal process parameters for certain cell type may not be suitable for another. Nair *et al.* have studied cell viability during EBB, and their study indicated that dispensing pressure affected the cell viability (Nair et al., 2009). In another study, it was observed that nozzle insulation improved the viability of HEK 293FT cells when printed with a gelatin-based bioink (Ouyang et al., 2015). Zhao *et al.* reported that bioink viscoelasticity was the key parameter for cellular viability and printability of polymers (Zhao et al., 2015). In microvalve-based DBB process, it has been observed that shear stress is the key factor to balance the printing resolution and cellular integrity (Blaeser et al., 2016). Previous study achieved approximately 90% viability of fibroblasts by controlling the shear stress within 5 kPa (Ouyang et al., 2016). DBB is suitable for handling with higher cellular densities. A study has reported that cellular homogeneity and viability could be enhanced by changing bioprinting parameters of polyvinyl pyrrolidone (PVP)-based bioink (Ng et al., 2017b). The effect of photo-crosslinking on cellular activity has been tested by Duan et al. (2014). In a study, methacrylated hyaluronic acid (MA-HA) and GelMA were crosslinked with UV for fabrication of valvular interstitial cell laden constructs. Approximately 92% of cellular viability was observed up to seven days after printing, which concluded that there was no noticeable toxic effect of photo-crosslinking on the encapsulated cells. They also optimized the compressive modulus of the bioink at about 13 kPa to obtain optimum polymer viscosity and effective photo-crosslinking. Printing of thermo-responsive polymers (i.e. poly (N-isopropylacrylamide)-grafted hyaluronan (HA-pNIPAAM) and MA-HA) has been investigated by Kesti et al. (2015), who produced printable constructs with high resolution and cell viability. However, in another study on thermo-responsive hydrogel bioprinting, the blend of PU/PCL was bioprinted through a two-step chemical reaction, and a low cell viability of mesenchymal stem cells (~ 40%) was observed a day after bioprinting (Tsai et al., 2015; Zhang et al., 2016a, 2016b). The effect of photo-initiators on cellular viability has been also intensively studied, and ~98% viability of hepatocarcinoma cells was observed using the VA-086 photo-initiator (Billiet et al., 2014). It has been reported that during temperature-based crosslinking process, the viability of cells is remarkably compromised, since cells can only survive in a narrow temperature range (Bianco and Robey, 2001). Gelation time is another factor; the longer gelation period generally reduces the cellular viability. Viscosity of hydrogel is often modulated for increasing the printability of bioink and resolution of tissue constructs. Such alteration induces stress on cell population, and hence reduces the viability of cells (Chang et al., 2008). Despite the capacity of bioprinter to deposit cells at high rates, the bioink composition (especially cell-laden bioink) also determines the practical speeds that can be attained, since cell viability and cell division post-bioprinting would be reduced, resulting from the high stress induced by higher extrusion speeds. Additionally, long standing time inside a reservoir due to slow printing rate can reduce the cell viability.

3.1.5. Solidification

Most of the available natural and synthetic bioinks are solidified through physical, chemical or enzymatic crosslinking methods. For example, alginate is ionotrophically crosslinked through calcium chloride ($CaCl_2$) or calcium sulphate ($CaSO_4$) solutions. Solidification of polymer occurs through transition of polymer solution to gel at a transition temperature. Hot solution (40-80 °C) of polymers such as agarose, gelatin, and methycellulose, are transformed into gel when printed on a cooled stage (Landers et al., 2002a, 2002b). Hydrogels prepared through physical crosslinking is mechanically weak, and reinforcement of other materials is required to enhance the stability. Photocurable hydrogels can be printed on illuminated stage through the incorporation of an appropriate photo-initiator (Skardal et al., 2010a). 3D printing of photocurable bioink with and without cell population was reported in several studies (Billiet et al., 2014; Dhariwala et al., 2004; Di Biase et al., 2011). Printing of photo-curable polymers has several advantages, one of which is that the printing process is very rapid, and has less detrimental effect on cells (Nguyen and West, 2002). Moreover, no additional crosslinking bath is required, and the degree of crosslinking can be easily adjusted by changing the intensity of light. Gelation of the extruded ionotropic polymers also occurs in a reactive substance bath (Khalil et al., 2005; Landers et al., 2002b). The advantage of reactive printing is the rapid solidification of polymers. Since gelation can occur at physiological temperature (i.e., 37 °C), the impact on cell population is minimal. Printing of gellan gum solutions by this method along with the cell culture media has also been reported (Ferris et al., 2013).

Material dispensing rate is impacted by the initial viscosity of bioink and the crosslinker density. Generally, bioinks with higher viscosity can be bioprinted in a faster rate requiring less amount of crosslinker, and bioprinted constructs are more stable under physiological conditions. In EBB, the extrusion force is exerted pneumatically or mechanically enabling bioprinting of highly viscous bioinks in comparison to DBB methods. Slower gelation kinetics can cause cell death and typically, the gelation time for alginate, and PEG-DA are shorter compared to that for collagen, and chitosan (Jana and Lerman, 2015). A highly viscous solution requires less time of crosslinking and hence, can be deposited at faster rates. Similarly, high crosslinker density can create fast solidification, and hence faster dispensing rate can be used. However, the toxicity of crosslinker with high concentration should be considered. In addition, EBB requires a fast gelation process for a desired fidelity, which can be adequately obtained by ionic crosslinking (Axpe and Oyen, 2016). Bioprinting with supporting nanoclays is able to minimize the impact of gelation speed on print fidelity (Jin et al., 2017). Another challenge in bioprinting is the selection of appropriate crosslinking density for achieving the structural integrity of construct without inducing any cytotoxic response (Jose et al., 2016). For optimum solidification, optimization of cellular density is also important since high cell concentration might interfere with the crosslinking mechanism of hydrogels occasionally (Skardal et al., 2010b).

3.1.6. Mechanical and chemical properties

For fabrication of stable and transplantable 3D bioprinted constructs, rheological properties of a bioink is necessary to be investigated to obtain sufficient printing accuracy and also provide an optimal environment for cellular migration and spreading (Khademhosseini et al.,

2006). In bioprinting, bioinks that are able to immediately solidify or regain structural integrity after extrusion, are desired (Murphy et al., 2012; Shim et al., 2011). Mechanical properties of constructs can be further improved through photo-crosslinking using a photo-sensitive bioink as a precursor material. The mechanical stability of physically-crosslinked constructs is relatively poor compared to that of chemically- or photo-crosslinked constructs (Salacinski et al., 2002). To improve the mechanical stability, some chemical functional groups can be incorporated, which form an irreversible crosslinked network through covalent crosslinking (Frantz et al., 2010; Geckil et al., 2010). Mechanical properties of the constructs can be further improved by using nanoparticle/hydrogel composites such as Laponite®/alginate and nanosilicate/collagen as evidenced from several studies (Ghadiri et al., 2013; Xavier et al., 2015).

Combination of physical and chemical crosslinking methods have also been employed for improving the stability (Geckil et al., 2010; Traver and Assimos, 2006). Physical crosslinking process is preferable during bioprinting, whereas chemical process is usually followed to enhance the stability of post-crosslinked products (Khademhosseini et al., 2006; Salacinski et al., 2002). Billiet *et al.* used photo-induced crosslinking after bioprinting of methacrylamide modified gelatin bioink (Billiet et al., 2014). Along with mechanical properties of a bioink, the cellular compatibility is also a matter of concern. Mauck *et al.* have tested the impact of density of encapsulated chondrocytes on mechanical properties of the resultant agarose hydrogel (Mauck et al., 2003). It is challenging to maintain the structural integrity of the construct during cell growth. Along with a physical support, maintaining the mechanical strength, which is alike *in vivo* conditions is also necessary for cellular proliferation and differentiation (Murphy et al., 2012; Seidlits et al., 2010). A recent study by Hölzl *et al.* showed a decrease in stiffness of hydrogels by 13% with the increase in cell density from 12 to 15 million cells/ml (Hölzl et al., 2016). Elsewhere, compressive modulus of constructs using collagen were at the range of 25kPa while those with alginate hydrogels were found from 15 to 20 kPa (Tabriz et al., 2015; You et al., 2016). The selection of a particular bioprinting modality should be made depending upon the target tissue. The greatest advantage of EBB is its ability for scale-up biofabrication, user friendliness and high mechanical strength of the constructs. Therefore, EBB should be explored for obtaining volumetric organs in clinical tissue engineering. On the other hand, in applications which require high bioprinting resolutions and closer cell-cell or cell-material interactions like tissue models for toxicity testing, DBB may be preferred. At present, LBB instruments are costlier but provide very high cell viability and resolutions and thus for stem cell research generally LBB may be recommended.

Therefore, EBB should be explored for obtaining volumetric organs in clinical tissue engineering. On the other hand, in applications which require high bioprinting resolutions and closer cell-cell or cell-material interactions like tissue models for toxicity testing, DBB may be preferred. At present, LBB instruments are costlier but provide very high cell viability and resolutions and thus for stem cell research generally LBB may be recommended.

3.1.7. Guiding cell growth and differentiation

Stem cells are the attractive cell types for tissue biofabrication due to their ability of multipotent differentiation. The growth and differentiation of stem cells requires a microenvironment with proper physical and chemical cues (Bianco and Robey, 2001). Hence, careful consideration of the bioink is essential for successful differentiation of stem cells (Peerani et al., 2007; Raof et al., 2011). Specific signaling molecules have been immobilized to control stem cell fate in bioprinting of stem cells through DBB. Bone morphogenic protein-2 (BMP-2) was used to control the differentiation of muscle-derived stem cells (MDSCs) blended with fibrin bioink (Phillippi et al., 2008). An *in vitro* study reported that MDSCs differentiated into osteogenic lineage in the presence of BMP-2, whereas whey differentiated into myogenic lineages in the absence of these signaling cues. Miller *et al.* used heparin-binding epidermal growth factor (EGF) as signaling molecules to control the differentiation of MSCs (Miller et al., 2011). In a recent study, growth factors (i.e. Wnt protein) were immobilized on bioactive beads that facilitated the asymmetric division of embryonic stem cell (ESCs) (Habib et al., 2013). After division, the daughter cells proximal to the beads showed more pluripotent characteristic, whereas daughter cells at the distal side showed increased expressions of differentiation markers (Brafman, 2013).

In addition, stem cell fate could be also regulated by signaling molecules (e.g. transforming growth factor- β (TGF-β), fibroblast growth factor (FGF), Wnt signaling proteins, and hedgehog proteins) during post-bioprinting incubation (Chen et al., 2012). Bioprinting of iPSC and ESCs with RGD coupled-alginate hydrogels has been found to differentiate into hepatocyte-like cells (Faulkner-Jones et al., 2015). In that study, the differentiation process was initiated prior to bioprinting, and allowed to continue for 11 days after bioprinting. This experiment indicated that bioprinting did not influence the cellular differentiation process. Hydrogels can instruct stem cell differentiation through mimicking the ECM network, in which they positioned cells in contact with tropic support, signaling cues and topographical information (Jones and Wagers, 2008). An interesting observation has been reported that differentiation of MSCs can be altered in the presence of different crosslinking agents for the same bioink. A study by Das *et al.* reported that crosslinking of bioprinted silk fibroin-gelatin hydrogels with tyrosinase showed the differentiation of MSCs towards chondrocytes (Das et al., 2015), whereas physical crosslinking of the bioinks by sonication tended the differentiation into osteocyte lineage.

3.1.8. Affordability

The affordability of bioinks depends on their raw material. For example, cell-laden bioinks are relatively expensive, since the incorporation of cells needs precise control, sophisticated instrumentation and skilled manpower. Maintenance of cell number in each batch also needs precise control. Moreover, the price of a bioink depends on the cell type, their doubling time, culture media, culture conditions and the rate of ECM deposition. Without considering cell incorporation, most of the printable hydrogels that are available commercially are affordable, except some natural hydrogels, such as collagen, laminin and hyaluronin, due to the complex isolation protocol (Malda and Frondoza, 2006). The abundance of biopolymer also influences the affordability of bio-printed constructs. For example, the synthetic polymers are more readily available, wherein the biomaterials from natural origin have limited resources. In addition, some polymers extracted from natural sources (e.g. alginate and chitosan) are comparatively affordable, due to more standardized convenient extraction procedures and abundance of their sources.

3.2. Bioprinter phase

Bioprinting technology had emerged as a cytoscribing technique by the pioneering work of Klebe in 1988, in which a Hewlett Packard (HP) modified printer was used. The evolution of bioprinters has been reviewed in details elsewhere (Ozbolat et al., 2017). In the last decade, several enterprises have innovated bioprinter products with different capabilities like generating functional perfusable tissues, which are important to be compared for their ability to produce constructs with different characteristics. Persistent efforts in bioprinter technology development are expected to produce hybrid vascularized tissues with the ability to scale up to clinically-relevant sizes and emergence of 4D bioprinting, and hybrid bioprinters. Below subsections discuss the essential requirements of an ideal bioprinter in order to successfully bioprint living tissue and organ constructs for clinical use in the future. The different quantitative aspects of the bioprinters are summarized in Table 2 and discussed below.

Table 2
Quantitative comparison of bioprinter technologies under different bioprinting modalities

Parameters	EBB	LBB	DBB	References
Compactness	+ +	+ + +	+	Ozbolat et al., 2017
Dimensions of the products	+ + +	+	+ +	Ozbolat et al., 2017
Bioprinter Resolution	Resolutions with micrometer ranges (5-15 μm)	Lateral plane resolution from 30 to 100 μm	Single cell resolution (50 μm) high lateral resolutions, their resolution in the z-direction is limited	Ozbolat et al., 2017; Bakhshinejad and D'souza, 2015; Jose et al., 2016
Nozzle size/ejected volumes	In micrometers	Picolitre droplet sizes	Droplet size in 1- 300 nano to picolitres	
Deposition rate	Slowest	Moderate	1–10,000 droplets per second	Murphy and Atala, 2014
Printing speed	10 μm s^{-1} – 700 mm s^{-1}	200–1,600 mm s^{-1}	1–10,000 droplets s^{-1}	Murphy and Atala, 2014; Ozbolat et al., 2017
Multi-material configurations	Multi-arm or multi-head extrusion-based bioprinter	Multi-array laser-based stereolithography	Multi-nozzle droplet	Park et al., 2015; Beke et al., 2012; Zhang et al., 2012
Commercialization	Fastest	Slowest for commercial transformation	Medium	
User friendliness	+ + +	+	+ +	
Price/Affordability	$5k-$250k	> $100k	$10k-$50k	Ozbolat et al., 2017
Versatility	+ + + (Biobot series are one example of versatile bioprinters Fab@Home offers remarkable versatility)	+	+ + (Nordson Pico® series and MD series from Microdrop Technologies, suitable for high-throughput applications, provide significant versatility)	
Bioink	Various different bioink materials with a wide range of viscosities	Only the bioink which can be irradiated by laser or photopolymerization	Bioinks with lower viscosities can be bioprinted as nozzle clogging is frequently observed for high viscosity bioinks	
Bioprinting resolution	100 μm	5 μm	50 μm	Gudapati et al., 2016; Li et al., 2016; Munaz et al., 2016; Ozbolat et al., 2017
Repeatability	+	+ +	+ + +	
External stresses on cells	Mechanical	Optical or thermal	Mechanical, thermal or electrical	Murphy and Atala, 2014
Cell viabilities	40-90%	95%	~85%	Murphy and Atala, 2014

3.2.1. Compactness

For the efficient clinical deployment, it is highly desirable that bioprinters are compact in size such that they can be directly placed inside a laminar flow unit for maintaining sterility, and easily fit inside an operation theatre. Most bioprinters are designed to fabricate tissue constructs in centimeter scale, but the hardware usually takes a large space. Thus, from the beginning of bioprinter development, compactness has been one of the important goals which the manufacturers are striving to achieve. For example, the upgraded version of BioBots bioprinter occupies only 28,317 cm^3 totally, and is easily accommodated inside a laminar-flow hood, while the previous Biobot2 model consumes 64,327 cm^3. Similarly, the inkjet bioprinter Autodrop Compact, which is manufactured by Microdrop Technologies GmbH, has dimensions of 562 × 772 × 550 mm. Similarly, Microfab technologies have Jetlab 4 model with a footprint of 63 × 57 cm. Compactness results in small dimensions of the products that can be printed, so the manufactures also supply models with larger size in most cases. For example, the substrate size for Jetlab 4 is 160 × 120 mm, and the advanced version has a working area of 200 × 200 mm. For example, Autodrop Compact model has a positional accuracy of 25 μm, maximum speed of 75 mm/s and a payload of 5 kg for Y axis compared to 5 μm, 125 mm/s and 10 kg values respectively for the larger model (Ozbolat et al., 2017).

The clinical translation also raises the demand for a compact bioprinter with a high accuracy, deposition velocity and resolution. Towards this end, miniaturized robotic arms with remote and wireless control possibilities (Huda et al., 2016; Jokic et al., 2014; Susilo et al., 2009) and light materials of construction with high specific strengths should be explored. Additionally, the type of tissue to be printed impacts the bioprinter selection. For example, a more compact bioprinter may be ideal for scaffold-free printing, as bioink volume would be small (Ozbolat, 2017). At the same time, scaffold-free bioprinting may also require higher resolutions to control cell-cell distances (Moldovan et al., 2017). To achieve this objective, there is a need for developing robotics at mesoscale-level (1–4 mm) with a number of degrees of freedom, so that even non-planar surface can be used as a substrate (Grames et al., 2016).

3.2.2. Bioprinter Resolution

One of the important considerations for the bioprinter selection is its resolution, which allows the fabrication of constructs with high fidelity. In fact, the resolution of bioprinted constructs is generally inferior to the nominal resolution of the bioprinter used, which is because of the additional factors of bioink stability, solidification and nozzle clogging observed in most bioprinting modalities. However, motion stages with micrometer scale resolution are vital to achieve bioprinted constructs in higher resolutions. In bioprinting, the size of nozzle is another consideration, which also determines the accuracy of final bioprinted constructs (Ozbolat et al., 2017). Droplet-based bioprinters can provide droplet size in 1-300 picolitres with single cell resolution (50 μm), and at the same time deposition rate of 1–10,000 droplets per second can be achieved (Murphy and Atala, 2014). There are many mechanisms on which DBB bioprinters base, and the droplet size has a bearing on the mechanism. With a similar orifice diameter, micro-valve print heads generate droplets of larger diameter (~100 μm) in comparison to thermal or piezoelectric (~50 μm) and acoustic droplet bioprinters (~10 μm). Example of micro-valve bioprinter is Biofactory, which produces droplets in range of 5 to 10 nL corresponding to > 100 μm droplet diameter (Gudapati et al., 2016). On the other hand, electrohydrodynamic jetting bioprinters can achieve resolutions which are not constrained by nozzle diameters, but they are not capable of generating one droplet at a time and thus reduce the precision of the system. Although DBB is capable of providing high lateral resolutions, their resolution in the z-direction is limited.

For extrusion-based bioprinters, positional resolutions with micrometer ranges are common (e.g. Allevi (previously Biobots): 5 μm, Fab@

Home: 15 μm, Inkredible: 10 μm). Recently, Suntornnoud *et al.* have proposed a mathematical method to predict the bioprinter resolution of EBB based on a function of printing velocity, nozzle diameter and applied pressure (Suntornnond et al., 2016). Most laser bioprinters can also achieve very high instrumental resolutions in lateral planes (30–100 μm) depending upon the wavelength of laser. Generally, laser-based direct write methods have higher instrument resolution than LIFT (Bakhshinejad and D'souza, 2015; Jose et al., 2016). Final resolution of LBB constructs is also determined by other factors such as fluence energy, surface properties and air gap (Ozler et al., 2015). Improvement of the resolution of bioprinters is often associated with increased costs and printing times due to deposition of larger bioink loads and more number of dots per square inch specified in the design.

3.2.3. Degree of freedom and motion speed

Earlier bioprinting technologies were mostly developed from commercial paper printers. Groups of Boland and Nakamura initiated studies to transform Epson or HP printers into bioprinters (Nishiyama et al., 2009; Wilson and Boland, 2003). Compared to the paper printers with a single movement direction, bioprinters need additional axes in order to build 3D constructs. Thus, several in-house modifications, such as providing integrated motorized table for a vertical axis movement, have been carried out with limited success. On the other hand, most commercial bioprinters are designed to only operate in 3-axis which is not adequate for intra-operative bioprinting of irregular-shaped defects in clinical settings. To bioprint non-planar surfaces and concavities, more degrees of freedom are required (Gazeau and Zeghloul, 2013; Tan and Yeong, 2014). The BioAssemblyBot with a 6-axis robotic arm, which is based on pneumatic micro-extrusion, is an improvement over the traditional extrusion bioprinters with 3 axes. In particular, the robotic arm is able to adjust the arm spacing (i.e. position level of the interconnected set of links and joints forming the robot manipulator in 2D Cartesian space location with respect to the taught location) to correspond with the porosity of designed constructs, along with additional options such as rotation about z-axis and allowing interchange of the lateral or dual rotation axis.

High printing speed is another important criterion for the bioprinter selection. The average speed of bioprinting in different modalities varies (e.g. LIFT: 200–1,600 mm s^{-1}, acoustic DBB: 1–10,000 droplets s^{-1}, and EBB: 10 μm s^{-1}–700 mm s^{-1} (Murphy and Atala, 2014; Ozbolat et al., 2017)). The process may take several hours to complete, especially for multi-layer constructs. In LBB, speed is limited as a single laser beam is used to irradiate each point of bioprinting. For example, the direct writing methods have high resolution but slow speed ($< 10^2$ drops per second), while forward transfer methods have lower resolutions but can print up to 5×10^3 drops per second (Bakhshinejad and D'souza, 2015). In commercially available extrusion based bioprinters, typical speed is 25 mm/s. The printing speeds are specified by the stepper motor configuration and driver. Recently, the use of multi-array laser-based stereolithography (Beke et al., 2012; Zhang et al., 2012), multi-nozzle droplet (Park et al., 2015) or extrusion-based bioprinters and a multi-arm robotic extrusion-based bioprinter have been proposed to reduce the bioprinting time (Zhang et al., 2012).

Despite the capacity of bioprinter to deposit cells at high rates, the bioink composition especially cell-laden bioinks also determines the practical speeds that can be attained, since cell viability and cell division post-printing would be reduced, resulting from the higher stresses induced by the higher deposition speed. Additionally, long standing time inside a reservoir due to slow printing rate can reduce the cell viability.

3.2.4. Commercialization

There has been great interest in 3D bioprinters and their potential to solve organ transplantation problems; however, commercialization of bioprinters have not kept as similar pace as the interest in exploring new applications of bioprinting. Overall, it can be concluded that extrusion-based bioprinters have achieved a more in-depth investigation compared to laser- or droplet-based bioprinters. Laser bioprinters have been the slowest for commercial transformation, due to their system complexities and tedious operations; though some commercial bioprinters based on stereolithography apparatus are available. In terms of extrusion-based bioprinters, there exists small difference between the working principles, and different manufacturers provide advanced functions such as automatic bioink cartridge filling and software control for robotic movement. Likewise, a wide range of droplet-based printers are available commercially, but most of them are not capable for printing mammalian cells, due to the small nozzle diameters compared to cell diameters (20–25 μm for cells and 150–500 μm for tissue spheroids (Lee and Yeong, 2016; Odde and Renn, 2000; Yu et al., 2014a)). Moreover, there exist many open-source 3D printers, which can be customized into bioprinters for early stage researchers (Xu et al., 2013a, 2013b). For example, a fused-deposition modeling (FDM)-based extruder can be modified into a pneumatically-controlled extrusion-based bioprinter for deposition of Pluronic F-127 hydrogels (Kang et al., 2016).

Some commercial bioprinters are packed and delivered in the form of parts, in which case the end-users are expected to self-assemble. Hence, it may be necessitated for clinical deployment that skilled service engineers from the manufacturers could work together with other clinical personnel. In the future, it would also be expected that well-defined industrial norms for bioprinters are developed, which can be conformed by the manufacturers to widen the acceptability of bioprinters in the medical community. Currently, software for many 3D printers is being standardized with respect to attributes such as error compensation, tolerance, temperature variations, dimensional performance (Galantucci et al., 2015) and they can also be used as platforms for bioprinters. Standardization of software will facilitate the compatibility among different bioprinters, which enables cross communications. Moreover, software should be able to not only communicate with the bioprinting hardware, but also enable the design of constructs. Such improvement will no doubt give a major fillip for fast commercialization of bioprinters, since it would be difficult for the end user to integrate different software from different vendors for certain operation. A bioprinter with wide range of deposition speed, high resolution, multiplicity of dispensation, and compatibility with various types of bioinks will be the ultimate goal for bioprinting instrumentation, so that different users can benefit from the same platform.

3.2.5. Automation

A concern with current bioprinting modalities is the absence of a completely automated workflow (Heller et al., 2016), which has been already achieved by some other 3D printing technologies. So far, most of the sub-operations of 3D printing ranging from extrusion of raw materials, fusion of metal powder, and photopolymerization have been automated (Bidare et al., 2017; Frketic et al., 2017; Ren et al., 2017). A major hurdle for automation of bioprinting is the nature of bioinks, which should undergo sol-gel transition in physiological ambient conditions without use of high temperature. Due to the shape distortions, sol-gel form is not readily bioprinted with high resolution deposition. In practice, it is often observed that either the nozzle or printed material does not contact the previous layer due to inherent hydrogel swelling or dehydration processes, which causes significant structural deformation and require manual intervention.

Moreover, in many bioprinting applications, multiple bioinks are co-printed, and each of them owns different swelling or shrinking kinetics which make the automation of bioprinting complicated. Such deficiencies are sought to be improved by implementation of real-time monitoring technologies, which use optical camera to observe construct height and provide feedback signal for subsequent dispensation (Wang et al., 2017). It must be noted that automation of dispensing should be compatible with other liquid handling and cell culture protocols. Several automated protocols for cell culture are now reported, and they

should be integrated with bioprinting modalities for *in situ* applications (Kato et al., 2009; Thomas and Ratcliffe, 2012; Triaud et al., 2003). Recently, an automated process for creation of surface topographic cues with a robotic bioink dispensation system has been demonstrated for tissue engineering applications (Bhuthalingam et al., 2016).

3.2.6. User friendliness

Since a large number of end-users are expected to be in medical and biotechnological areas, it is desirable that the user interface of bioprinters is user-friendly. User-friendliness can be evaluated by the time and steps required to get functional outputs and the minimum time required to train a new user. The end-users should not be bothered much with the intricate instrumentation operation, and should be allowed to focus more on the clinical problems. Therefore, user-friendliness should be taken into account seriously for the bioprinter development. It may be seen that most of the extrusion- and some droplet-based bioprinters are quite user-friendly. In fact, some of the bioprinters are transshipped as separated parts, which the users can be assembled by end users themselves. Besides ease of installation, they also allow ease of operation with interactive software. During operation, point to be noted is the change of bioink after dispensation of a unit quantity initially loaded. In this respect, bioprinters with attached peristaltic pumps are desirable. Apart from operation, troubleshooting is also important and a manual with clear descriptions should be provided. Since a bioprinter is made up of several small electronic and mechanical components, such as microchips, microcontrollers, stepper motors, gears, and belts, it is essential to use the components following international standard. Bioprinters such as Inkredible and Biobots are quite user-friendly, whereas Envisiontec and Gesim Bioscaffolder are sophisticated, which required professional training for operation and troubleshooting (Lee et al., 2017a, 2017b). Moreover, laser-based bioprinters are generally less user-friendly as they require more learning time and they are more intricate to operate.

3.2.7. Affordability

The high cost of bioprinters remains a bottleneck for mass deployment of the technology in regular clinical use. It is also emphasized that bioprinting processes are quite expensive as the essential sterility required. However, cost of any instrument is known to plummet as demand increases. Therefore, it may be predicted that with rising number of users and proof-of-concept demonstration of applications, bioprinters will start finding commercial demand and price will drop as seen in plastic 3D printers. At present, most of clinically-relevant bioprinters are available at pricing of $150–200k. However, several start-up companies are trying to develop affordable bioprinters for customers across the country, though most of these bioprinters are based on extrusion principle and have inferior fabrication properties. Certain pneumatic extrusion bioprinters can also be very expensive (e.g. BioAssembly bots at ~ $160k and nSrypt at > $200k). The recently launched bioprinters in this category like BioBots and Inkredible are available in range of $10k. Laser-based bioprinters, which can be developed from scratches, are around $100k. On contrary, bi-axial droplet-based bioinks without live-cell dispensing capabilities can be developed using commercial paper-jet printers at very low cost. For biological application, however, the cost may increase to $20–70k. Generally, the system automation, resolution, number of print-heads is important determinants of the cost. For instance, dual-head bioprinter with photo-crosslinking capability costs $5–10k while a basic one excluding bioink extruder only cost as little as $500. It is essential that a component cost analysis is performed to find out strategies for cost reduction. In a recent study, Reid *et al.* have developed an automated bioprinting system with the protocol of human-induced pluripotent cell differentiation. A low cost Felix 3D printer was adapted and the resolution of conventional extrusion process were improved by the use of finite element modeling (Reid et al., 2016).

3.2.8. Versatility

Another important property of bioprinters is the necessity of versatility, which refers to the compatibility with various types of bioinks, bioinks with wide range of viscosities and different gelation processes and various bioprinting processes. Versatile bioprinters should also allow end-users to customize the instrument for specific applications. Amongst different bioprinters, the Biobot series are one example of versatile bioprinters. The open source Fab@Home also offers bioprinter with remarkable versatility. In the droplet-based category, different series of bioprinters such as Nordson Pico® series and MD series from Microdrop Technologies, which are suitable for high-throughput applications, provide significant versatility by allowing enhanced control on generation of droplets and their spatial deposition. It can be deduced that extrusion-based bioprinters are more versatile as bioinks with wide ranges of viscosities can be dispensed. Comparatively, laser-based bioprinters are limited by the bioink which can be irradiated by laser or photopolymerization. In droplet-based bioprinters, different bioinks can be printed, but clogging of nozzles is frequently observed for high viscosity bioinks, which limits their versatility. As an example, most bioprinters are developed for alginate or Pluronic bioinks, which have limited clinical utility for tissue regeneration. Therefore, a system automation based on these bioinks may not be exactly suitable for an end-user, who seeks functional bioinks.

3.3. Bioprinting Phase

After the selection of bioink formulation and appropriate bioprinter technology, physical bioprinting assumes significance, as process parameters comprise a range of selection which should be optimized in case-to-case basis to obtain the desired constructs. There is a need for process automation in this stage to generate constructs rapidly for clinical applications. Bioprinting process should also be carried out under highly defined and controlled environments with proper controls to allow for repetitive results. Some of the salient requirements of this stage are described below:

3.3.1. Bioprinting Resolution

The resolution of a bioprinting process, which can be evaluated in terms of the smallest pattern that can be achieved, differs from the instrumental resolution of a bioprinter due to the rheological properties and non-instantaneous nature of solidification of most hydrogels. In practice, process bioprinting resolution of around 5, 50 and 100 μm are typically obtained by LBB, DBB and EBB, respectively (Gudapati et al., 2016; Li et al., 2016; Munaz et al., 2016; Ozbolat et al., 2017). Likewise, resolution deteriorates as bioink is changed from hydrogel to cell aggregates (i.e., tissue spheroids or strands). One of the effective ways to improve bioprinting resolution is to allow quick crosslinking, but this often results in nozzle clogging and adherence of nozzle to bioprinted layers. Moreover, reduction in nozzle diameter is also not an effective solution, as it would increase shear force on the cells, resulting in decreased viability.

In case of DBB, ejection of one droplet is often accompanied by several satellite droplets, reducing its bioprinting resolution (Li et al., 2015). Other factors that influence bioprinting process resolution are the mechanism of actuation, droplet-nozzle and droplet-substrate interactions. For example, hydrophilicity of inner walls of the nozzle and the surface tension of bioink affect the print quality. Decreasing hydrophilicity of nozzle inner walls and lowering the surface tension of the bioink result in delayed droplet disintegration time and reduce droplet ejection velocities. Similarly, contact angle of substrate determines the spreading of bioink, and hence influences the resolution of the bioprinting process.

In LBB, process parameters that influence resolution include jet dynamics and impact of ejected bioink. These forces can be modulated by the bioink rheology and by adjusting the distance between the ribbon and collector. Based on the above process understanding, Ali

et al. have successfully bioprinted MSCs with minimal shear stress and high process resolution (Ali et al., 2014). Additionally, the study of Guillotin also showed the effect of bioink viscosity and laser parameters on the bioprinting resolution (Guillotin et al., 2010). In many cases, improving the bioprinting resolution often results in decrease of cellular functionality parameters (e.g. stem cell integrity, high dehydration time), and hence process parameters like shear stress are required to be optimized (Blaeser et al., 2016). LBB can result in generally high bioprinting resolution compared to DBB and EBB. For EBB, bioprinting resolution should be endeavored to be improved by using a tapered nozzle to reduce the exposure time of cells to high shear stress, hyphenation with electrohydrodynamic effects (Eagles et al., 2006; Gasperini et al., 2014) or ultimately using a nozzle-free extrusion system.

3.3.2. Repeatability

Tissue engineered constructs are required to meet specific and quantitative standards of safety and performance for clinical use (Nawroth and Parker, 2013; Salih, 2013). Bioprinted constructs are more complex and customized compared to traditional constructs, making the standardization more difficult. In this respect, it has been observed that the use of tissue strands as a bioink without liquid medium or molds, allows for repeatable bioprinting (Yu et al., 2016). The major criteria of estimation of the repeatability of bioprinted structures for standardization include bioprint fidelity, mechanical properties, and cell viability. It must be noted that some properties such as mechanical strength are dynamic in nature and would change with time as cells deposit their own ECM. Therefore, standardized protocols should also be dynamic (i.e. analysis at multiple time points). Several automated methods for cell viability and mechanical property measurements of tissue *in situ* have been developed (Dougherty et al., 2013). One of the example is to use microscope for label-free cell viability determination, which should be more widely applied (Cadena-Herrera et al., 2015; Ke et al., 2011; Louis and Siegel, 2011). Amongst the bioprinting modalities, process repeatability is higher in DBB compared to LBB or EBB. EBB often suffers from unpredictable process interruptions due to swelling or shrinkage of hydrogels (He et al., 2016). Though LBB is nozzle-free bioprinting and hence, the repeatability is not affected by clogging problems, the limited range of viscosities that can be handled restricts the mechanical strengths of the printed construct. In LBB, the processes are highly complicated with nonlinear physical relationship of parameters resulting in poor repeatability of the process.

3.3.3. Biocompatibility

Process biocompatibility is unarguably one of the most important considerations for bioprinting. One of the principal aims of bioprinting is to maintain viability and function. In addition, the process must not induce any phenotypic and genotypic changes. Depending upon the modality, cells may be exposed to different external stresses including mechanical in EBB, mechanical, acoustic, thermal or electrical in DBB, and optical or thermal in LBB, all of which can result in cell morbidities. In general, typical viabilities of 40-80% for EBB, 85% for DBB and 95% for LBB are observed (Murphy and Atala, 2014). From these, it can be deduced that shear stress is most detrimental to cells (Ouyang et al., 2016). For each modality, apart from bioink compatibility, certain common stressors also exist (e.g. flow rate and bioprinting time), which may result in lower cell viabilities. In case of LBB, additional parameters such as laser pulse time and air gap between receiver and collector plates also determine the biocompatibility of the process (Catros et al., 2011). In many cases, solidification is achieved by UV, which may become another factor to impact viability. Application of stereolithography in bioprinting commenced with the experiments of Boland and coworkers in 2004. In this method, cells and a photocurable hydrogel was charged onto a vat, and positioned on a table in which movement could be controlled in vertical axis. UV radiation was then made incident on the bioink, triggering generation of radical from photoinitiators and subsequent polymerization of the bioink. UV light traced the toolpath according to the CAD file, thus curing the bioink at designated places inside the vat. The process was repeated for each layer to generate the 3D constructs, which can be of few hundred μm to few mm in size. Initially, Chinese hamster ovary cells were bioprinted in PEO and PEO-dimethacrylate (PEGDMA) hydrogels with over 90% viability. Subsequently, SLA-based bioprinting of cylindrical constructs were shown for 3T3 fibroblasts within PEGDMA hydrogels. Other commonly used hydrogel for SLA bioprinting has been acrylate polymers with urethane segments and trimethylolpropane triacrylate. Apart from photocurable polymers, photoinitiators, e.g. Irgacure, are also a major component of this modality in order to improve solidification. Thus, the optimization of photo-initiator concentation in a bioink composition becomes crucial. Further, care is to be taken to determine the ideal photo-initiator concentration due to its toxicity (Dhariwala et al., 2004; Fedorovich et al., 2009). Recently, the use of visible light induced crosslinking of poly(ethylene glycol diacrylate), gelatin methacrylate and eosin Y photo-initiator have shown promise to maintain high cell viability (Wang et al., 2015a).

4. Post-bioprinting Stage

After bioprinting of constructs, tissue maturation is a time-dependent process and post-bioprinting should be performed under tightly controlled conditions, especially in bioreactors (see Fig. 5A). Cell-cell interactions are highly influenced by these conditions and kinetics of any differentiation process can be modulated with wide variations of stimuli that can be exerted during post-bioprinting processes. Such conditions can be optimized to mimic *in vivo* environment, which can be further enhanced by providing *in vivo* like environment such as explant culture as can be seen in Fig. 5B.

4.1. Conditioning of bioprinted constructs

Lack of mass transfer of nutrients and metabolites is one of the prime reasons for failure of generating tissue constructs with clinically-relevant thickness *in vitro,* since the absence of internal vascular network restricts oxygen supply from the peripheral regions of the construct to the deeper regions even after homogeneous seeding (Chan and Chong, 2009). This is also an issue for bioprinted tissue constructs. Though bioprinted constructs have been designed with vasculature as shown in Fig. 5C, effective oxygen supply is not readily achieved in conventional static tissue culture methods. Therefore, perfusion of bioprinted constructs in bioreactors becomes a necessary and essential step.

A bioreactor is broadly defined to be a vessel, in which a biochemical process can be carried out under controlled conditions, and allows simultaneous monitoring. In bioprinted tissue constructs, bioreactors also allow to create various stimulating conditions to regulate the maturation of the tissues. Several types of bioreactors including spinner flask, rotating wall, compression, strain, hydrostatic pressure, flow perfusion and some combined bioreactors, have been used for engineering tissue constructs (Plunkett and O'Brien, 2010). Amongst them, flow perfusion bioreactor is made up of a pump system and a chamber for tissue construct connected by tubes, such that media can flow through the tissue construct to enhance fluid transport.

Bioreactors have shown their utility in different types of tissues including bone, skin, cardiovascular and cartilage. For example, in rotating wall vessel bioreactor, mature chondrocytes were observed after 6 weeks of culture from cartilage progenitor cells or 3 weeks from bone marrow stromal cells. In addition, cartilaginous tissues, approximately 1.25×0.60 cm in dimensions, have been obtained after 12 weeks of culture (Zhao et al., 2016). In spinner flask bioreactor, cartilage formation after 4 weeks is observed. Bone tissue type mineralization is obtained in spinner bioreactors after 3-5 weeks of culture. Several

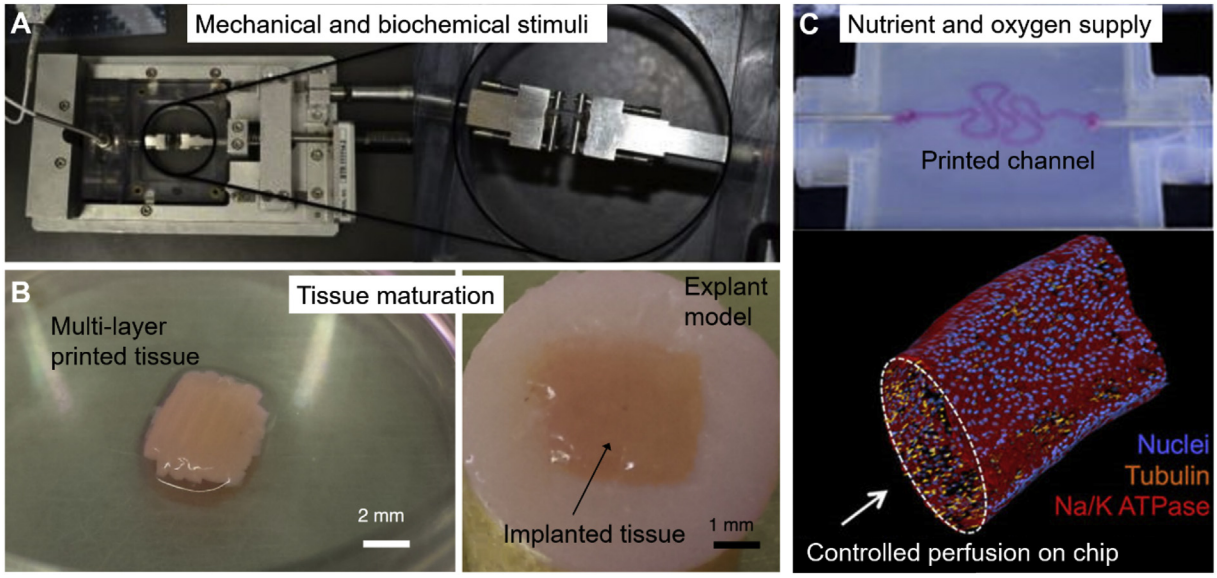

Fig. 5. A) A biotense perfusion bioreactor with a bioprinted vasculature (modified with permission from (Dolati et al., 2014)); B) Explant culture improved the maturation of bioprinted cartilage into a native-like cartilage (modified from (Yu et al., 2016)); C) 3D Bioprinted convoluted renal proximal tubule where an open lumen circumscribed with an epithelial lining was perfused on chip (modified from (Homan et al., 2016).

microfluidic perfusion bioreactors have also been developed, which allow bioprinted construct to differentiate at accelerated rate into desired tissues such as heart (Zhang et al., 2016a, 2016b) and bone (Detsch and Boccaccini, 2015). However, technological breakthrough of bioreactors should be performed for wider clinical translation through offering substantial user-friendliness. Further, process consistency and volume output are also necessary to be improved. This can be achieved by increasing the automation of bioreactors. For example, the perfusion bioreactor from Aastrom Bioscience Inc. allows for automated expansion of cells from bone marrow as raw material. Recent advances in bioreactors allow real time monitoring and feedback control of several vital parameters including temperature, oxygen level and pH, to allow optimal cell growth. In addition, novel oxygen-imaging sensor has been developed, which can be integrated with bioreactors to map oxygen distribution in 3D scaffolds (Westphal et al., 2017). The other physiological ambient conditions required to be maintained in bioreactor are oxygen partial pressure (pO_2), pH, CO_2 and temperature, as well as maintained concentrations of growth factor and nutrients.

In the classical paradigm of tissue engineering, cells, scaffold and growth factors composed the triad which needs to be engineered to obtain functional tissues. However, it was realized that external stimuli can also induce differentiation of progenitor cells into specific cell types. Thus, apart from designing scaffold with architecture for cell infiltration and growth, it is necessary that physiologically-mimetic mechanical and biochemical stimuli are exerted on tissue constructs in a bioreactor for cells to mature into relevant tissues (Bhuthalingam et al., 2016). Many bioreactors have been developed to exert such mechanical stimuli such as hydrostatic pressure, compression, shear and tension (Plunkett and O'Brien, 2010).

Methods have also been developed to exert mechanical/biochemical or mechanical/electrical stimuli for accelerated maturation of some specific tissue types. For example, in cartilage tissue engineering, mechanical stimuli are applied to compress the cartilage to produce more ECM to improve mechanical strength. Mechanical stimulation can also aid in better integration of cartilage construct with host tissue. For example, in cartilage tissue engineering, stimulation with 0.4 MPa pulsatile hydrostatic pressure or 1 Hz compression can lead enhanced chondrocytes differentiation, GAG production and ECM synthesis (Correia et al., 2012). Another study by Wernike et al. found that dynamic compression (10–20% strain; 0.5 Hz; 1 h/day) and low oxygen tension (5%) was able to show a more stable phenotype of chondrocytes (Wernike et al., 2008). Similarly, for osteoblasts differentiation and alkaline phosphatase (ALP) activities were observed to be enhanced, when they were cultured with the shear stress of 0.16–32 N/m^2. For cardiac tissue engineering, electrical (e.g. 5 V for 2 ms, 1 Hz) or mechanical (e.g. 2 Hz) stimulation has been shown to improve tissue formation (Trumbull et al., 2016). The extent and values of stimuli exerted in different studies for maturation of tissues in bioreactors have been mentioned and extensively detailed in other studies (Li et al., 2017; Rauh et al., 2011). Recently, bioreactor systems for clinical heart valve tissue engineering have also been reported (Converse et al., 2013).

4.2. Practicality

One important parameter that is critical for success of bioprinting is the practicality with which mass-scale tissue production can be carried out. Prevalent technologies can result in production of proliferation/differentiation of cells into numbers, which are adequate only for laboratory scale studies. However, organ bioprinting for clinically-relevant volumes and amounts require scale-up manufacturing of cells. Advanced, automated bioprocessing technologies conforming to good manufacturing practices and strict quality monitoring are thus needed to be implemented in clinical bioprinting establishments (Placzek et al., 2009). The source of cell in itself may have some constrains, for example, stem cells from relatively younger patients can be passaged upto 40 generations and those from patients of higher age group can be limited to only 25 population cycles only (Stenderup et al., 2003). For example, Organovo company has been successfully producing liver tissue lines for drug toxicity testing (Nguyen et al., 2016) and has also started making progress in kidney and skin tissue bioprinting. Apart from tissue constructs, bioprinting-assisted fabrication of tumor-on-chip platforms is emerging to provide practical solutions for cancer research (Knowlton et al., 2016).

4.3. Affordability

The bioreactor should not add significant costs to the whole system. Bioreactors are mostly composed of peristaltic pumps, filters, chamber vessel, tubings and integrated sensors. Of these, filters have generally

the highest cost contribution, apart from number of sensors that are integrated inside the system. Though addition of advanced monitoring and control systems for vital parameters as well as cellular phenotypes may contribute to cost of maturation bioreactors and hence tissue constructs, progresses and commercialization of systems like BioProfilew 400 (Nova Biomedical), Advanced Clinical Tissue Engineering System ACTESe, or Stat Profilew Critical Care Xpress, present an encouraging scenario (Martin et al., 2004). Affordability of bioreactors is also determined by the tissue types and differentiation media to be used.

5. Conclusions and future remarks

It is widely speculated that future bioprinting will soon move towards fabrication of mechanically robust constructs with high resolutions as well as translation of bioprinters into operating rooms. Clinical translation of bioprinting demands scale-up to clinically-relevant volume of tissues along with efficient vascularization for ready implantation. Rapid expansion in efforts for bioprinting of several organs like pancreas (Ravnic et al., 2017), osteochondral (Datta et al., 2017b), bone, stem cells are visible (Datta et al., 2017c; Leberfinger et al., 2017). To achieve this, bioprinting technological advancements are needed to be firmly supported by organic synchronization of all components of bioprinting. Since this is a multi-step process, ultimate construct fabrication will be dependent on how each step is coordinated with others and appropriately optimized. Though one of the major milestones in bioprinter development may be considered to be started with the modification of desktop 3D printers for printing of live cells (Xu et al., 2005), bioprinting industry is still in its infancy with limited technological achievements in attaining a complete process chain for functional tissue biofabrication. The ExVive™ 3D bioprinted human tissues developed by the Organovo company is, however, an important milestone in bioprinting process chain. Similarly, in immediate past, a bioresorbable 3D-printed airway splint has been implanted in human infant. Approval of food and drug administration (FDA) was sought by the University of Michigan- institutional review board of and the device was granted emergency-use exemption and has performed well in initial evaluations. It is expected that more of such milestones may be witnessed in the near future. On the other hand, inability to generate functional vascular network in bioprinted constructs is the weakest link in bioprinting process chain, and it would require specific solutions to overcome the limitations. Likewise, ample achievements have also been made in scale up of bioprinted constructs, which had been thought to be a limitation initially (Yu et al., 2014b). Bioprinting of microvascular network is more challenging compared to bioprinting macro-level vasculature. Fugitive inks are often employed to fabricate the vascular networks (Kolesky et al., 2016). Moreover, some recent achievements in intra-vascularization of tissue spheroids (such as pancreatic islets) indicate that it is possible to make significant inroads in overcoming this limitation for bioprinting (Hospodiuk et al., 2018). Broadly, it is expected that major milestones in transplantation of organs not requiring vascularization for significant effects (like cartilage or skin) may be achieved sooner than organs with high metabolic activity (e.g. liver or heart) (Datta et al., 2017a).

In the pre-bioprinting stage, minimally invasive cell harvesting followed by efficient expansion technologies of stem cell are essential to generate rapid and cost-effective tissue-specific constructs from autologous cells. Different new cell types like pericytes are also attractive for functional bioprinting applications (Potjewyd et al., 2018). This apart, high resolution images and more robust blueprint modeling should develop to ensure full potential of bioprinting is harnessed clinically. In the bioprinting stage, there is need for focused research on bioprintable biomaterials, which form the important component of bioinks since not all novel biomaterials are amenable to bioprinting. Instructive biomaterials that direct cells to a defined lineage apart from supporting adequate cell adhesion, proliferation, appropriate host response, are emerging but their bioprintability cannot be always guaranteed and hence needs special attention. Specifically, quick gelation in a physiologically-acceptable environment (pH, temperature, radiation etc.) is expected from these compatible biomaterials for successful bioprinting. In the bioprinting stage, another crucial area is the evolution of bioprinting technologies and the bioprinter themselves. Bioprinter should have high degree of freedom in multi-axis, multiple arms as well as designed to reduce chances of bioink coagulation during long operating hours. Another important dimension would be full automation of the bioprinting process maintain highest levels of aseptic conditions inside the operating rooms. Affordability and ease of operation would also require to be considered for use in clinical establishments. The advances in bioprinters and bioinks are needed to be complimented with process innovations to allow precise fabrication of constructs mimicking native tissue microenvironment causing minimal cell damages. Several in situ monitoring and sensing mechanisms are needed to be built in to enable detection of deviations and feedback control of the process. Subsequently, bioprinted constructs are transferred to bioreactors where tissue maturation is accelerated with aid of mechanical, electrical and/or biochemical stimulation to obtain rigid, and functional tissue construct, and monitored with the aid of biosensors.

Indeed, bioprinting technology is expected to provide constructs with improved functional quality, resolution, 3D design and material complexities with spatial variations mimicking natural tissue, in the future. Deposition of various different bioinks with different physicochemical properties simultaneously, appears to be a realistic prospect. However, it can be concluded that a well-coordinated, multi-disciplinary approach is necessary to ensure that tissue constructs of high-quality, high reproducibility are obtained for human transplantation.

Acknowledgement

This work has been supported by National Science Foundation Award # 1600118 awarded to I.T.O. The authors also acknowledge Department of Science and Technology, Government of India, INSPIRE Faculty Award to P.D. The authors are grateful to International Postdoctoral Research Scholarship Program (BIDEP 2219) of the Scientific and Technological Research Council of Turkey for providing scholarship to V. O and the support from the Turkish Ministry of National Education for providing graduate scholarship to B. A. *The authors confirm that there are no known conflicts of interest associated with this publication and there has been no significant financial support for this work that could have influenced its outcome.*

References

Actis, P., Maalouf, M.M., Kim, H.J., Lohith, A., Vilozny, B., Seger, R.A., Pourmand, N., 2014. Compartmental genomics in living cells revealed by single-cell nanobiopsy. ACS Nano 8, 546–553. http://dx.doi.org/10.1021/nn405097u.

Afshar, M., Anaraki, A.P., Montazerian, H., Kadkhodapour, J., 2016. Additive manufacturing and mechanical characterization of graded porosity scaffolds designed based on triply periodic minimal surface architectures. J. Mech. Behav. Biomed. Mater. 62, 481–494. http://dx.doi.org/10.1016/j.jmbbm.2016.05.027.

Ahmed, T.A.E., Dare, E.V., Hincke, M., 2008. Fibrin: a versatile scaffold for tissue engineering applications. Tissue Eng. Part B Rev. 14, 199–215. http://dx.doi.org/10.1089/ten.teb.2007.0435.

Ahsan, A.M.N., Xie, R., Khoda, B., 2017. Direct Bio-printing with Heterogeneous Topology Design. Proc. Manuf. 10, 945–956. http://dx.doi.org/10.1016/j.promfg.2017.07.085.

Akkouch, A., Yu, Y., Ozbolat, I.T., 2015. Microfabrication of scaffold-free tissue strands for three-dimensional tissue engineering. Biofabrication 7, 31002. http://dx.doi.org/10.1088/1758-5090/7/3/031002.

Alexandrescu, L., Syverud, K., Gatti, A., Chinga-Carrasco, G., 2013. Cytotoxicity tests of cellulose nanofibril-based structures. Cellulose 20, 1765–1775. http://dx.doi.org/10.1007/s10570-013-9948-9.

Ali, M., Pages, E., Ducom, A., Fontaine, A., Guillemot, F., 2014. Controlling laser-induced jet formation for bioprinting mesenchymal stem cells with high viability and high resolution. Biofabrication 6, 045001. http://dx.doi.org/10.1088/1758-5082/6/4/045001.

Appel, A.A., Anastasio, M.A., Larson, J.C., Brey, E.M., 2013. Imaging challenges in

biomaterials and tissue engineering. Biomaterials 34, 6615–6630. http://dx.doi.org/10.1016/j.biomaterials.2013.05.033.

Arai, K., Iwanaga, S., Toda, H., Genci, C., Nishiyama, Y., Nakamura, M., 2011. Three-dimensional inkjet biofabrication based on designed images. Biofabrication 3, 34113. http://dx.doi.org/10.1088/1758-5082/3/3/034113.

Arai, K., Tsukamoto, Y., Yoshida, H., Sanae, H., Ahmad Mir, T., Sakai, S., Yoshida, T., Okabe, M., Nikaido, T., Taya, M., Nakamura, M., 2016. The development of cell-adhesive hydrogel for 3D printing. Int. J. Bioprinting 2 (2). http://dx.doi.org/10.18063/IJB.2016.02.002.

Axpe, E., Oyen, M.L., 2016. Applications of alginate-based bioinks in 3D bioprinting. Int. J. Mol. Sci. 17, 1976. http://dx.doi.org/10.3390/ijms17121976.

Bakhshinejad, A., D'souza, R.M., 2015. A brief comparison between available bio-printing methods. In: 2015 IEEE Gt. Lakes Biomed. Conf, http://dx.doi.org/10.1109/GLBC.2015.7158294.

Ballyns, J.J., Bonassar, L.J., 2009. Image-guided tissue engineering. J. Cell. Mol. Med. 13, 1428–1436. http://dx.doi.org/10.1111/j.1582-4934.2009.00836.x.

Beke, S., Anjum, F., Tsushima, H., Ceseracciu, L., Chieregatti, E., Diaspro, A., Athanassiou, A., Brandi, F., 2012. Towards excimer-laser-based stereolithography: a rapid process to fabricate rigid biodegradable photopolymer scaffolds. J. R. Soc. Interface 9, 3017–3026. http://dx.doi.org/10.1098/rsif.2012.0300.

Bhattacharjee, T., Zehnder, S.M., Rowe, K.G., Jain, S., Nixon, R.M., Sawyer, W.G., Angelini, T.E., 2015. Writing in the granular gel medium. Sci. Adv. 1, e1500655. http://dx.doi.org/10.1126/sciadv.1500655.

Bhuthalingam, R., Lim, P.Q., Irvine, S.A., Venkatraman, S.S., 2016. Automated robotic dispensing technique for surface guidance and bioprinting of cells. J. Vis. Exp. 117. http://dx.doi.org/10.3791/54604.

Bianco, P., Robey, P.G., 2001. No Title. Nature 414, 118–121. http://dx.doi.org/10.1038/35102181.

Bianconi, E., Piovesan, A., Facchin, F., Beraudi, A., Casadei, R., Frabetti, F., Vitale, L., Pelleri, M.C., Tassani, S., Piva, F., Perez-Amodio, S., Strippoli, P., Canaider, S., 2013. An estimation of the number of cells in the human body. Ann. Hum. Biol. 40, 463–471. http://dx.doi.org/10.3109/03014460.2013.807878.

Bidare, P., Maier, R.R.J., Beck, R.J., Shephard, J.D., Moore, A.J., 2017. An open-architecture metal powder bed fusion system for in-situ process measurements. Addit. Manuf. 16, 177–185. http://dx.doi.org/10.1016/j.addma.2017.06.007.

Billiet, T., Gevaert, E., De Schryver, T., Cornelissen, M., Dubruel, P., 2014. The 3D printing of gelatin methacrylamide cell-laden tissue-engineered constructs with high cell viability. Biomaterials 35, 49–62. http://dx.doi.org/10.1016/j.biomaterials.2013.09.078.

Blaeser, A., Duarte Campos, D.F., Puster, U., Richtering, W., Stevens, M.M., Fischer, H., 2016. Controlling shear stress in 3D bioprinting is a key factor to balance printing resolution and stem cell integrity. Adv. Healthc. Mater. 5, 326–333. http://dx.doi.org/10.1002/adhm.201500677.

Boitano, A.E., Wang, J., Romeo, R., Bouchez, L.C., Parker, A.E., Sutton, S.E., Walker, J.R., Flaveny, C.A., Perdew, G.H., Denison, M.S., Schultz, P.G., Cooke, M.P., 2010. Aryl hydrocarbon receptor antagonists promote the expansion of human hematopoietic stem cells. Science 329, 1345–1348. http://dx.doi.org/10.1126/science.1191536.

Brafman, D.A., 2013. Constructing stem cell microenvironments using bioengineering approaches. Physiol. Genomics 45, 1123–1135. http://dx.doi.org/10.1152/physiolgenomics.00099.2013.

Bücking, T.M., Hill, E.R., Robertson, J.L., Maneas, E., Plumb, A.A., Nikitichev, D.I., 2017. From medical imaging data to 3D printed anatomical models. PLoS One 12, 1–10. http://dx.doi.org/10.1371/journal.pone.0178540.

Buehr, M., Meek, S., Blair, K., Yang, J., Ure, J., Silva, J., McLay, R., Hall, J., Ying, Q.-L., Smith, A., 2008. Capture of authentic embryonic stem cells from rat blastocysts. Cell 135, 1287–1298. http://dx.doi.org/10.1016/j.cell.2008.12.007.

Cadena-Herrera, D., Esparza-De Lara, J.E., Ramírez-Ibañez, N.D., López-Morales, C.A., Pérez, N.O., Flores-Ortiz, L.F., Medina-Rivero, E., 2015. Validation of three viable-cell counting methods: manual, semi-automated, and automated. Biotechnol. Rep. 7, 9–16. http://dx.doi.org/10.1016/j.btre.2015.04.004.

Cao, X., Ban, E., Baker, B.M., Lin, Y., Burdick, J.A., Chen, C.S., Shenoy, V.B., 2017. Multiscale model predicts increasing focal adhesion size with decreasing stiffness in fibrous matrices. Proc. Natl. Acad. Sci. U. S. A. 114, E4549–E4555. http://dx.doi.org/10.1073/pnas.1620486114.

Catros, S., Guillotin, B., Bacakova, M., Fricain, J.-C., Guillemot, F., 2011. Applied surface science effect of laser energy, substrate film thickness and bioink viscosity on viability of endothelial cells printed by laser-assisted bioprinting. Appl. Surf. Sci. 257, 5142–5147. http://dx.doi.org/10.1016/j.apsusc.2010.11.049.

Cavo, M., Fato, M., Peñuela, L., Beltrame, F., Raiteri, R., Scaglione, S., 2016. Microenvironment complexity and matrix stiffness regulate breast cancer cell activity in a 3D in vitro model. Sci. Rep. 6, 35367. http://dx.doi.org/10.1038/srep35367.

Ceusters, J., Lejeune, J.-P., Sandersen, C., Niesten, A., Lagneaux, L., Serteyn, D., 2017. From skeletal muscle to stem cells: an innovative and minimally-invasive process for multiple species. Sci. Rep. 7, 696. http://dx.doi.org/10.1038/s41598-017-00803-7.

Chan, W.Y., Chong, C.K., 2009. Perfusion bioreactors improve oxygen transport and cell distribution in esophageal smooth muscle construct. In: International Conference on Biomedical Engineering. IFMBE Proceedings. Heidelberg, pp. 1523–1526. http://dx.doi.org/10.1007/978-3-540-92841-6_377.

Chang, S.C.N., Rowley, J.A., Tobias, G., Genes, N.G., Roy, A.K., Mooney, D.J., Vacanti, C.A., Bonassar, L.J., 2001. Injection molding of chondrocyte/alginate constructs in the shape of facial implants. J. Biomed. Mater. Res. 55, 503–511. http://dx.doi.org/10.1002/1097-4636(20010615)55:4<503::AID-JBM1043>3.0.CO;2-S.

Chang, R., Nam, J., Sun, W., 2008. Effects of dispensing pressure and nozzle diameter on cell survival from solid freeform fabrication–based direct cell writing. Tissue Eng. Part A 14, 41–48.

Chen, L., Bouley, D., Yuh, E., D'Arceuil, H., Butts, K., 1999. Study of focused ultrasound tissue damage using MRI and histology. J. Magn. Reson. Imaging 10, 146–153. http://dx.doi.org/10.1002/(SICI)1522-2586(199908)10:2<146::AID-JMRI6>3.0.CO;2-C.

Chen, S., Do, J.T., Zhang, Q., Yao, S., Yan, F., Peters, E.C., Schöler, H.R., Schultz, P.G., Ding, S., 2006. Self-renewal of embryonic stem cells by a small molecule. Proc. Natl. Acad. Sci. 103, 17266–17271. http://dx.doi.org/10.1073/pnas.0608156103.

Chen, G., Deng, C., Li, Y.-P., 2012. TGF-β and BMP signaling in osteoblast differentiation and bone formation. Int. J. Biol. Sci. 8, 272–288. http://dx.doi.org/10.7150/ijbs.2929.

Cheng, G., Youssef, B.B., Markenscoff, P., Zygourakis, K., 2006. Cell population dynamics modulate the rates of tissue growth processes. Biophys. J. 90, 713–724. http://dx.doi.org/10.1529/biophysj.105.063701.

Cheng, G., Markenscoff, P., Zygourakis, K., 2009. A 3D hybrid model for tissue growth: the interplay between cell population and mass transport dynamics. Biophys. J. 97, 401–414. http://dx.doi.org/10.1016/j.bpj.2009.03.067.

Chimene, D., Lennox, K.K., Kaunas, R.R., Gaharwar, A.K., 2016. Advanced bioinks for 3D printing: a materials science perspective. Ann. Biomed. Eng. 44, 2090–2102. http://dx.doi.org/10.1007/s10439-016-1638-y.

Christensen, K., Zhang, Z., Xu, C., Huang, Y., 2017. Deformation compensation during buoyancy-enabled inkjet printing of three-dimensional soft tubular structures. J. Manuf. Sci. Eng. 140, 011011. http://dx.doi.org/10.1115/1.4037996.

Chung, J.H.Y., Naficy, S., Yue, Z., Kapsa, R., Quigley, A., Moulton, S.E., Wallace, G.G., 2013. Bio-ink properties and printability for extrusion printing living cells. Biomater. Sci. 1, 763. http://dx.doi.org/10.1039/c3bm00012e.

Clarke, B., 2008. Normal bone anatomy and physiology. Clin. J. Am. Soc. Nephrol. 3, S131–S139. http://dx.doi.org/10.2215/CJN.04151206.

Cline, H.E., Hynynen, K., Watkins, R.D., Adams, W.J., Schenck, J.F., Ettinger, R.H., Freund, W.R., Vetro, J.P., Jolesz, F.A., 1995. Focused US system for MR imaging-guided tumor ablation. Radiology 194, 731–737. http://dx.doi.org/10.1148/radiology.194.3.7862971.

Coakley, M.F., Hurt, D.E., Weber, N., Mtingwa, M., Fincher, E.C., Alekseyev, V., Chen, D.T., Yun, A., Gizaw, M., Swan, J., Yoo, T.S., Huyen, Y., 2014. The NIH 3D print exchange: a public resource for bioscientific and biomedical 3D Prints. 3D print. Addit. Manuf. 1, 137–140. http://dx.doi.org/10.1089/3dp.2014.1503.

Cohen, D.E., Melton, D., 2011. Turning straw into gold: directing cell fate for regenerative medicine. Nat. Rev. Genet. 12, 243–252.

Collins, S.F., 2014. Bioprinting is changing regenerative medicine forever. Stem Cells Dev. 23, 79–82. http://dx.doi.org/10.1089/scd.2014.0322.

Colosi, C., Shin, S.R., Manoharan, V., Massa, S., Costantini, M., Barbetta, A., Dokmeci, M.R., Dentini, M., Khademhosseini, A., 2016. Microfluidic bioprinting of heterogeneous 3D tissue constructs using low-viscosity bioink. Adv. Mater. 28, 677–684. http://dx.doi.org/10.1002/adma.201503310.

Converse, G.L., Buse, E.E., Hopkins, R.A., 2013. Bioreactors and operating room centric protocols for clinical heart valve tissue engineering. Prog. Pediatr. Cardiol. 35, 95–100. http://dx.doi.org/10.1016/j.ppedcard.2013.09.001.

Cornelissen, D.-J., Faulkner-Jones, A., Shu, W., 2017. Current developments in 3D bioprinting for tissue engineering. Curr. Opin. Biomed. Eng. 2, 76–82. http://dx.doi.org/10.1016/j.cobme.2017.05.004.

Correia, C., Pereira, A.L., Duarte, A.R.C., Frias, A.M., Pedro, A.J., Oliveira, J.T., Sousa, R.A., Reis, R.L., 2012. Dynamic culturing of cartilage tissue: the significance of hydrostatic pressure. Tissue Eng. Part A 18, 1979–1991. http://dx.doi.org/10.1089/ten.tea.2012.0083.

Ćwikła, G., Grabowik, C., Kalinowski, K., Paprocka, I., Ociepka, P., 2017. The influence of printing parameters on selected mechanical properties of FDM/FFF 3D-printed parts. In: IOP Conf. Ser. Mater. Sci. Eng. 227, http://dx.doi.org/10.1088/1757-899X/227/1/012033.

Daley, W.P., Yamada, K.M., 2013. Cell–ECM interactions and the regulation of epithelial branching morphogenesis. In: DeSimone, D.W., Mecham, R.P. (Eds.), Extracellular Matrix in Development. Springer Berlin Heidelberg, Berlin, Heidelberg, pp. 75–104. http://dx.doi.org/10.1007/978-3-642-35935-4_4.

Darabi, R., Arpke, R.W., Irion, S., Dimos, J.T., Grskovic, M., Kyba, M., Perlingeiro, R.C.R., 2012. Human ES- and iPS-derived myogenic progenitors restore DYSTROPHIN and improve contractility upon transplantation in dystrophic mice. Cell Stem Cell 10, 610–619. http://dx.doi.org/10.1016/j.stem.2012.02.015.

Das, S., Pati, F., Choi, Y.-J., Rijal, G., Shim, J.-H., Kim, S.W., Ray, A.R., Cho, D.-W., Ghosh, S., 2015. Bioprintable, cell-laden silk fibroin–gelatin hydrogel supporting multilineage differentiation of stem cells for fabrication of three-dimensional tissue constructs. Acta Biomater. 11, 233–246. http://dx.doi.org/10.1016/j.actbio.2014.09.023.

Datta, P., Ayan, B., Ozbolat, I.T., 2017a. Bioprinting for vascular and vascularized tissue biofabrication. Acta Biomater. 51, 1–20. http://dx.doi.org/10.1016/j.actbio.2017.01.035.

Datta, P., Dhawan, A., Yu, Y., Hayes, D., Gudapati, H., Ozbolat, I.T., 2017b. Bioprinting of osteochondral tissues: a perspective on current gaps and future trends. Int. J. Bioprinting 3 (2). http://dx.doi.org/10.18063/IJB.2017.02.007.

Datta, P., Ozbolat, V., Ayan, B., Dhawan, A., Ozbolat, I.T., 2017c. Bone tissue bioprinting for craniofacial reconstruction. Biotechnol. Bioeng. 114, 2424–2431. http://dx.doi.org/10.1002/bit.26349.

Derakhshanfar, S., Mbeleck, R., Xu, K., Zhang, X., Zhong, W., Xing, M., 2018. 3D bioprinting for biomedical devices and tissue engineering: a review of recent trends and advances. Bioact. Mater. 3, 144–156. http://dx.doi.org/10.1016/J.BIOACTMAT.2017.11.008.

Detsch, R., Boccaccini, A.R., 2015. The role of osteoclasts in bone tissue engineering. J. Tissue Eng. Regen. Med. 9, 1133–1149. http://dx.doi.org/10.1002/term.1851.

Dhariwala, B., Hunt, E., Boland, T., 2004. Rapid prototyping of tissue-engineering constructs, using photopolymerizable hydrogels and stereolithography. Tissue Eng. 10,

1316–1322.
Di Biase, M., Saunders, R.E., Tirelli, N., Derby, B., 2011. Inkjet printing and cell seeding thermoreversible photocurable gel structures. Soft Matter 7, 2639–2646. http://dx.doi.org/10.1039/C0SM00996B.
Do, A.-V., Akkouch, A., Green, B., Ozbolat, I., Debabneh, A., Geary, S., Salem, A.K., 2017. Controlled and sequential delivery of fluorophores from 3D printed alginate-PLGA tubes. Ann. Biomed. Eng. 45, 297–305. http://dx.doi.org/10.1007/s10439-016-1648-9.
Dolati, F., Yu, Y., Zhang, Y., De Jesus, A.M., Sander, E.A., Ozbolat, I.T., 2014. In vitro evaluation of carbon-nanotube-reinforced bioprintable vascular conduits. Nanotechnology 25, 145101. http://dx.doi.org/10.1088/0957-4484/25/14/145101.
Dougherty, J., Schaefer, E., Nair, K., Kelly, J., Masi, A., 2013. Repeatability, Reproducibility, and Calibration of the MyotonPro® on Tissue Mimicking Phantoms. In: SME 2013 Summer Bioengineering Conference, SBC 2013. Sunriver, OR, United States, p. V01AT20A026, http://dx.doi.org/10.1115/SBC2013-14622.
Duan, B., Hockaday, L.A., Kang, K.H., Butcher, J.T., 2013. 3D Bioprinting of heterogeneous aortic valve conduits with alginate/gelatin hydrogels. J. Biomed. Mater. Res. Part A 101A, 1255–1264. http://dx.doi.org/10.1002/jbm.a.34420.
Duan, B., Kapetanovic, E., Hockaday, L.A., Butcher, J.T., 2014. Three-dimensional printed trileaflet valve conduits using biological hydrogels and human valve interstitial cells. Acta Biomater. 10. http://dx.doi.org/10.1016/j.actbio.2013.12.005.
Eagles, P.M., Qureshi, A., Jayasinghe, S., 2006. Electrohydrodynamic jetting of mouse neuronal cells. Biochem. J. 394, 375–378. http://dx.doi.org/10.1042/BJ20051838.
Elomaa, L., Teixeira, S., Hakala, R., Korhonen, H., Grijpma, D.W., Seppälä, J.V., 2011. Preparation of poly(ε-caprolactone)-based tissue engineering scaffolds by stereolithography. Acta Biomater. 7, 3850–3856. http://dx.doi.org/10.1016/j.actbio.2011.06.039.
Elson, E.L., Genin, G.M., 2016. Tissue constructs: platforms for basic research and drug discovery. Interface Focus 6, 20150095. http://dx.doi.org/10.1098/rsfs.2015.0095.
Eshraghi, S., Das, S., 2012. Micromechanical finite-element modeling and experimental characterization of the compressive mechanical properties of polycaprolactone–hydroxyapatite composite scaffolds prepared by selective laser sintering for bone tissue engineering. Acta Biomater. 8, 3138–3143. http://dx.doi.org/10.1016/j.actbio.2012.04.022.
Faulkner-Jones, A., Fyfe, C., Cornelissen, D.-J., Gardner, J., King, J., Courtney, A., Shu, W., 2015. Bioprinting of human pluripotent stem cells and their directed differentiation into hepatocyte-like cells for the generation of mini-livers in 3D. Biofabrication 7, 044102. http://dx.doi.org/10.1088/1758-5090/7/4/044102.
Fedorovich, N.E., Oudshoorn, M.H., van Geemen, D., Hennink, W.E., Alblas, J., Dhert, W.J., 2009. The effect of photopolymerization on stem cells embedded in hydrogels. Biomaterials 30, 344–353. http://dx.doi.org/10.1016/j.biomaterials.2008.09.037.
Ferris, C.J., Gilmore, K.J., Beirne, S., McCallum, D., Wallace, G.G., in het Panhuis, M., 2013. Bio-ink for on-demand printing of living cells. Biomater. Sci. 1, 224–230. http://dx.doi.org/10.1039/C2BM00114D.
Fine, R.E., Whitworth, P.W., Kim, J.A., Harness, J.K., Boyd, B.A., Burak, W.E., 2003. Low-risk palpable breast masses removed using a vacuum-assisted hand-held device. Am. J. Surg. 186, 362–367. http://dx.doi.org/10.1016/S0002-9610(03)00263-0.
Frantz, C., Stewart, K.M., Weaver, V.M., 2010. The extracellular matrix at a glance. J. Cell Sci. 123, 4195–4200. http://dx.doi.org/10.1242/jcs.023820.
Frketic, J., Dickens, T., Ramakrishnan, S., 2017. Automated manufacturing and processing of fiber-reinforced polymer (FRP) composites: An additive review of contemporary and modern techniques for advanced materials manufacturing. Addit. Manuf. 14, 69–86. http://dx.doi.org/10.1016/j.addma.2017.01.003.
Fu, F., Qin, Z., Xu, C., Chen, X.Y., Li, R.X., Wang, L.N., Peng, D.W., Sun, H.T., Tu, Y., Chen, C., Zhang, S., Zhao, M.L., Li, X.H., 2017. Magnetic resonance imaging-three-dimensional printing technology fabricates customized scaffolds for brain tissue engineering. Neural Regen. Res. 12, 614–622. http://dx.doi.org/10.4103/1673-5374.205101.
Galantucci, L.M., Bodi, I., Kacani, J., Lavecchia, F., 2015. Analysis of Dimensional performance for a 3D open-source printer based on fused deposition modeling technique. Proc. CIRP 28, 82–87. http://dx.doi.org/10.1016/J.PROCIR.2015.04.014.
Gao, B., Yang, Q., Zhao, X., Jin, G., Ma, Y., Xu, F., 2016a. 4D bioprinting for biomedical applications. Trends Biotechnol. 34, 746–756. http://dx.doi.org/10.1016/J.TIBTECH.2016.03.004.
Gao, F., Chiu, S.M., Motan, D.A.L., Zhang, Z., Chen, L., Ji, H.-L., Tse, H.-F., Fu, Q.-L., Lian, Q., 2016b. Mesenchymal stem cells and immunomodulation: current status and future prospects. Cell Death Dis. 7, e2062. http://dx.doi.org/10.1038/cddis.2015.327.
Gardiner, B.S., Wong, K.K.L., Joldes, G.R., Rich, A.J., Tan, C.W., Burgess, A.W., Smith, D.W., 2015. Discrete Element Framework for Modelling Extracellular Matrix, Deformable Cells and Subcellular Components. PLoS Comput. Biol. 11, e1004544. http://dx.doi.org/10.1371/journal.pcbi.1004544.
Gasperini, L., Maniglio, D., Motta, A., Migliaresi, C., 2014. An electrohydrodynamic bioprinter for alginate hydrogels containing living cells. Tissue Eng. Part C Methods 21, 123–132. http://dx.doi.org/10.1089/ten.tec.2014.0149.
Gauvin, R., Chen, Y.-C., Lee, J.W., Soman, P., Zorlutuna, P., Nichol, J.W., Bae, H., Chen, S., Khademhosseini, A., 2012. Microfabrication of complex porous tissue engineering scaffolds using 3D projection stereolithography. Biomaterials 33, 3824–3834. http://dx.doi.org/10.1016/J.BIOMATERIALS.2012.01.048.
Gazeau, J.-P., Zeghloul, S., 2013. Design and operation of two service robot arms: a wide surface printing robot and an artist robot. In: Information Resources Management Association (Ed.), Robotics: Concepts, Methodologies, Tools, and Applications. IGI Global, USA, pp. 474–500.
Geckil, H., Xu, F., Zhang, X., Moon, S., Demirci, U., 2010. Engineering hydrogels as extracellular matrix mimics. Nanomedicine (London) 5, 469–484. http://dx.doi.org/10.2217/nnm.10.12.
Ghadiri, M., Chrzanowski, W., Lee, W.H., Fathi, A., Dehghani, F., Rohanizadeh, R., 2013. Physico-chemical, mechanical and cytotoxicity characterizations of Laponite®/alginate nanocomposite. Appl. Clay Sci. 85, 64–73. http://dx.doi.org/10.1016/j.clay.2013.08.049.
Gillette, B.M., Jensen, J.A., Wang, M., Tchao, J., Sia, S.K., 2010. Dynamic Hydrogels: Switching of 3D Microenvironments Using Two-Component Naturally Derived Extracellular Matrices. Adv. Mater. 22, 686–691. http://dx.doi.org/10.1002/adma.200902265.
Gomes, M.E., Rodrigues, M.T., Domingues, R.M.A., Reis, R.L., 2017. Tissue engineering and regenerative medicine: new trends and directions—a year in review. Tissue Eng. Part B Rev. 23, 211–224. http://dx.doi.org/10.1089/ten.teb.2017.0081.
Goody, M.F., Henry, C.A., 2010. Dynamic interactions between cells and their extracellular matrix mediate embryonic development. Mol. Reprod. Dev. 77, 475–488. http://dx.doi.org/10.1002/mrd.21157.
Gou, M., Qu, X., Zhu, W., Xiang, M., Yang, J., Zhang, K., Wei, Y., Chen, S., 2014. Bio-inspired detoxification using 3D-printed hydrogel nanocomposites. Nat. Commun. 5, 3774.
Grames, C.L., Jensen, B.D., Magleby, S.P., Howell, L.L., 2016. A Compact 2 Degree of Freedom Wrist for Robot-actuated Surgery and Other Applications 1–12. http://dx.doi.org/10.1115/DETC2016-60070.
Gruene, M., Deiwick, A., Koch, L., Schlie, S., Unger, C., Hofmann, N., Bernemann, I., Glasmacher, B., Chichkov, B., 2011b. Laser printing of stem cells for biofabrication of scaffold-free autologous grafts. Tissue Eng. Part C Methods 17, 79–87. http://dx.doi.org/10.1089/ten.TEC.2010.0359.
Gruene, M., Pflaum, M., Deiwick, A., Koch, L., Schlie, S., Unger, C., Wilhelmi, M., Haverich, A., Chichkov, B.N., 2011a. Adipogenic differentiation of laser-printed 3D tissue grafts consisting of human adipose-derived stem cells. Biofabrication 3. http://dx.doi.org/10.1088/1758-5082/3/1/015005.
Gudapati, H., Dey, M., Ozbolat, I., 2016. A comprehensive review on droplet-based bioprinting: past, present and future. Biomaterials 102, 20–42. http://dx.doi.org/10.1016/j.biomaterials.2016.06.012.
Guillemot, F., Souquet, A., Catros, S., Guillotin, B., Lopez, J., Faucon, M., Pippenger, B., Bareille, R., Rémy, M., Bellance, S., Chabassier, P., Fricain, J.C., Amédée, J., 2010. High-throughput laser printing of cells and biomaterials for tissue engineering. Acta Biomater. 6, 2494–2500. http://dx.doi.org/10.1016/j.actbio.2009.09.029.
Guillotin, B., Souquet, A., Catros, S., Duocastella, M., Pippenger, B., Bellance, S., Bareille, R., Rémy, M., Bordenave, L., Amédée, J., Guillemot, F., 2010. Laser assisted bioprinting of engineered tissue with high cell density and microscale organization. Biomaterials 31, 7250–7256. http://dx.doi.org/10.1016/j.biomaterials.2010.05.055.
Guo, T., Lembong, J., Zhang, L.G., Fisher, J.P., 2016. Three-dimensional printing articular cartilage: recapitulating the complexity of native tissue. Tissue Eng. Part B Rev. 23, 225–236. http://dx.doi.org/10.1089/ten.teb.2016.0316.
Guvendiren, M., Molde, J., Soares, R.M.D., Kohn, J., 2016. Designing biomaterials for 3D printing. ACS Biomater. Sci. Eng. 2, 1679–1693. http://dx.doi.org/10.1021/acsbiomaterials.6b00121.
Habib, S.J., Chen, B.-C., Tsai, F.-C., Anastassiadis, K., Meyer, T., Betzig, E., Nusse, R., 2013. A localized wnt signal orients asymmetric stem cell division in vitro. Science 339, 1445–1448. http://dx.doi.org/10.1126/science.1231077.
Hamazoe, R., Maeta, M., Murakami, A., Yamashiro, H., Kaibara, N., 1991. Heating efficiency of radiofrequency capacitive hyperthermia for treatment of deep-seated tumors in the peritoneal cavity. J. Surg. Oncol. 48, 176–179. http://dx.doi.org/10.1002/jso.2930480307.
Hasegawa, K., Zhang, P., Wei, Z., Pomeroy, J.E., Lu, W., Pera, M.F., 2010. Comparison of reprogramming efficiency between transduction of reprogramming factors, cell–cell fusion, and cytoplast fusion. Stem Cells 28, 1338–1348. http://dx.doi.org/10.1002/stem.466.
He, Y., Yang, F., Zhao, H., Gao, Q., Xia, B., Fu, J., 2016. Research on the printability of hydrogels in 3D bioprinting. Sci. Rep. 6, 29977. http://dx.doi.org/10.1038/srep29977.
Heller, M., Bauer, H.-K., Goetze, E., Gielisch, M., Ozbolat, I.T., Moncal, K.K., Rizk, E., Seitz, H., Gelinsky, M., Schroder, H.C., Wang, X.H., Muller, W.E.G., Al-Nawas, B., 2016. Materials and scaffolds in medical 3D printing and bioprinting in the context of bone regeneration. Int. J. Comput. Dent. 19, 301–321.
Hinton, T.J., Feinberg, A., 2016. 3D printing hydrogel and elastomer scaffolds in a fugitive support. In: Frontiers in Bioengineering and Biotechnology Conference Abstract: 10th World Biomaterials Congress. Montréal, Canada, pp. 3031. http://dx.doi.org/10.3389/conf.FBIOE.2016.01.03031.
Hinton, T.J., Jallerat, Q., Palchesko, R.N., Park, J.H., Grodzicki, M.S., Shue, H.J., Ramadan, M.H., Hudson, A.R., Feinberg, A.W., 2015. Three-dimensional printing of complex biological structures by freeform reversible embedding of suspended hydrogels. Sci. Adv. 1, e1500758. http://dx.doi.org/10.1126/sciadv.1500758.
Hinton, T.J., Hudson, A., Pusch, K., Lee, A., Feinberg, A.W., 2016. 3D Printing PDMS Elastomer in a Hydrophilic Support Bath via Freeform Reversible Embedding. ACS Biomater. Sci. Eng. 2, 1781–1786. http://dx.doi.org/10.1021/acsbiomaterials.6b00170.
Hölzl, K., Lin, S., Tytgat, L., Van Vlierberghe, S., Gu, L., Ovsianikov, A., 2016. Bioink properties before, during and after 3D bioprinting. Biofabrication 8, 32002. http://dx.doi.org/10.1088/1758-5090/8/3/032002.
Homan, K.A., Kolesky, D.B., Skylar-Scott, M.A., Herrmann, J., Obuobi, H., Moisan, A., Lewis, J.A., 2016. Bioprinting of 3D convoluted renal proximal tubules on perfusable chips. Sci. Rep. 6, 34845. http://dx.doi.org/10.1038/srep34845.
Hospodiuk, M., Dey, M., Sosnoski, D., Ozbolat, I.T., 2017. The bioink: a comprehensive review on bioprintable materials. Biotechnol. Adv. 35, 217–239. http://dx.doi.org/10.1016/j.biotechadv.2016.12.006.
Hospodiuk, M., Dey, M., Ayan, B., Sosnoski, D., Moncal, K.K., Wu, Y., Ozbolat, I.T., 2018. Sprouting angiogenesis in engineered pseudo islets. In: Biofabrication, http://dx.doi.org/10.1088/1758-5090/aab002.

Hsieh, F.-Y., Lin, H.-H., Hsu, S., 2015. 3D bioprinting of neural stem cell-laden thermoresponsive biodegradable polyurethane hydrogel and potential in central nervous system repair. Biomaterials 71, 48–57. http://dx.doi.org/10.1016/j.biomaterials.2015.08.028.

Huang, P., Zhang, L., Gao, Y., He, Z., Yao, D., Wu, Z., Cen, J., Chen, X., Liu, C., Hu, Y., Lai, D., Hu, Z., Chen, L., Zhang, Y., Cheng, X., Ma, X., Pan, G., Wang, X., Hui, L., 2014. Direct reprogramming of human fibroblasts to functional and expandable hepatocytes. Cell Stem Cell 14, 370–384. http://dx.doi.org/10.1016/j.stem.2014.01.003.

Huda, M.N., Yu, H., Cang, S., 2016. Robots for minimally invasive diagnosis and intervention. Robot. Comput. Manuf. 41, 127–144. http://dx.doi.org/10.1016/j.rcim.2016.03.003.

Ieda, M., Fu, J.-D., Delgado-Olguin, P., Vedantham, V., Hayashi, Y., Bruneau, B.G., Srivastava, D., 2010. Direct reprogramming of fibroblasts into functional cardiomyocytes by defined factors. Cell 142, 375–386. http://dx.doi.org/10.1016/j.cell.2010.07.002.

Irvine, S.A., Venkatraman, S.S., 2016. Bioprinting and differentiation of stem cells. Molecules 21, E1188.

Itskovitz-Eldor, J., Schuldiner, M., Karsenti, D., Eden, A., Yanuka, O., Amit, M., Soreq, H., Benvenisty, N., 2000. Differentiation of human embryonic stem cells into embryoid bodies compromising the three embryonic germ layers. Mol. Med. 6, 88–95.

Iyer, S.R., Xu, S., Stains, J.P., Bennett, C.H., Lovering, R.M., 2016. Superparamagnetic iron oxide nanoparticles in musculoskeletal biology. Tissue Eng. Part B Rev. 23, 373–385. http://dx.doi.org/10.1089/ten.teb.2016.0437.

Jana, S., Lerman, A., 2015. Bioprinting a cardiac valve. Biotechnol. Adv. 33, 1503–1521. http://dx.doi.org/10.1016/j.biotechadv.2015.07.006.

Ji, S., Guvendiren, M., 2017. Recent advances in bioink design for 3D bioprinting of tissues and organs. Front. Bioeng. Biotechnol. 5, 1–8. http://dx.doi.org/10.3389/fbioe.2017.00023.

Jia, J., Richards, D.J., Pollard, S., Tan, Y., Rodriguez, J., Visconti, R.P., Trusk, T.C., Yost, M.J., Yao, H., Markwald, R.R., Mei, Y., 2014. Engineering alginate as bioink for bioprinting. Acta Biomater. 10, 4323–4331. http://dx.doi.org/10.1016/J.ACTBIO.2014.06.034.

Jin, Y., He, Y., Xue, G., Fu, J., 2015. A parallel-based path generation method for fused deposition modeling. Int. J. Adv. Manuf. Technol. 77, 927–937. http://dx.doi.org/10.1007/s00170-014-6530-z.

Jin, Y., Compaan, A., Bhattacharjee, T., Huang, Y., 2016. Granular gel support-enabled extrusion of three-dimensional alginate and cellular structures. Biofabrication 8, 025016.

Jin, Y., Liu, C., Chai, W., Compaan, A., Huang, Y., 2017. Self-supporting nanoclay as internal scaffold material for direct printing of soft hydrogel composite structures in air. ACS Appl. Mater. Interfaces 9, 17456–17465. http://dx.doi.org/10.1021/acsami.7b03613.

Jokic, S., Novikov, P., Maggs, S., Sadan, D., Jin, S., Nan, C., 2014. Robotic positioning device for three-dimensional printing. In: CoRR abs/1406.3, arXiv:1406.3400.

Jones, D.L., Wagers, A.J., 2008. No place like home: anatomy and function of the stem cell niche. Nat. Rev. Mol. Cell Biol. 9, 11–21.

Jose, R.R., Rodriguez, M.J., Dixon, T.A., Omenetto, F., Kaplan, D.L., 2016. Evolution of bioinks and additive manufacturing technologies for 3D bioprinting. ACS Biomater. Sci. Eng. 2, 1662–1668. http://dx.doi.org/10.1021/acsbiomaterials.6b00088.

Kang, H.-W., Lee, S.J., Ko, I.K., Kengla, C., Yoo, J.J., Atala, A., 2016. A 3D bioprinting system to produce human-scale tissue constructs with structural integrity. Nat. Biotechnol. 34, 312–319. http://dx.doi.org/10.1038/nbt.3413.

Kato, R., Iejima, D., Agata, H., Asahina, I., Okada, K., Ueda, M., Honda, H., Kagami, H., 2009. A compact, automated cell culture system for clinical scale cell expansion from primary tissues. Tissue Eng. Part C Methods 16, 947–956. http://dx.doi.org/10.1089/ten.tec.2009.0305.

Ke, N., Wang, X., Xu, X., Abassi, Y.A., 2011. In: Stoddart, M.J. (Ed.), The xCELLigence system for real-time and label-free monitoring of cell viability BT - mammalian cell viability: methods and protocols. Humana Press, Totowa, NJ, pp. 33–43. http://dx.doi.org/10.1007/978-1-61779-108-6_6.

Kesti, M., Müller, M., Becher, J., Schnabelrauch, M., D'Este, M., Eglin, D., Zenobi-Wong, M., 2015. A versatile bioink for three-dimensional printing of cellular scaffolds based on thermally and photo-triggered tandem gelation. Acta Biomater. 11, 162–172. http://dx.doi.org/10.1016/j.actbio.2014.09.033.

Kesti, M., Fisch, P., Pensalfini, M., Mazza, E., Zenobi-Wong, M., 2016. Guidelines for standardization of bioprinting: A systematic study of process parameters and their effect on bioprinted structures. BioNanoMaterials 17, 193–204. http://dx.doi.org/10.1515/bnm-2016-0004.

Khademhosseini, A., Langer, R., Borenstein, J., Vacanti, J.P., 2006. Microscale technologies for tissue engineering and biology. Proc. Natl. Acad. Sci. U. S. A. 103, 2480–2487. http://dx.doi.org/10.1073/pnas.0507681102.

Khalil, S., Nam, J., Sun, W., 2005. Multi-nozzle deposition for construction of 3D biopolymer tissue scaffolds. Rapid Prototyp. J. 11, 9–17. http://dx.doi.org/10.1108/13552540510573347.

Khati, V., 2016. Development of a robust decellularized extracellular matrix bioink for 3D bioprinting. Tampere University of Technology. https://dspace.cc.tut.fi/dpub/handle/123456789/23772?show=full.

Khattak, S.F., Bhatia, S.R., Roberts, S.C., 2005. Pluronic F127 as a cell encapsulation material: utilization of membrane-stabilizing agents. Tissue Eng. 11, 974–983. http://dx.doi.org/10.1089/ten.2005.11.974.

Khoda, B., 2014. Build direction for improved process plan in multi-material additive manufacturing. 3D print. Addit. Manuf. 1, 210–218. http://dx.doi.org/10.1115/DETC2014-35060.

Khoda, A.K.M., Ozbolat, I.T., Koc, B., 2013. Designing heterogeneous porous tissue scaffolds for additive manufacturing processes. Comput. Des. 45, 1507–1523. http://dx.doi.org/10.1016/J.CAD.2013.07.003.

Kim, J.S., Sun, S.X., 2009. Continuum modeling of forces in growing viscoelastic cytoskeletal networks. J. Theor. Biol. 256, 596–606. http://dx.doi.org/10.1016/j.jtbi.2008.10.023.

Kim, J.D., Choi, J.S., Kim, B.S., Chan Choi, Y., Cho, Y.W., 2010. Piezoelectric inkjet printing of polymers: stem cell patterning on polymer substrates. Polymer (Guildf) 51, 2147–2154. http://dx.doi.org/10.1016/j.polymer.2010.03.038.

Kirchmajer, D.M., Gorkin III, R., in het Panhuis, M., 2015. An overview of the suitability of hydrogel-forming polymers for extrusion-based 3D-printing. J. Mater. Chem. B 3, 4105–4117. http://dx.doi.org/10.1039/C5TB00393H.

Knowlton, S., Joshi, A., Yenilmez, B., Ozbolat, I.T., Chua, C.K., Khademhosseini, A., Tasoglu, S., 2016. Advancing cancer research using bioprinting for tumor-on-a-chip platforms. Int. J. Bioprinting 2, 3–8. http://dx.doi.org/10.18063/IJB.2016.02.003.

Kolesky, D.B., Homan, K.A., Skylar-scott, M.A., Lewis, J.A., 2016. Three-dimensional bioprinting of thick vascularized tissues. Proc. Natl. Acad. Sci. Am. 113, 3179–3184. http://dx.doi.org/10.1073/pnas.1521342113.

Kurosawa, H., 2007. Methods for inducing embryoid body formation: in vitro differentiation system of embryonic stem cells. J. Biosci. Bioeng. 103, 389–398. http://dx.doi.org/10.1263/jbb.103.389.

Kyle, S., Jessop, Z.M., Al-Sabah, A., Whitaker, I.S., 2017. "Printability" of candidate biomaterials for extrusion based 3D printing: state-of-the-art. Adv. Healthc. Mater. 6, 1700264. http://dx.doi.org/10.1002/adhm.201700264.

Landers, R., Hübner, U., Schmelzeisen, R., Mülhaupt, R., 2002a. Rapid prototyping of scaffolds derived from thermoreversible hydrogels and tailored for applications in tissue engineering. Biomaterials 23, 4437–4447. http://dx.doi.org/10.1016/S0142-9612(02)00139-4.

Landers, R., Pfister, A., Hübner, U., John, H., Schmelzeisen, R., Mülhaupt, R., 2002b. Fabrication of soft tissue engineering scaffolds by means of rapid prototyping techniques. J. Mater. Sci. 37, 3107–3116. http://dx.doi.org/10.1023/A:1016189724389.

Lanza, R., Langer, R., Vacanti, J. (Eds.), 2007. Principles of Tissue Engineering, 3rd ed. Elsevier.

Larobina, M., Murino, L., 2014. Medical image file formats. J. Digit. Imaging 27, 200–206. http://dx.doi.org/10.1007/s10278-013-9657-9.

Leberfinger, A.N., Ravnic, D.J., Dhawan, A., Ozbolat, I.T., 2017. Concise review: bioprinting of stem cells for transplantable tissue fabrication. Stem Cells Transl. Med. 6, 1940–1948. http://dx.doi.org/10.1002/sctm.17-0148.

Lee, J.M., Yeong, W.Y., 2016. Design and printing strategies in 3D bioprinting of cell-hydrogels: a review. Adv. Healthc. Mater. 5, 2856–2865. http://dx.doi.org/10.1002/adhm.201600435.

Lee, H.-Y., Kim, H.-W., Lee, J.H., Oh, S.H., 2015. Controlling oxygen release from hollow microparticles for prolonged cell survival under hypoxic environment. Biomaterials 53, 583–591. http://dx.doi.org/10.1016/J.BIOMATERIALS.2015.02.117.

Lee, H., Koo, Y., Yeo, M., Kim, S., Kim, G.H., 2017a. Recent Cell printing systems for tissue engineering. Int. J. Bioprinting 3, 27–41. http://dx.doi.org/10.18063/IJB.2017.01.004.

Lee, J., Kim, K.E., Bang, S., Noh, I., Lee, C., 2017b. A desktop multi-material 3D bioprinting system with open-source hardware and software. Int. J. Precis. Eng. Manuf. 18, 605–612. http://dx.doi.org/10.1007/s12541-017-0072-x.

Levato, R., Visser, J., Planell, J.A., Engel, E., Malda, J., Mateos-Timoneda, M.A., 2014. Biofabrication of tissue constructs by 3D bioprinting of cell-laden microcarriers. Biofabrication 6, 35020. http://dx.doi.org/10.1088/1758-5082/6/3/035020.

Levin, M.L., Lober, C., Levin, R.R., 1989. Harvesting auricular cartilage. J. Dermatol. Surg. Oncol. 15, 712–713. http://dx.doi.org/10.1111/j.1524-4725.1989.tb03617.x.

Li, J.P., de Wijn, J.R., van Blitterswijk, C.A., de Groot, K., 2010. The effect of scaffold architecture on properties of direct 3D fiber deposition of porous Ti6Al4V for orthopedic implants. J. Biomed. Mater. Res. A 92, 33–42. http://dx.doi.org/10.1002/jbm.a.32330.

Li, J., Rossignol, F., Macdonald, J., 2015. Inkjet printing for biosensor fabrication: combining chemistry and technology for advanced manufacturing. Lab Chip 15, 2538–2558. http://dx.doi.org/10.1039/C5LC00235D.

Li, J., Chen, M., Fan, X., Zhou, H., 2016. Recent advances in bioprinting techniques: approaches, applications and future prospects. J. Transl. Med. 14, 271. http://dx.doi.org/10.1186/s12967-016-1028-0.

Li, P., Tong, C., Mehrian-Shai, R., Jia, L., Wu, N., Yan, Y., Maxson, R.E., Schulze, E.N., Song, H., Hsieh, C.L., Pera, M.F., Ying, Q.-L., 2008. Germline competent embryonic stem cells derived from rat blastocysts. Cell 135, 1299–1310. http://dx.doi.org/10.1016/j.cell.2008.12.006.

Li, K., Zhang, C., Qiu, L., Gao, L., Zhang, X., 2017. Advances in application of mechanical stimuli in bioreactors for cartilage tissue engineering. Tissue Eng. Part B Rev. 23, 399–411. http://dx.doi.org/10.1089/ten.teb.2016.0427.

Lin, L., Zhang, H., Yao, Y., Tong, A., Hu, Q., Fang, M., 2007. In: Li, K., Li, X., Irwin, G.W., He, G. (Eds.), Application of Image Processing and Finite Element Analysis in Bionic Scaffolds' Design Optimizing and Fabrication BT - Life System Modeling and Simulation: International Conference, LSMS 2007, Shanghai, China, September 14-17, 2007. Proceedings. Springer Berlin Heidelberg, Berlin, Heidelberg, pp. 136–145. http://dx.doi.org/10.1007/978-3-540-74771-0_16.

Louis, K.S., Siegel, A.C., 2011. In: Stoddart, M.J. (Ed.), Cell viability analysis using trypan blue: manual and automated methods BT - mammalian cell viability: methods and protocols. Humana Press, Totowa, NJ, pp. 7–12. http://dx.doi.org/10.1007/978-1-61779-108-6_2.

Lukovic, D., Diez Lloret, A., Stojkovic, P., Rodríguez-Martínez, D., Perez Arago, M.A., Rodriguez-Jimenez, F.J., González-Rodríguez, P., López-Barneo, J., Sykova, E., Jendelova, P., Kostic, J., Moreno-Manzano, V., Stojkovic, M., Bhattacharya, S.S., Erceg, S., 2017. Highly efficient neural conversion of human pluripotent stem cells in adherent and animal-free conditions. Stem Cells Transl. Med. 6, 1217–1226. http://dx.doi.org/10.1002/sctm.16-0371.

Lyu, J., Cao, J., Zhang, P., Liu, Y., Cheng, H., 2016. Coupled Hybrid Continuum-Discrete

Model of Tumor Angiogenesis and Growth. PLoS One 11, e0163173. http://dx.doi.org/10.1371/journal.pone.0163173.
Madrigal, M., Rao, K.S., Riordan, N.H., 2014. A review of therapeutic effects of mesenchymal stem cell secretions and induction of secretory modification by different culture methods. J. Transl. Med. 12, 260. http://dx.doi.org/10.1186/s12967-014-0260-8.
Mahmoud, S., Eldeib, A., Samy, S., 2015. The design of 3D scaffold for tissue engineering using automated scaffold design algorithm. Australas. Phys. Eng. Sci. Med. 38, 223–228. http://dx.doi.org/10.1007/s13246-015-0339-4.
Malda, J., Frondoza, C.G., 2006. Microcarriers in the engineering of cartilage and bone. Trends Biotechnol. 24, 299–304. http://dx.doi.org/10.1016/j.tibtech.2006.04.009.
Malda, J., Visser, J., Melchels, F.P., Jüngst, T., Hennink, W.E., Dhert, W.J.A., Groll, J., Hutmacher, D.W., 2013. 25th anniversary article: Engineering hydrogels for biofabrication. Adv. Mater. 25, 5011–5028. http://dx.doi.org/10.1002/adma.201302042.
Mandrycky, C., Wang, Z., Kim, K., Kim, D.-H., 2016. 3D bioprinting for engineering complex tissues. Biotechnol. Adv. 34, 422–434. http://dx.doi.org/10.1016/j.biotechadv.2015.12.011.
Margaliot, M., 2008. Biomimicry and fuzzy modeling: a match made in heaven. IEEE Comput. Intell. Mag. 3, 38–48. http://dx.doi.org/10.1109/MCI.2008.926602.
Markstedt, K., Mantas, A., Tournier, I., Martínez Ávila, H., Hägg, D., Gatenholm, P., 2015. 3D bioprinting human chondrocytes with nanocellulose–alginate bioink for cartilage tissue engineering applications. Biomacromolecules 16, 1489–1496. http://dx.doi.org/10.1021/acs.biomac.5b00188.
Martin, G.R., 1981. Isolation of a pluripotent cell line from early mouse embryos cultured in medium conditioned by teratocarcinoma stem cells. Proc. Natl. Acad. Sci. U. S. A. 78, 7634–7638.
Martin, I., Wendt, D., Heberer, M., 2004. The role of bioreactors in tissue engineering. Trends Biotechnol. 22, 80–86. http://dx.doi.org/10.1016/j.tibtech.2003.12.001.
Massarwi, F., Elber, G., 2016. A B-spline based framework for volumetric object modeling. Comput. Aided Des. 78, 36–47. http://dx.doi.org/10.1016/j.cad.2016.05.003.
Matthew, J.E., Nazario, Y.L., Roberts, S.C., Bhatia, S.R., 2002. Effect of mammalian cell culture medium on the gelation properties of Pluronic® F127. Biomaterials 23, 4615–4619. http://dx.doi.org/10.1016/S0142-9612(02)00208-9.
Mauck, R.L., Wang, C.B., Oswald, E.S., Ateshian, G.A., Hung, C.T., 2003. The role of cell seeding density and nutrient supply for articular cartilage tissue engineering with deformational loading. Osteoarthr. Cartil. 11, 879–890. http://dx.doi.org/10.1016/j.joca.2003.08.006.
McCormick, M., Liu, X., Jomier, J., Marion, C., Ibanez, L., 2014. ITK: enabling reproducible research and open science. Front. Neuroinform. 8, 13. http://dx.doi.org/10.3389/fninf.2014.00013.
McDannold, N., Hynynen, K., Wolf, D., Wolf, G., Jolesz, F., 1998. MRI evaluation of thermal ablation of tumors with focused ultrasound. J. Magn. Reson. Imaging 8, 91–100. http://dx.doi.org/10.1002/jmri.1880080119.
Megerian, C.A., Weitzner, B.D., Dore, B., Bonassar, L.J., 2000. Minimally invasive technique of auricular cartilage harvest for tissue engineering. Tissue Eng. 6, 69–74. http://dx.doi.org/10.1089/107632700320900.
Mehdizadeh, H., Bayrak, E.S., Lu, C., Somo, S.I., Akar, B., Brey, E.M., Cinar, A., 2015. Agent-based modeling of porous scaffold degradation and vascularization: Optimal scaffold design based on architecture and degradation dynamics. Acta Biomater. 27, 167–178. http://dx.doi.org/10.1016/j.actbio.2015.09.011.
Melchels, F.P.W., Feijen, J., Grijpma, D.W., 2009. A poly(d,l-lactide) resin for the preparation of tissue engineering scaffolds by stereolithography. Biomaterials 30, 3801–3809. http://dx.doi.org/10.1016/j.biomaterials.2009.03.055.
Miller, E.D., Li, K., Kanade, T., Weiss, L.E., Walker, L.M., Campbell, P.G., 2011. Spatially directed guidance of stem cell population migration by immobilized patterns of growth factors. Biomaterials 32, 2775–2785. http://dx.doi.org/10.1016/j.biomaterials.2010.12.005.
Moldovan, L., Babbey, C., Murphy, M., Moldovan, N.I., 2017. Comparison of biomaterial-dependent and -independent bioprinting methods for cardiovascular medicine. Curr. Opin. Biomed. Eng. 2, 124–131. http://dx.doi.org/10.1016/j.cobme.2017.05.009.
Möller, T., Amoroso, M., Hägg, D., Brantsing, C., Rotter, N., Apelgren, P., Lindahl, A., Kölby, L., Gatenholm, P., 2017. In vivo chondrogenesis in 3D bioprinted human cell-laden hydrogel constructs. Plast. Reconstr. Surg. Glob. Open 5, e1227. http://dx.doi.org/10.1097/GOX.0000000000001227.
Munaz, A., Vadivelu, R.K., St. John, J., Barton, M., Kamble, H., Nguyen, N.-T., 2016. Three-dimensional printing of biological matters. J. Sci. Adv. Mater. Devices 1, 1–17. http://dx.doi.org/10.1016/j.jsamd.2016.04.001.
Murphy, S.V., Atala, A., 2014. 3D bioprinting of tissues and organs. Nat. Biotechnol. 32, 773–785. http://dx.doi.org/10.1038/nbt.2958.
Murphy, C.M., Matsiko, A., Haugh, M.G., Gleeson, J.P., O'Brien, F.J., 2012. Mesenchymal stem cell fate is regulated by the composition and mechanical properties of collagen–glycosaminoglycan scaffolds. J. Mech. Behav. Biomed. Mater. 11, 53–62. http://dx.doi.org/10.1016/j.jmbbm.2011.11.009.
Murray, P.J., Walter, A., Fletcher, A.G., Edwards, C.M., Tindall, M.J., Maini, P.K., 2011. Comparing a discrete and continuum model of the intestinal crypt. Phys. Biol. 8, 26011. http://dx.doi.org/10.1088/1478-3975/8/2/026011.
Mycek, M.-A., 2015. Clinical translation of optical molecular imaging to tissue engineering: opportunities & challenges. In: Optics in the Life Sciences, OSA Technical Digest. Optical Society of America, Vancouver (p. OT1C.1).
Nagahara, S., Matsuda, T., 1996. Cell-substrate and cell-cell interactions differently regulate cytoskeletal and extracellular matrix protein gene expression. J. Biomed. Mater. Res. 32, 677–686.
Nair, K., Gandhi, M., Khalil, S., Yan, K.C., Marcolongo, M., Barbee, K., Sun, W., 2009. Characterization of cell viability during bioprinting processes. Biotechnol. J. 4, 1168–1177. http://dx.doi.org/10.1002/biot.200900004.
Nam, S.Y., Ricles, L.M., Suggs, L.J., Emelianov, S.Y., 2014. Imaging strategies for tissue engineering applications. Tissue Eng. Part B. Rev. 21, 1–44. http://dx.doi.org/10.1089/ten.TEB.2014.0180.
Nawroth, J.C., Parker, K.K., 2013. Design standards for engineered tissues. Biotechnol. Adv. 31, 632–637. http://dx.doi.org/10.1016/j.biotechadv.2012.12.005.
Newby, G.E., Hamley, I.W., King, S.M., Martin, C.M., Terrill, N.J., 2009. Structure, rheology and shear alignment of Pluronic block copolymer mixtures. J. Colloid Interface Sci. 329, 54–61. http://dx.doi.org/10.1016/J.JCIS.2008.09.054.
Ng, W.L., Lee, J.M., Yeong, W.Y., Win Naing, M., 2017a. Microvalve-based bioprinting - process, bio-inks and applications. Biomater. Sci. 5, 632–647. http://dx.doi.org/10.1039/C6BM00861E.
Ng, W.L., Yeong, W.Y., Naing, M.W., 2017b. Polyvinylpyrrolidone-based bio-ink improves cell viability and homogeneity during drop-on-demand printing. Materials (Basel) 10. http://dx.doi.org/10.3390/ma10020190.
Nguyen, K.T., West, J.L., 2002. Photopolymerizable hydrogels for tissue engineering applications. Biomaterials 23, 4307–4314. http://dx.doi.org/10.1016/S0142-9612(02)00175-8.
Nguyen, D.G., Funk, J., Robbins, J.B., Crogan-Grundy, C., Presnell, S.C., Singer, T., Roth, A.B., 2016. Bioprinted 3D primary liver tissues allow assessment of organ-level response to clinical drug induced toxicity in vitro. PLoS One 11, e0158674.
Nicodemus, G.D., Bryant, S.J., 2008. Cell encapsulation in biodegradable hydrogels for tissue engineering applications. Tissue Eng. B Rev. 14, 149–165. http://dx.doi.org/10.1089/ten.teb.2007.0332.
Nishiyama, Y., Nakamura, M., Henmi, C., Yamaguchi, K., Mochizuki, S., Nakagawa, H., Takiura, K., 2009. Development of a three-dimensional bioprinter: construction of cell supporting structures using hydrogel and state-of-the-art inkjet technology. J. Biomech. Eng. 131, 35001. http://dx.doi.org/10.1115/1.3002759.
Norotte, C., Marga, F.S., Niklason, L.E., Forgacs, G., 2009. Scaffold-free vascular tissue engineering using bioprinting. Biomaterials 30, 5910–5917. http://dx.doi.org/10.1016/j.biomaterials.2009.06.034.
Obeng-Gyasi, S., Grimm, L.J., Hwang, E.S., Klimberg, V.S., Bland, K.I., 2018. 28 - Indications and Techniques for Biopsy BT - The Breast (Fifth Edition). Elsevier, pp. 377–385. e2. https://doi.org/10.1016/B978-0-323-35955-9.00028-3.
Odde, D.J., Renn, M.J., 2000. Laser-guided direct writing of living cells. Biotechnol. Bioeng. 67, 312–318. http://dx.doi.org/10.1002/(SICI)1097-0290(20000205)67:3<312::AID-BIT7>3.0.CO;2-F.
Ouyang, L., Yao, R., Chen, X., Na, J., Sun, W., 2015. 3D printing of HEK 293FT cell-laden hydrogel into macroporous constructs with high cell viability and normal biological functions. Biofabrication 7, 015010. http://dx.doi.org/10.1088/1758-5090/7/1/015010.
Ouyang, L., Yao, R., Zhao, Y., Sun, W., 2016. Effect of bioink properties on printability and cell viability for 3D bioplotting of embryonic stem cells. Biofabrication 8, 035020. http://dx.doi.org/10.1088/1758-5090/8/3/035020.
Ozbolat, I.T., 2017. 3D Bioprinting: Fundamentals, Principles and Apllications. Academic Press, London, United Kingdom.
Ozbolat, I.T., Gudapati, H., 2016. A review on design for bioprinting. Bioprinting 3–4, 1–14. http://dx.doi.org/10.1016/j.bprint.2016.11.001.
Ozbolat, I.T., Hospodiuk, M., 2016. Current advances and future perspectives in extrusion-based bioprinting. Biomaterials 76, 321–343. http://dx.doi.org/10.1016/j.biomaterials.2015.10.076.
Ozbolat, I.T., Khoda, A.K.M.B., 2014. Design of a new parametric path plan for additive manufacturing of hollow porous structures with functionally graded materials. J. Comput. Inf. Sci. Eng. 14, 41005–41013.
Ozbolat, I.T., Koc, B., 2012. 3D hybrid wound devices for spatiotemporally controlled release kinetics. Comput. Methods Prog. Biomed. 108, 922–931. http://dx.doi.org/10.1016/j.cmpb.2012.05.004.
Ozbolat, I.T., Moncal, K.K., Gudapati, H., 2017. Evaluation of bioprinter technologies. Addit. Manuf. 13, 179–200. http://dx.doi.org/10.1016/j.addma.2016.10.003.
Ozler, S.B., Kucukgul, C., Koc, B., 2015. Bioprinting with live cells. In: Turksen, K. (Ed.), Bioprinting in Regenerative Medicine. Springer International Publishing, Cham, pp. 67–88. http://dx.doi.org/10.1007/978-3-319-21386-6_3.
Park, H.-L., Kim, L.S., 2011. The current role of vacuum assisted breast biopsy system in breast disease. J. Breast Cancer 14, 1–7. http://dx.doi.org/10.4048/jbc.2011.14.1.1.
Park, S., Kim, S., Choi, J., 2015. Development of a multi-nozzle bioprinting system for 3D tissue structure fabrication. In: 2015 15th Int. Conf. Control. Autom. Syst, http://dx.doi.org/10.1109/ICCAS.2015.7364668.
Park, S.H., Kang, B.K., Lee, J.E., Chun, S.W., Jang, K., Kim, Y.H., Jeong, M.A., Kim, Y., Kang, K., Lee, N.K., Choi, D., Kim, H.J., 2017. Design and fabrication of a thin-walled free-form scaffold on the basis of medical image data and a 3D printed template: its potential use in bile duct regeneration. ACS Appl. Mater. Interfaces 9, 12290–12298. http://dx.doi.org/10.1021/acsami.7b00849.
Pati, F., Cho, D.-W., 2017. In: Koledova, Z. (Ed.), Bioprinting of 3D Tissue Models Using Decellularized Extracellular Matrix Bioink BT - 3D Cell Culture: Methods and Protocols. Springer New York, New York, NY, pp. 381–390. http://dx.doi.org/10.1007/978-1-4939-7021-6_27.
Pawlowski, M., Ortmann, D., Bertero, A., Tavares, J.M., Pedersen, R.A., Vallier, L., Kotter, M.R.N., 2017. Inducible and deterministic forward programming of human pluripotent stem cells into neurons, skeletal myocytes, and oligodendrocytes. Stem Cell Rep. 8, 803–812. http://dx.doi.org/10.1016/j.stemcr.2017.02.016.
Peerani, R., Rao, B.M., Bauwens, C., Yin, T., Wood, G.A., Nagy, A., Kumacheva, E., Zandstra, P.W., 2007. Niche-mediated control of human embryonic stem cell self-renewal and differentiation. EMBO J. 26, 4744–4755. http://dx.doi.org/10.1038/sj.emboj.7601896.
Peltola, S.M., Melchels, F.P.W., Grijpma, D.W., Kellomäki, M., 2008. A review of rapid prototyping techniques for tissue engineering purposes. Ann. Med. 40, 268–280. http://dx.doi.org/10.1080/07853890701881788.

Peng, W., Unutmaz, D., Ozbolat, I.T., 2016. Bioprinting towards physiologically relevant tissue models for pharmaceutics. Trends Biotechnol. 34, 722–732. http://dx.doi.org/10.1016/J.TIBTECH.2016.05.013.

Peng, W., Datta, P., Ayan, B., Ozbolat, V., Sosnoski, D., Ozbolat, I.T., 2017. 3D bioprinting for drug discovery and development in pharmaceutics. Acta Biomater. 57, 26–46. http://dx.doi.org/10.1016/j.actbio.2017.05.025.

Pepper, M.E., Seshadri, V., Burg, T.C., Burg, K.J.L., Groff, R.E., 2012. Characterizing the effects of cell settling on bioprinter output. Biofabrication 4, 11001. http://dx.doi.org/10.1088/1758-5082/4/1/011001.

Phillippi, J.A., Miller, E., Weiss, L., Huard, J., Waggoner, A., Campbell, P., 2008. Microenvironments engineered by inkjet bioprinting spatially direct adult stem cells toward muscle- and bone-like subpopulations. Stem Cells 26, 127–134. http://dx.doi.org/10.1634/stemcells.2007-0520.

Pirraco, R.P., Marques, A.P., Reis, R.L., 2010. Cell interactions in bone tissue engineering. J. Cell. Mol. Med. 14, 93–102. http://dx.doi.org/10.1111/j.1582-4934.2009.01005.x.

Placzek, M.R., Chung, I.M., Macedo, H.M., Ismail, S., Mortera Blanco, T., Lim, M., Cha, J.M., Fauzi, I., Kang, Y., Yeo, D.C., Ma, C.Y., Polak, J.M., Panoskaltsis, N., Mantalaris, A., 2009. Stem cell bioprocessing: fundamentals and principles. J. R. Soc. Interface 209–232. http://dx.doi.org/10.1098/rsif.2008.0442.

Plunkett, N., O'Brien, F.J., 2010. Bioreactors in tissue engineering. Stud. Health Technol. Inform. 152, 214–230. http://dx.doi.org/10.3233/THC-2011-0605.

Pohlig, F., Kirchhoff, C., Lenze, U., Schauwecker, J., Burgkart, R., Rechl, H., von Eisenhart-Rothe, R., 2012. Percutaneous core needle biopsy versus open biopsy in diagnostics of bone and soft tissue sarcoma: a retrospective study. Eur. J. Med. Res. 17, 29. http://dx.doi.org/10.1186/2047-783X-17-29.

Poser, B.A., Setsompop, K., 2017. Pulse sequences and parallel imaging for high spatiotemporal resolution MRI at ultra-high field. NeuroImage 1–18. http://dx.doi.org/10.1016/j.neuroimage.2017.04.006.

Potjewyd, G., Moxon, S., Wang, T., Domingos, M., Hooper, N.M., 2018. Tissue engineering 3D neurovascular units: a biomaterials and bioprinting perspective. Trends Biotechnol. 36, 457–472. http://dx.doi.org/10.1016/j.tibtech.2018.01.003.

Raof, N.A., Schiele, N.R., Xie, Y., Chrisey, D.B., Corr, D.T., 2011. The maintenance of pluripotency following laser direct-write of mouse embryonic stem cells. Biomaterials 32, 1802–1808. http://dx.doi.org/10.1016/j.biomaterials.2010.11.015.

Rauh, J., Milan, F., Günther, K.-P., Stiehler, M., 2011. Bioreactor systems for bone tissue engineering. Tissue Eng. Part B. Rev. 17, 263–280. http://dx.doi.org/10.1089/ten.teb.2010.0612.

Ravnic, D.J., Leberfinger, A.N., Ozbolat, I.T., 2017. Bioprinting and cellular therapies for type 1 diabetes. Trends Biotechnol. 35, 1025–1034. http://dx.doi.org/10.1016/J.TIBTECH.2017.07.006.

Reid, J.A., Mollica, P.A., Johnson, G.D., Ogle, R.C., Bruno, R.D., Sachs, P.C., 2016. Accessible bioprinting: adaptation of a low-cost 3D-printer for precise cell placement and stem cell differentiation. Biofabrication 8, 025017. http://dx.doi.org/10.1088/1758-5090/8/2/025017.

Reiffel, A.J., Kafka, C., Hernandez, K.A., Popa, S., Perez, J.L., Zhou, S., Pramanik, S., Brown, B.N., Ryu, W.S., Bonassar, L.J., Spector, J.A., 2013. High-fidelity tissue engineering of patient-specific auricles for reconstruction of pediatric microtia and other auricular deformities. PLoS One 8, e56506. http://dx.doi.org/10.1371/journal.pone.0056506.

Ren, L., Zhou, X., Song, Z., Zhao, C., Liu, Q., Xue, J., Li, X., 2017. Process parameter optimization of extrusion-based 3D metal printing utilizing PW–LDPE–SA binder system. Materials (Basel) 10, 305. http://dx.doi.org/10.3390/ma10030305.

Requicha, A.G., 1980. Representations for rigid solids: theory, methods, and systems. ACM Comput. Surv. 12, 437–464. http://dx.doi.org/10.1145/356827.356833.

Rezende, R.A., Bártolo, P.J., Mendes, A., Filho, R.M., 2009. Rheological behavior of alginate solutions for biomanufacturing. J. Appl. Polym. Sci. 113, 3866–3871. http://dx.doi.org/10.1002/app.30170.

Rodriguez, M.J., Brown, J., Giordano, J., Lin, S.J., Omenetto, F.G., Kaplan, D.L., 2017. Silk based bioinks for soft tissue reconstruction using 3-dimensional (3D) printing with in vitro and in vivo assessments. Biomaterials 117, 105–115. http://dx.doi.org/10.1016/j.biomaterials.2016.11.046.

Rodríguez-Salvador, M., Rio-Belver, R.M., Garechana-Anacabe, G., 2017. Scientometric and patentometric analyses to determine the knowledge landscape in innovative technologies: The case of 3D bioprinting. PLoS One 12, e0180375. http://dx.doi.org/10.1371/journal.pone.0180375.

Rutz, A.L., Lewis, P.L., Shah, R.N., 2017. Toward next-generation bioinks: Tuning material properties pre- and post-printing to optimize cell viability. MRS Bull. 42, 563–570. http://dx.doi.org/10.1557/mrs.2017.162.

Sadelain, M., Papapetrou, E.P., Bushman, F.D., 2011. Safe harbours for the integration of new DNA in the human genome. Nat. Rev. Cancer 12, 51–58. http://dx.doi.org/10.1038/nrc3179.

Salacinski, H.J., Tai, N.R., Carson, R.J., Edwards, A., Hamilton, G., Seifalian, A.M., 2002. In vitro stability of a novel compliant poly(carbonate-urea)urethane to oxidative and hydrolytic stress. J. Biomed. Mater. Res. 59, 207–218. http://dx.doi.org/10.1002/jbm.1234.

Salih, V., 2013. Introduction, in: Standardisation in Cell and Tissue Engineering' Woodhead Publishing Series in Biomaterials. Woodhead Publishing, pp. xxiii–xxvi. http://dx.doi.org/10.1016/B978-0-85709-419-3.50017-0.

Seidel, J., Ahlfeld, T., Adolph, M., Kümmritz, S., Steingroewer, J., Krujatz, F., Bley, T., Gelinsky, M., Lode, A., 2017. Green bioprinting: extrusion-based fabrication of plant cell-laden biopolymer hydrogel scaffolds. Biofabrication 9, 45011. http://dx.doi.org/10.1088/1758-5090/aa8854.

Seidlits, S.K., Khaing, Z.Z., Petersen, R.R., Nickels, J.D., Vanscoy, J.E., Shear, J.B., Schmidt, C.E., 2010. The effects of hyaluronic acid hydrogels with tunable mechanical properties on neural progenitor cell differentiation. Biomaterials 31, 3930–3940. http://dx.doi.org/10.1016/j.biomaterials.2010.01.125.

Shen, H., Goldstein, A.S., Wang, G., 2011. Biomedical imaging and image processing in tissue engineering BT - tissue engineering: from lab to clinic. In: Pallua, N., Suscheck, C.V. (Eds.), Tissue Eng. Springer Berlin Heidelberg, Berlin, Heidelberg, pp. 155–178. http://dx.doi.org/10.1007/978-3-642-02824-3_9.

Shim, J.-H., Kim, J.Y., Park, M., Park, J., Cho, D.-W., 2011. Development of a hybrid scaffold with synthetic biomaterials and hydrogel using solid freeform fabrication technology. Biofabrication 3, 034102. http://dx.doi.org/10.1088/1758-5082/3/3/034102.

Skardal, A., Zhang, J., Mccoard, L., Xu, X., Oottamasathien, S., Prestwich, G.D., 2010a. Photocrosslinkable hyaluronan-gelatin hydrogels for two-step bioprinting. Tissue Eng. Part A 16, 2675–2685. http://dx.doi.org/10.1089/ten.tea.2009.0798.

Skardal, A., Zhang, J., Prestwich, G.D., 2010b. Bioprinting vessel like constructs using hyaluronan hydrogels crosslinked with tetrahedral polyethylene glycol tetracrylates. Biomaterials 31, 6173–6184. http://dx.doi.org/10.1016/j.biomaterials.2010.04.045.

Skardal, A., Devarasetty, M., Kang, H.-W., Mead, I., Bishop, C., Shupe, T., Lee, S.J., Jackson, J., Yoo, J., Soker, S., Atala, A., 2015. A hydrogel bioink toolkit for mimicking native tissue biochemical and mechanical properties in bioprinted tissue constructs. Acta Biomater. 25, 24–34. http://dx.doi.org/10.1016/j.actbio.2015.07.030.

Smadbeck, P., Stumpf, M.P.H., 2016. Coalescent models for developmental biology and the spatio-temporal dynamics of growing tissues. J. R. Soc. Interface 13, 20160112. http://dx.doi.org/10.1098/rsif.2016.0112.

Stenderup, K., Justesen, J., Clausen, C., Kassem, M., 2003. Aging is associated with decreased maximal life span and accelerated senescence of bone marrow stromal cells. Bone 33, 919–926. http://dx.doi.org/10.1016/j.bone.2003.07.005.

Stockwell, R.A., 1967. The cell density of human articular and costal cartilage. J. Anat. 101, 753–763.

Sudarmadji, N., Chua, C.K., Leong, K.F., 2012. The development of computer-aided system for tissue scaffolds (CASTS) system for functionally graded tissue-engineering scaffolds BT - computer-aided tissue engineering. In: Liebschner, M.A.K. (Ed.), Humana Press. Totowa, NJ, pp. 111–123. http://dx.doi.org/10.1007/978-1-61779-764-4_7.

Sun, W., Starly, B., Darling, A., Gomez, C., 2004. Computer-aided tissue engineering: application to biomimetic modelling and design of tissue scaffolds. Biotechnol. Appl. Biochem. 39, 49. http://dx.doi.org/10.1042/BA20030109.

Suntornnond, R., Tan, E.Y.S., An, J., Chua, C.K., 2016. A mathematical model on the resolution of extrusion bioprinting for the development of new bioinks. Materials (Basel) 9. http://dx.doi.org/10.3390/ma9090756.

Susilo, E., Valdastri, P., Menciassi, A., Dario, P., 2009. A miniaturized wireless control platform for robotic capsular endoscopy using advanced pseudokernel approach. Sensors Actuators A Phys. 156, 49–58. http://dx.doi.org/10.1016/j.sna.2009.03.036.

Tabriz, A.G., Hermida, M.A., Leslie, N.R., Shu, W., 2015. Three-dimensional bioprinting of complex cell laden alginate hydrogel structures. Biofabrication 7, 045012.

Tait, A., Charalambous, X., Proctor, T., Tsagovits, K., Hamilton, N., Veraitch, F., Birchall, M.A., Lowdell, M., 2017. Creating gmp epithelial and fibroblast cells from a single biopsy for the potential use in tissue engineering. Cytotherapy 19, S194. http://dx.doi.org/10.1016/j.jcyt.2017.02.283.

Takahashi, K., Yamanaka, S., 2006. Induction of pluripotent stem cells from mouse embryonic and adult fibroblast cultures by defined factors. Cell 126, 663–676. http://dx.doi.org/10.1016/j.cell.2006.07.024.

Tan, Y.S.E., Yeong, W.Y., 2014. Direct Bioprinting of alginate-based tubular constructs using multi-nozzle extrusion-based technique, in: Kai, C.C., Yee, Y.W., Jen, T.M., Erjia, L. 1st International Conference on Progress in Additive Manufacturing. Singapore, p. 93. https://doi.org/10.3850/978-981-09-0446-3_093

Tasoglu, S., Demirci, U., 2013. Bioprinting for stem cell research. Trends Biotechnol. 31, 10–19. http://dx.doi.org/10.1016/j.tibtech.2012.10.005.

Teodori, L., Crupi, A., Costa, A., Diaspro, A., Melzer, S., Tarnok, A., 2017. Three-dimensional imaging technologies: a priority for the advancement of tissue engineering and a challenge for the imaging community. J. Biophotonics 10, 24–45. http://dx.doi.org/10.1002/jbio.201600049.

Thomas, R., Ratcliffe, E., 2012. Automated adherent human cell culture (mesenchymal stem cells). In: Mitry, R.R., Hughes, R.D. (Eds.), Human Cell Culture Protocols. Humana Press, Totowa, NJ, pp. 393–406. http://dx.doi.org/10.1007/978-1-61779-367-7_26.

Traver, M.A., Assimos, D.G., 2006. New generation tissue sealants and hemostatic agents: innovative urologic applications. Rev. Urol. 8, 104–111.

Triaud, F., Clenet, D.-H., Cariou, Y., Le Neel, T., Morin, D., Truchaud, A., 2003. Evaluation of automated cell culture incubators. JALA J. Assoc. Lab. Autom. 8, 82–86. http://dx.doi.org/10.1016/s1535-5535(03)00018-2.

Trumbull, A., Subramanian, G., Yildirim-Ayan, E., 2016. Mechanoresponsive musculoskeletal tissue differentiation of adipose-derived stem cells. Biomed. Eng. Online 15, 43. http://dx.doi.org/10.1186/s12938-016-0150-9.

Tsai, Y.-C., Li, S., Hu, S.-G., Chang, W.-C., Jeng, U.-S., Hsu, S., 2015. Synthesis of thermoresponsive amphiphilic polyurethane gel as a new cell printing material near body temperature. ACS Appl. Mater. Interfaces 7, 27613–27623. http://dx.doi.org/10.1021/acsami.5b10697.

Van Hoorick, J., Declercq, H., De Muynck, A., Houben, A., Van Hoorebeke, L., Cornelissen, R., Van Erps, J., Thienpont, H., Dubruel, P., Van Vlierberghe, S., 2015. Indirect additive manufacturing as an elegant tool for the production of self-supporting low density gelatin scaffolds. J. Mater. Sci. Mater. Med. 26, 247. http://dx.doi.org/10.1007/s10856-015-5566-4.

Van Lenthe, G., Hagenmuller, H., Bohner, M., Hollister, S., Meinel, L., Muller, R., 2007. Nondestructive micro-computed tomography for biological imaging and quantification of scaffold–bone interaction in vivo. Biomaterials 28, 2479–2490. http://dx.doi.org/10.1016/j.biomaterials.2007.01.017.

Van Vlierberghe, S., Dubruel, P., Lippens, E., Masschaele, B., Van Hoorebeke, L., Cornelissen, M., Unger, R., Kirkpatrick, C.J., Schacht, E., 2008. Toward modulating the architecture of hydrogel scaffolds: curtains versus channels. J. Mater. Sci. Mater. Med. 19, 1459–1466. http://dx.doi.org/10.1007/s10856-008-3375-8.

Vartiainen, J., Pöhler, T., Sirola, K., Pylkkänen, L., Alenius, H., Hokkinen, J., Tapper, U., Lahtinen, P., Kapanen, A., Putkisto, K., Hiekkataipale, P., Eronen, P., Ruokolainen, J., Laukkanen, A., 2011. Health and environmental safety aspects of friction grinding and spray drying of microfibrillated cellulose. Cellulose 18, 775–786. http://dx.doi.org/10.1007/s10570-011-9501-7.

Vlastos, G., Verkooijen, H.M., 2007. Minimally invasive approaches for diagnosis and treatment of early-stage breast cancer. Oncologia 12, 1–10. http://dx.doi.org/10.1634/theoncologist.12-1-1.

Wang, Z., Abdulla, R., Parker, B., Samanipour, R., Ghosh, S., Kim, K., 2015a. A simple and high-resolution stereolithography-based 3D bioprinting system using visible light crosslinkable bioinks. Biofabrication 7, 045009. http://dx.doi.org/10.1088/1758-5090/7/4/045009.

Wang, Z., Min, J.K., Xiong, G., 2015b. Robotics-driven printing of curved 3D structures for manufacturing cardiac therapeutic devices. In: 2015 IEEE Int. Conf. Robot. Biomimetics, http://dx.doi.org/10.1109/ROBIO.2015.7419120.

Wang, Z., Jin, X., Dai, R., Holzman, J.F., Kim, K., 2016. An ultrafast hydrogel photo-crosslinking method for direct laser bioprinting. RSC Adv. 6, 21099–21104. http://dx.doi.org/10.1039/C5RA24910D.

Wang, T., Kwok, T.-H., Zhou, C., 2017. In-situ droplet inspection and control system for liquid metal jet 3D printing process. Proc. Manuf. 10, 968–981. http://dx.doi.org/10.1016/j.promfg.2017.07.088.

Wernike, E., Li, Z., Alini, M., Grad, S., 2008. Effect of reduced oxygen tension and long-term mechanical stimulation on chondrocyte-polymer constructs. Cell Tissue Res. 331, 473–483.

Westphal, I., Jedelhauser, C., Liebsch, G., Wilhelmi, A., Aszodi, A., Schieker, M., 2017. Oxygen mapping: Probing a novel seeding strategy for bone tissue engineering. Biotechnol. Bioeng. 114, 894–902. http://dx.doi.org/10.1002/bit.26202.

Wilson, W.C., Boland, T., 2003. Cell and organ printing 1: protein and cell printers. Anat. Rec. Part A Discov. Mol. Cell. Evol. Biol. 272A, 491–496. http://dx.doi.org/10.1002/ar.a.10057.

Wojcik, M., Koszalka, L., Pozniak-koszalka, I., Kasprzak, A., 2015. MZZ-GA Algorithm for Solving Path Optimization in 3D Printing. In: ICONS 2015 Tenth Int. Conf. Syst. MZZ-GA, pp. 30–35.

Xavier, J.R., Thakur, T., Desai, P., Jaiswal, M.K., Sears, N., Cosgriff-Hernandez, E., Kaunas, R., Gaharwar, A.K., 2015. Bioactive nanoengineered hydrogels for bone tissue engineering: A growth-factor-free approach. ACS Nano 9, 3109–3118. http://dx.doi.org/10.1021/nn507488s.

Xing, Q., Yates, K., Vogt, C., Qian, Z., Frost, M.C., Zhao, F., 2014. Increasing mechanical strength of gelatin hydrogels by divalent metal ion removal. Sci. Rep. 4, 4706. http://dx.doi.org/10.1038/srep04706.

Xu, T., Jin, J., Gregory, C., Hickman, J.J., Boland, T., 2005. Inkjet printing of viable mammalian cells. Biomaterials 26, 93–99. http://dx.doi.org/10.1016/j.biomaterials.2004.04.011.

Xu, F., Sridharan, B., Wang, S., Gurkan, U.A., Syverud, B., Demirci, U., 2011. Embryonic stem cell bioprinting for uniform and controlled size embryoid body formation. Biomicrofluidics 5, 22207. http://dx.doi.org/10.1063/1.3580752.

Xu, S., Mundra, P.A., Li, H., Zhu, S., Welsch, R.E., Rajapakse, J.C., 2013a. Image analysis for cellular and tissue engineering. In: Yu, H., Rahim, N.A.A. (Eds.), Imaging in Cellular and Tissue Engineering. CRC Press, Boca Raton, pp. 223.

Xu, T., Zhao, W., Zhu, J., Albanna, M.Z., Yoo, J.J., Atala, A., 2013b. Complex heterogeneous tissue constructs containing multiple cell types prepared by inkjet printing technology. Biomaterials 34, 130–139. http://dx.doi.org/10.1016/j.biomaterials.2012.09.035.

Yanagimachi, M.D., Niwa, A., Tanaka, T., Honda-Ozaki, F., Nishimoto, S., Murata, Y., Yasumi, T., Ito, J., Tomida, S., Oshima, K., Asaka, I., Goto, H., Heike, T., Nakahata, T., Saito, M.K., 2013. Robust and highly-efficient differentiation of functional monocytic cells from human pluripotent stem cells under serum- and feeder cell-free conditions. PLoS One 8, e59243. http://dx.doi.org/10.1371/journal.pone.0059243.

You, F., Wu, X., Zhu, N., Lei, M., Eames, B.F., Chen, X., 2016. 3D printing of porous cell-laden hydrogel constructs for potential applications in cartilage tissue engineering. ACS Biomater. Sci. Eng. 2, 1200–1210. http://dx.doi.org/10.1021/acsbiomaterials.6b00258.

Youssef, A.A., Ross, E.G., Bolli, R., Pepine, C.J., Leeper, N.J., Yang, P.C., 2016. The promise and challenge of induced pluripotent stem cells for cardiovascular applications. JACC Basic to Transl. Sci. 1, 510–523. http://dx.doi.org/10.1016/j.jacbts.2016.06.010.

Yu, Y., Wen, H., Ma, J., Lykkemark, S., Xu, H., Qin, J., 2014a. Flexible fabrication of biomimetic bamboo-like hybrid microfibers. Adv. Mater. 26, 2494–2499. http://dx.doi.org/10.1002/adma.201304974.

Yu, Y., Zhang, Y., Ozbolat, I.T., 2014b. A hybrid bioprinting approach for scale-up tissue fabrication. J. Manuf. Sci. Eng. 136 061013–1. https://doi.org/10.1115/1.4028511.

Yu, Y., Moncal, K.K., Li, J., Peng, W., Rivero, I., Martin, J.A., Ozbolat, I.T., 2016. Three-dimensional bioprinting using self-assembling scalable scaffold-free “tissue strands” as a new bioink. Sci. Rep. 6, 28714. http://dx.doi.org/10.1038/srep28714.

Zhang, A.P., Qu, X., Soman, P., Hribar, K.C., Lee, J.W., Chen, S., He, S., 2012. Rapid fabrication of complex 3D extracellular microenvironments by dynamic optical projection stereolithography. Adv. Mater. 24, 4266–4270. http://dx.doi.org/10.1002/adma.201202024.

Zhang, Y., Li, W., Laurent, T., Ding, S., 2013. Small molecules, big roles – the chemical manipulation of stem cell fate and somatic cell reprogramming. J. Cell Sci. 125 5609 LP-5620. https://doi.org/10.1242/jcs.096032.

Zhang, Y., Yu, Y., Akkouch, A., Dababneh, A., Dolati, F., Ozbolat, I.T., 2015. In vitro study of directly bioprinted perfusable vasculature conduits. Biomater. Sci. 3, 134–143. http://dx.doi.org/10.1039/C4BM00234B.

Zhang, H.-B., Xing, T.-L., Yin, R.-X., Shi, Y., Yang, S.-M., Zhang, W.-J., 2016a. Three-dimensional bioprinting is not only about cell-laden structures. Chin. J. Traumatol. 19, 187–192. http://dx.doi.org/10.1016/j.cjtee.2016.06.007.

Zhang, Y.S., Arneri, A., Bersini, S., Shin, S.R., Zhu, K., Goli-Malekabadi, Z., Aleman, J., Colosi, C., Busignani, F., Dell’Erba, V., Bishop, C., Shupe, T., Demarchi, D., Moretti, M., Rasponi, M., Dokmeci, M.R., Atala, A., Khademhosseini, A., 2016b. Bioprinting 3D microfibrous scaffolds for engineering endothelialized myocardium and heart-on-a-chip. Biomaterials 110, 45–59. http://dx.doi.org/10.1016/j.biomaterials.2016.09.003.

Zhang, Y., Pak, C., Han, Y., Ahlenius, H., Zhang, Z., Chanda, S., Marro, S., Patzke, C., Acuna, C., Covy, J., Xu, W., Yang, N., Danko, T., Chen, L., Wernig, M., Südhof, T.C., 2017. Rapid single-step induction of functional neurons from human pluripotent stem cells. Neuron 78, 785–798. http://dx.doi.org/10.1016/j.neuron.2013.05.029.

Zhao, Y., Li, Y., Mao, S., Sun, W., Yao, R., 2015. The influence of printing parameters on cell survival rate and printability in microextrusion-based 3D cell printing technology. Biofabrication 7, 045002. http://dx.doi.org/10.1088/1758-5090/7/4/045002.

Zhao, J., Griffin, M., Cai, J., Li, S., Bulter, P.E.M., Kalaskar, D.M., 2016. Bioreactors for tissue engineering: an update. Biochem. Eng. J. 109, 268. http://dx.doi.org/10.1016/j.bej.2016.01.018.

Zhou, H., Li, W., Zhu, S., Joo, J.Y., Do, J.T., Xiong, W., Kim, J.B., Zhang, K., Schöler, H.R., Ding, S., 2010. Conversion of mouse epiblast stem cells to an earlier pluripotency state by small molecules. J. Biol. Chem. 285, 29676–29680. http://dx.doi.org/10.1074/jbc.C110.150599.